

SOME OPTICAL CONSIDERATIONS OF  
SYNTHETIC HYDROGEL POLYMERS  
FOR CONTACT LENS USAGE

by

NABIL FATHY EL-NASHAR

A thesis submitted for the degree of  
Doctor of Philosophy  
in the  
University of Aston in Birmingham

September 1979

Some Optical Considerations of Synthetic Hydrogel  
Polymers for Contact Lens Usage

Nabil Fathy El-Nashar

PhD

1979

Summary

The accurate measurement of hydrogel contact lenses presents a number of problems. The inherent flexibility of the material and its similarity to saline, in terms of refractive index, make measurements unpredictable and difficult.

The aim of the experimental work was to develop an accurate method for measuring the radii of curvature, thickness and refractive index of hydrogel contact lenses. The construction of novel apparatus allowed interference patterns to be generated using a Linnik micro-interferometer. The generated patterns were analysed and the radii of curvature of a series of Bausch and Lomb SOFLENSES were calculated to an accuracy of  $10^{-3}$  mm. The experimental results showed a good agreement with the theoretical results published by the manufacturer. The micro-interferometer was also employed to determine the refractive index of a range of hydrogel materials.

The spherical aberration of SOFLENSES in air and in situ on the human eye was investigated using a commercially available photoelectric keratoscope, the "PEK" system 2000. The results present a comprehensive view of the changes in the lens parameters when applied to the cornea.

Key words:

Contact lenses  
Hydrogel  
Interferometry  
Refractive indices  
Spherical aberration

## ACKNOWLEDGEMENTS

I would like to express my most sincere thanks to my supervisor, Dr. John Larke, for suggesting the project, his helpful suggestions, encouragement and patient reading throughout this thesis.

I am indebted to: Professor T. Mulvey of the Department of Physics for his interest in the project; to Dr. K. G. Birch of the National Physical Laboratory for his help, advice and access to the Linnik micro-interferometer; and to Dr. M. J. Kidger for providing the computer program used in Chapter Five.

I would like to thank the staff and technicians of the Departments of Physics and Ophthalmic Optics who have kindly given me all the help which I needed.

I would also like to thank my colleagues in the Soft Contact Lens laboratory, in particular Miss C. Haggerty for fitting the SOFLENSES and Mr. J. Pointer for reading the manuscript. I am grateful to the Egyptian Government for the award of the financial assistance and to the University of Hellwan for granting me the study leave.

Many thanks to my typist, Mrs. B. Drinkwater, whose skill and endeavour has been greatly appreciated.

## ABBREVIATIONS

MMA	Methyl Methacrylate
PMMA	Polymethyl Methacrylate
HEMA	Hydroxyethyl methacrylate
PHEMA	Poly 2-hydroxyethyl methacrylate
VP	Vinyl Pyrrolidone
PVP	Poly-vinyl Pyrrolidone
mm	millimetre
$\mu$	micron
$\text{A}^{\circ}$	Angstrom
$\text{C}^{\circ}$	Degree centigrade
F.C.O.R.	Front central optic radius
B.C.O.R.	Back central optic radius
$\lambda$	wave length of monochromatic light
N.A.	numerical aperture
S.D.	standard deviation

## C O N T E N T S

Summary	i
Acknowledgements	ii
Abbreviations	iii
CHAPTER 1 Introduction: Contact lenses as a refractive correction	
1.1 The optical system of eye and its properties	1
1.2 The early development in contact lenses	5
1.3 The optics of contact lenses	8
1.3.1 Optical principles of spherical contact lenses	8
1.3.2 Magnification properties	12
1.3.3 Residual Astigmatism	13
1.3.4 Aberrations	16
1.4 The development of contact lens materials	17
1.4.1 General development	17
1.4.2 Hydrogels as a contact lens material	19
1.5 Methods of manufacturing hydrogel contact lenses	21
1.5.1 Spin casting	21
1.5.2 Lathe cutting	25
CHAPTER 2 Methods of measuring the radii of curvature of optical surfaces	
2.1 Introduction	26

2.2	Principles of curvature	27
2.2.1	Mechanical spherometers	27
2.2.2	Optical spherometers	29
2.2.2a	Autocollimation method	29
2.2.2b	Microscope method	31
2.2.2c	Interference fringes method	32
2.3	Measurements of corneal contact lenses	33
2.3.1	Bier contact lens spherometer	33
2.3.2	Radiuscope	34
2.3.3	Keratometer (associated with a special attachment)	35
2.3.4	Focimeter	36
2.3.5	Toposcope	40
2.3.6	Newton's rings	43
2.4	Measurements of soft hydrophilic lenses (Hydrogel lenses)	44
2.4.1	Hemispherical convex template (plastic radius gauge)	44
2.4.2	Radiuscope	45
2.4.3	Keratometry	48
2.4.4	Profile projection technique	49
2.4.5	Sagittal height (Sagometer principle)	51
2.4.6.	Other methods (laser, tool maker microscope and moire fringes)	54

CHAPTER 3    Measurements of central optic radii and  
                 thickness of hydrogel lenses SOFLENS<sup>R</sup>  
                 by interferometry

3.1	Introduction	56
3.2	Preliminary experiment	57
3.3	Interference Microscopy	58
3.3.1	Definition and classification	58
3.3.2	The Linnik interference microscope	61
3.3.3	Description of the instrument	64
3.3.3a	General construction	64
3.3.3b	Inner construction	66
3.3.3c	Cell-lens design	69
3.4	Experimental procedure	71
3.4.1	Calibration	71
3.4.2	Measurement of central optic radii of hydrogel lenses	73
3.4.3	Measurement of central thickness	75
3.5	Theoretical considerations	76
3.6	Experimental results	82
3.7	Source of Errors	92
3.7.1	Fringe spacing error	93
3.7.2	Errors due to wave front and spherical aberration	97

CHAPTER 4    Measurement of refractive index of the  
                 hydrogel material

4.1	Introduction	100
-----	--------------	-----

4.2	Experiment 1: Apparatus and methodology	102
4.3	Experiment 2: Apparatus and methodology	106
4.4	Experiment 3: Apparatus and methodology	107
4.5	Results and Conclusion	111

CHAPTER 5    The evaluation of spherical aberration  
and change in the parameters for the  
hydrogel lenses on the human eye

5.1	Introduction	115
5.2	Spherical aberration of the human eye	115
5.3	Effect of contact lenses on the spherical aberration of the human eye	119
5.4	Apparatus	122
5.5	Experimental procedure	123
5.6	Calculation of the spherical aberration of the SOFLENS in air	124
5.7	Calculation of the spherical aberration of the SOFLENS in situ on the human eye	125
5.8	Calculation of the changes in SOFLENSES parameters in situ on the human eye	130
	5.8.1    Equal change hypothesis	134
	5.8.2    Percentage change hypothesis	134
	Analysis of the results	
5.9	Analysis of the results	135

CHAPTER 6    Conclusion

6.1	General discussion and conclusion	137
6.2	Suggestions for further work	141

Appendix I	143
Appendix II	146
Appendix III	188
References	

## CHAPTER 1

### INTRODUCTION: CONTACT LENSES AS A REFRACTIVE CORRECTION

#### 1.1 The optical system of the eye and its properties

The eye is a complex optical system, comprising an approximately spherical body about 2.5 cm in diameter. The greater part of the eye is bounded by a tough, opaque, white membrane known as the sclera. At the front, this merges into a transparent rather horny tissue known as the cornea. The general shape is preserved by the internal pressure in the eye which is equivalent to 15 - 25 mm of mercury. The diameter of the cornea is about 12 mm horizontally and 11 mm vertically, the thickness at the pole being somewhat less than at the periphery. The cornea is kept moist and transparent by a surface film of lachrymal fluid, constantly distributed by the involuntary action of the lids during blinking. The chamber behind the cornea contains a liquid; the aqueous humor, and has an axial length of about 1.3 mm posterior to the aqueous humor is the crystalline lens which is double convex in form and composed of a number of transparent fibrous coats which are hardest at centre and become progressively softer towards the outer layers. The crystalline lens is held in place by ligaments which are attached to the ciliary muscle. Under the action of the ciliary muscle the lens can be made to change its shape, and the power

of the system is adjusted to focus images of objects at different distances on to the retina. This focusing effect is known as accommodation. In front of the crystalline lens is the iris which automatically controls the amount of light entering the eye. The circular aperture in the iris, known as the pupil, can be varied from about 2 mm diameter in very bright light to about 8 mm diameter in darkness, while in ordinary light the diameter may be 3 to 4 mm. The space behind the crystalline lens is filled with a transparent, thin gel called the vitreous humor, having a refractive index similar to the aqueous humor. The outer coating of the eyeball (the sclera) is about 1 mm thick, opaque, usually white in colour and merges into the transparent cornea in the region known as the limbus. The inner layer adjacent to the sclera is called the choroid and contains dark pigmented cells for absorbing any light which might penetrate the sclera, thus preventing any such stray light from reaching the retina. The retina-proper consists of a delicate layer of nerve fibre and covers a large part of the inner surface of the eye. The microstructure of the retina is very complicated, and no less than ten layers have been distinguished. The thickness of the retina at no point exceeds 0.4 mm. The field of view of the immobile eye is extensive, amounting to about  $150^{\circ}$  laterally and  $120^{\circ}$  vertically.

The eye has four refracting surfaces, the front and back surfaces of the cornea and the front and back surfaces of the lens. The main optical characteristic of these surfaces are their curvature, and the separation and refractive indices of the media between them. Duke-Elder (1970) has reported the data for the optical system of the eye, summarised in table 1.1 which would closely represent the human eye with completely relaxed accommodation.

Table 1.1

The optical system of the eye (in mm)

	Von Helmholtz	Tschering	Gullstrand
<u>Position of surfaces</u>			
Cornea, Front surface	0	0	0
Cornea, Back "	-	1.15	0.5
Lens, Front "	3.6	3.54	3.6
Lens, Back "	7.2	7.60	7.2
Lens,Core, Front surface	-	-	4.146*
Lens,Core, Back "	-	-	6.565*
<u>Radii of Curvature</u>			
Cornea, Front surface	8.0	7.98	7.7
Cornea, Back "	-	6.22	6.8
Lens, Front "	10.0	10.20	10.0
Lens, Back "	-6.0	-6.17	-6.0
Lens,Core, Front surface	-	-	7.911*
Lens,Core, Back "	-	-	-5.76*
<u>Refractive indices</u>			
Cornea	-	1.377	1.376
Aqueous and vitreous	1.336	1.3365	1.336 (cortex)
Lens	1.44*	1.42*	1.406 (core)

\*Calculated values

## 1.2 The early development in contact lenses

Ferrero (1952) was the first to make a complete English translation of Leonardo Da Vinci's Codex of the eye from the Ravaisson-Mollien facsimile edition of 1883. He shows that the idea of neutralizing the cornea was proposed by Da Vinci in 1508, who suggested immersing the eye in a hollow glass bowl containing water. The idea of neutralizing the cornea was later made by Descartes in 1636 which was reported by Enoch (1956). De la Hire (1685) suggested the use of a concave glass upon the eye, the inner surface having the same convexity as the cornea so that the corneal refraction was eliminated; Crombie and Hoskin (1967).

Young (1801) introduced an apparatus called a hydrodiascope, the object of which was to abolish the action of the cornea as a refracting medium by placing in front of it a lens of known power separated from it by a layer of water of known thickness. Herschel (1830) suggested that corneal astigmatism could be corrected by applying to the eye a small glass capsule containing a transparent animal Jelly in contact with the cornea, the glass being moulded to correspond to the shape of the eye.

In 1887, Saemisch suggested to A. C. Müller the possibility of a protective glass shell for a patient who had his eye-lid surgically removed. The patient was able to wear the contact

glass with comfort and complete preservation of corneal transparency till his death twenty-one years later. Three ophthalmologists independently attempted to produce a contact glass in different ways and for different reasons. Fick (1888) of Zürich, who introduced the term contact lens, had in mind the correction of conical cornea, and used glasses blown to a form obtained by taking a mould. Kalt (1888) of Paris, used a moulded lens as an orthopaedic splint in the same condition to mould the cornea into a more normal shape. Müller of Gladbach (1889) recognised that the main cause of the pain and lachrymation often experienced by patients in contact lens wear came from the pressure exerted on the conjunctival vessels by the edge of the glass lens, and not from the pressure of the glass on the cornea. Other people became interested and development and experience accumulated rapidly.

Between 1880-1932 experiments continued with blown contact lenses. The type of lenses most commonly used in this period were the scleral lenses. The majority of these lenses were blown by the Müller Company and were ground and polished by Carl Zeiss of Jena.

Feinbloom (1937) was the first American who used plastic to manufacture contact lens. His lenses were made of a glass corneal portion and a plastic scleral band.

Obrig and Salvatori (1940) produced scleral contact lenses made of all plastic (Polymethyl methacrylate). These lenses were advantageous in having transparency of the corneal and scleral portions, and being light in weight and producing diminished ocular sensation. Obrig also reported the use of a 2% sodium fluorescein solution and ultraviolet light for checking the fit of contact lenses. Nugent (1949) reported that the corneal lens was patented by Tuohy (1948) to replace the scleral lens. The Tuohy lens shape was circular and had a standard 11.5 mm diameter which covered nearly the whole of the cornea. The lens had two back curves, the back central optic diameter was 10.5 mm and the peripheral bevel was 0.5 mm. The back surface of the lens was fitted so as to be slightly flatter than the flattest meridian of the cornea.

Dickenson et al (1954) made another step in developing corneal lenses by reducing the overall diameter to 9.5 mm and the centre thickness to 0.2 mm. This lens was called the Microlens.

In 1955, Bier introduced a corneal lens having multiple inside radii which was known as the contour lens. This lens had three back curves, a central optical zone, a peripheral curve varying from 0.4 mm to 0.8 mm flatter than the central zone, and an intermediate transitional curve 0.25 mm wide.

The back central optic diameter was 6.5 mm and the overall size varied from 8.0 mm to 10.5 mm. The main advantage of this lens was the presence of a flatter peripheral curve which allowed the central curve to align the flattest meridian of the cornea, and also enabled lenses to be fitted with central optical clearance.

### 1.3 The optics of contact lenses

#### 1.3.1 Optical principles of spherical contact lenses

Physically we can consider the contact lens as a thin lens but optically this assumption cannot be accepted because the radii of curvature of the contact lens are large as compared to its thickness. The surface powers of a contact lens are given by the expressions:-

$$F_1 = (\mu_1 - \mu_0) / R_1$$

$$F_2 = (\mu_0 - \mu_1) / R_2$$

where	$F_1$	Front surface power in diopters
	$F_2$	Back " " "
	$\mu_1$	Index of refraction of contact lens material
	$\mu_0$	" " " " surrounding medium (air $\approx 1$ )
	$R_1$	Radius of curvature of front surface in metres
	$R_2$	" " " " back " " "

The vertex powers are given by the equations:-

$$F_{\text{vCL}} = F_1 + F_2 - \frac{t}{\mu_1} F_1 F_2 \quad / \quad 1 - \frac{t}{\mu_1} F_2 \quad 1.1$$

$$\overset{\wedge}{F}_{\text{vCL}} = F_1 + F_2 - \frac{t}{\mu_1} F_1 F_2 \quad / \quad 1 - \frac{t}{\mu_1} F_1 \quad 1.2$$

$$F_{\text{V}} = F_1 + F_2 - \frac{t}{\mu_1} F_1 F_2 \quad 1.3$$

where

- $F_{\text{vCL}}$  Front vertex power in dioptries
- $\overset{\wedge}{F}_{\text{vCL}}$  Back " " " "
- $F_{\text{V}}$  equivalent lens power
- $t$  central optic thickness in metres

Westheimer (1961) gave the equation for the back vertex power of the three-surface contact lens-fluid lens system in air (Figure 1.1) as follows,

$$\overset{\wedge}{F}_{\text{V}_3} = \frac{F_1 + F_2 + F_3 - d_1 F_1 (F_2 + F_3) - d_2 F_3 (F_1 + F_2) + d_1 d_2 F_1 F_2 F_3}{1 - d_1 F_1 - d_2 (F_1 + F_2) + d_1 d_2 F_1 F_2}$$

..... 1.4

where,

- $F_1 = (\mu_1 - \mu_0) / R_1$       and     $d_1 = t_1 / \mu_1$
- $F_2 = (\mu_2 - \mu_1) / R_2$       "     $d_2 = t_2 / \mu_2$
- $F_3 = (\mu_0 - \mu_2) / R_3$

Equation 1.4 is too complicated for clinical application.

Sarver (1963); and independently Bennet (1966), simplified the case by separating the plastic contact lens and fluid lens with an infinitely thin layer of air (Figure 1.2).

Assuming that the fluid lens is infinitely thin,

$$F_2 = F_{2a} + F_{2b} \quad 1.5$$

substitute by equation 1.5 in 1.4 considering,

$$d_2 = 0$$

$$F_{2b} = K_2 = \text{the keratometer value of the base curve of the contact lens}$$

and,

$$-F_3 = K_c = \text{the keratometer value of corneal curvature}$$

Then equation 1.4 can be written as follows,

$$\hat{F}_{V_3} = \hat{F}_{VcL} + K_2 - K_c \quad 1.6$$

Equation 1.6 shows that the back vertex power of the contact lens and fluid lens system is equal to the sum of the contact lens back vertex power in air plus the thin lens power of the fluid lens in air.

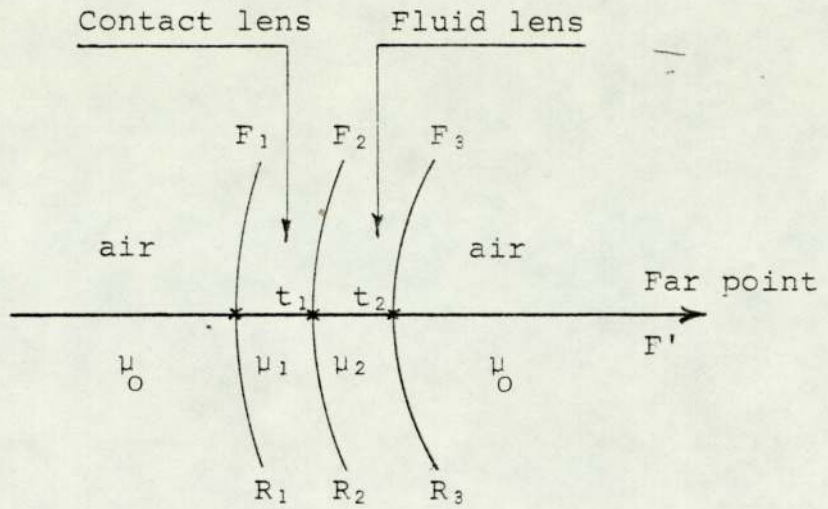


Figure 1.1 Three surface contact lens - fluid lens system

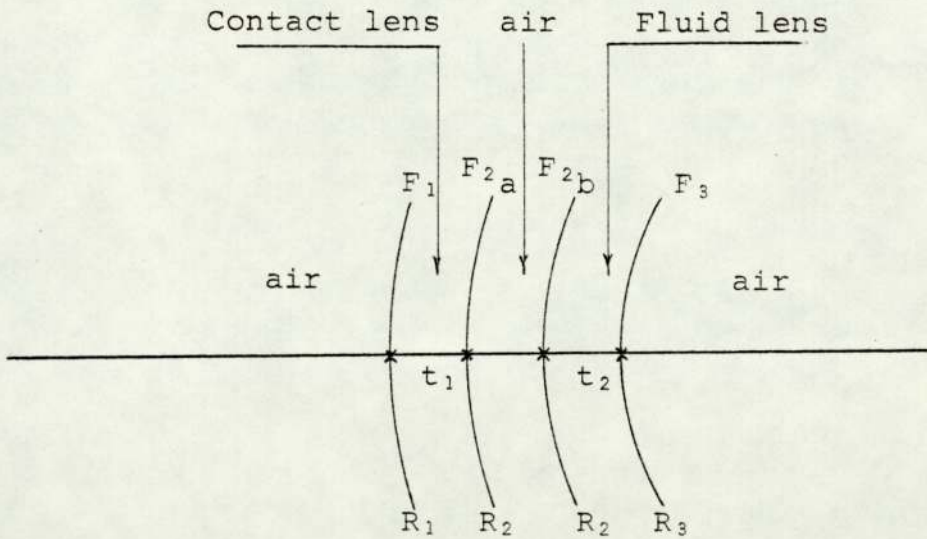


Figure 1.2 Three surface contact lens - fluid lens system with  $F_2 = F_{2a} + F_{2b}$  and  $t_2 = 0$

### 1.3.2 Magnification properties

The change in the retinal image size brought about by the wearing of lenses is termed "Spectacle magnification" and is defined as the ratio of the retinal image size in the corrected ametropic eye to the retinal image size in the uncorrected eye.

#### (a) Power factor

The power factor is given by the expression  $1 / (1 - aF_v)$

where,

$F_v$  is the back vertex power of the lens (in dioptries)

$a$  is the distance between the back vertex of the lens and entrance pupil of eye (in metres)

usually the eye's entrance pupil is about 3 mm behind the corneal vertex. For the spectacle lens "a" is about 0.015 - 0.018 m. As a result of the power factor the retinal image size could be altered by up to 50%. In the case of contact lens where " $F_v$ " represent the back vertex power of the contact lens system, the value of "a" is 0.003 m. So the effect of the power factor on the retinal image size is negligible.

#### (b) Shape factor

The shape factor is  $1 / (1 - (t/\mu)F_1)$  therefore the shape factor increases with centre thickness and front surface power of the lens. For contact lenses the value of the shape factor can be disregarded for the most minus power lenses, but may be considered significant for the strong plus lenses.

### 1.3.3 Residual Astigmatism

Mandell (1969) defined residual astigmatism as the astigmatic refractive error that is present when a contact lens is placed upon the cornea to correct an existing ametropia. Residual astigmatism can be subdivided into physiological residual astigmatism which is due to the eye's refractive system, and the induced residual astigmatism which is the product of the contact lens itself whose causes may be due to:-

- i) The tilt or decentration of the contact lens  
(Tocher, 1962; Sarver, 1963)
- ii) Toric anterior and/or posterior surface of the contact lens (Korb, 1960)
- iii) Flexure of a very thin contact lens (Bailey 1961; Marano, 1962; Harris, 1970)

There are different ways to calculate the residual astigmatism. A direct method was given by Mandell (1969) as follows:-

- i) Determine the amount of anterior corneal cylinder that is neutralized by the fluid lens by measuring the difference between the keratometer readings  $\Delta K$  of the two principal meridians of the cornea (Note that keratometer should be calibrated for an index of refraction equal to the refractive index of the fluid lens)

- ii) Subtract  $\Delta K$  from the total astigmatism of the eye referred to the plane of the cornea

The calculation of residual astigmatism was done by Kratz 1949; Carter 1963; Sarver 1969; Dellande 1970.

The mean calculated residual astigmatism was about  $-0.50D$  axis  $90$ . The relation between the measured and calculated residual astigmatism was studied by Sarver (1969) and was given by the linear regression equation,

$$Y = 0.247 X + 0.086 \quad S.D = \pm 0.25D, N = 408 \quad 1.7$$

Dellande (1970) introduced the regression line that gives the best fit for his results as follows,

$$Y = 0.510 X + 0.026 \quad S.D = \pm 0.26D, N = 83 \quad 1.8$$

Grosvenor (1963) reported that if the calculated residual astigmatism is  $0.75D$  or more the visual acuity through ordinary contact lens may be poor. To correct the residual astigmatism a contact lens with toric surfaces could be used. A non rotating lens design should be used so that the cylinder axis can maintain its axis.

Goldberg (1964) suggested that the corneal contact lens may become a non-rotating design by using any one, of a combination,

of the following:-

1. Prism base down
2. Double truncation
3. Single truncation at the base of a prism design lens
4. Toric peripheral curve
5. Toric base curve

Also the residual astigmatism could be corrected by spherical corneal lenses as was explained by Harris (1970). The results of Harris (1970) indicate that thin lenses (< 0.12 mm thick) flex on toric corneas. A spherical lens that flexes on a-with-rule toric cornea will reduce an against-the-rule-residual astigmatism. But if the residual astigmatism and corneal toricity are both against-the-rule or both with-the-rule, the residual astigmatism will increase and thin lenses should not be used.

Harris and Appelquist (1974) demonstrated that varying the contact lens power did not alter lens flexure or residual astigmatism on spherical corneas, whilst contact lenses with higher minus power caused significantly less flexure and residual astigmatism than did contact lenses with lower minus power. They also indicate that varying contact lens diameter did not alter lens flexure or residual astigmatism on any of the corneas.

#### 1.3.4 Aberrations

Westheimer (1961) maintained that aberrations of a visual aid can only be discussed in the context of the use of the device in association with the eyes. In the case of spectacle lenses, the spherical aberration and coma do not play an important role, since the cone of light entering the pupil is usually small compared to the curvature of such lenses. Because the eye moves with respect to the spectacle lens, oblique astigmatism, distortion and curvature of the field should be considered. In the case of contact lenses the eye moves with the contact lens and since the sensitivity of the peripheral retina is limited, extra axial imagery is not a critical factor. For this reason oblique astigmatism, distortion, curvature of the field and the coma are not highly significant aberrations of contact lenses as long as the lens stays centred on the pupil.

Spherical aberration is the most important aberration in contact lenses, since contact lenses have a relatively high curvature over a relatively small entrance pupil.

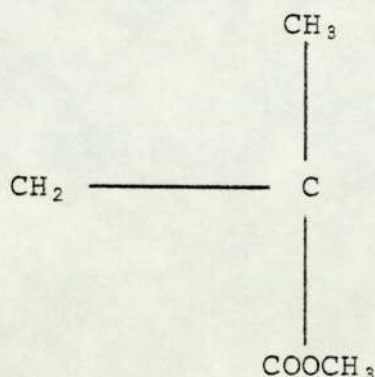
Millodot (1969) found that visual acuity was not affected by the spherical aberration when contact lenses were worn under conditions of high luminance. When luminance was reduced and the pupil dilated, the visual acuity with contact lenses decreases more rapidly than with spectacle lenses. However,

the difference in visual acuity was not as large as would be predicted from spherical aberration alone because of the Stiles-Crawford effect. Chromatic aberration is not significant for either spectacle or contact lenses and was ignored in the study.

#### 1.4 The development of contact lens materials

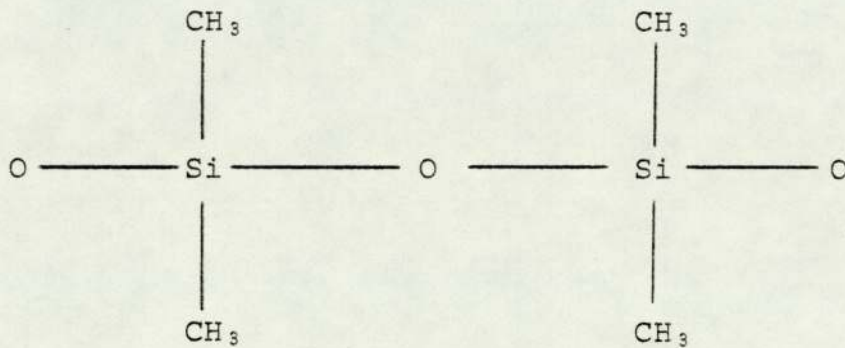
##### 1.4.1 General development

As previously stated, Feinbloom (1937) was the first to report the use of plastic in the manufacture of contact lenses. Feinbloom's lenses consisted of a ground glass corneal portion and a moulded plastic scleral band. The first moulded all plastic scleral contact lenses were made (1938), following the development of polymethylmethacrylate whose structure is as follows:-



The second change in contact lens materials came in the mid 1950's with the invention of synthetic hydrogels by Professor Lim and Wichterle (1956).

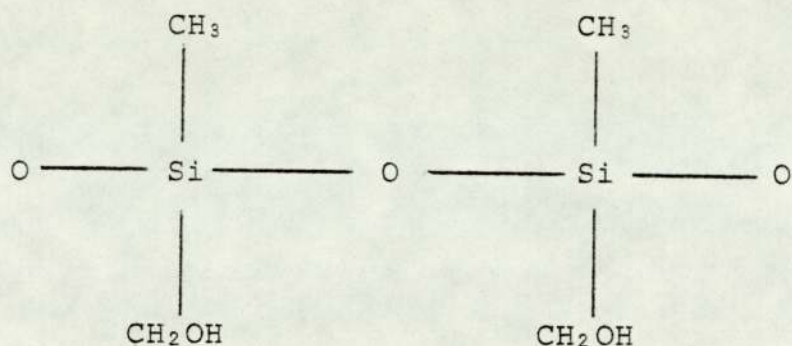
In 1966, Becker reported a further material for contact lens usage, Silicone rubber, a poly (dimethylsiloxane) whose chemical structure is as follows:-



The silicone rubber is a non-toxic material which is highly permeable to oxygen and carbon dioxide, it is flexible and soft even in dry state, and its rigidity and elasticity are important in the correction of corneal astigmatism.

Unfortunately, it is a hydrophobic material and, since it cannot be readily machined or polished, there are problems of forming a satisfactory edge.

Mizutani and Miwa (1977) developed a technique to treat the silicone rubber contact lens to make the surface of the lens hydrophilic. They called this process Molecular Bond Treatment (M.B.T.). The formula of silicone rubber treated by M.B.T. is:-



They concluded from the results of various investigations that a hydrophilic silicone rubber contact lens is practical in daily wear.

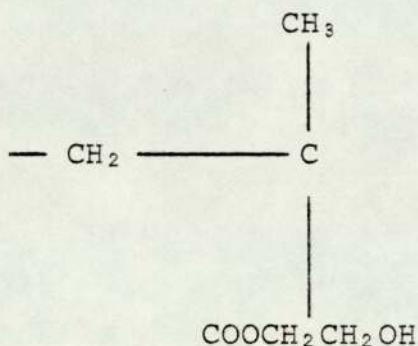
The materials which can be used for manufacturing contact lenses may then be summarised as follows:-

1. Poly(methyl methacrylate) PMMA hard material
2. Poly (2-hydroxyethyl methacrylate) PHEMA hydrogel soft material
3. Silicone rubber poly (dimethyl siloxane) flexible material

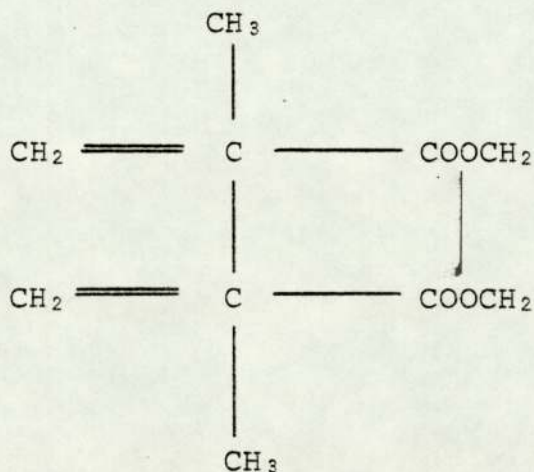
#### 1.4.2 Hydrogels as a contact lens material

In 1956, Wichterle proposed the use of covalently cross-linked glycol methacrylates for a surgical prostheses and contact lenses. The developed materials were called hydrogels because

of their ability to absorb water. The original hydrogel contact lenses were made from infrequently cross-linked poly 2-hydroxyethyl methacrylate (PHEMA):-



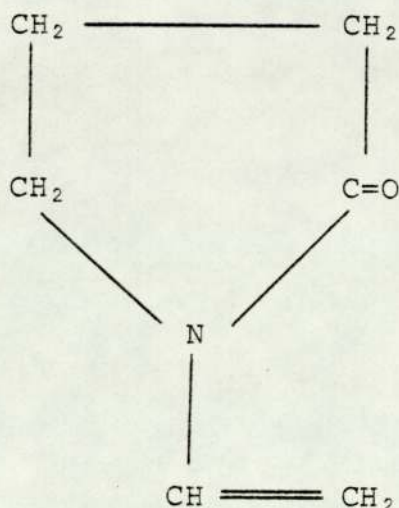
The material was cross-linked with Ethylene glycol dimethacrylate (EGDM):-



In the preparation of HEMA monomer, EGDM usually exists in small amounts as an impurity.

Commercially available PHEMA lenses contain approximately 38% water. To improve the ability of the gel to imbibe

more than 40% water at equilibrium, the Wichterle group copolymerized HEMA with other hydrophilic monomers such as Vinyl pyrrolidone (VP), Refoja (1978).



VP has a double bond on its vinyl group which allows it to polymerise to yield the polymer PVP.

### 1.5 Methods of manufacturing hydrogel contact lenses

There are two methods currently available for the commercial production of contact lenses from hydrogels.

#### 1.5.1 Spin Casting

The first technique used to manufacture hydrogel contact lenses was spin casting in Czechoslovakia (Wichterle 1966, 1968). At present, the Bausch and Lomb, inc. in the U.S.A. is the only manufacturer that uses spin casting for the

manufacture of hydrogel contact lenses (Soflens). The theory and practice of the method will be briefly described.

The fabrication of Soflens (2 hydroxyethylmethacrylate) begins with a mixture of two liquid monomers; ethylene glycol monoethacrylate and ethylene dimethacrylate.

The liquid mixture is injected into a concave spinning mould. Mandell (1974) illustrates that the polymerisation takes place in the spinning mould in the presence of carbon dioxide at 65°C until it reaches a state of equilibrium. Water at 80°C is then pumped in to remove any unreacted monomer or other water soluble substances and to hydrate the lens. The lens is then inspected, measured for power, placed in a glass vial filled with 0.9% saline and sterilized.

The anterior surface of Soflens is a replica of the spherical surface of the mould. Its value is constant for each series of lenses. The posterior surface of the Soflens is aspheric, Anon (1976) and is the product of the forces at play on the lens at the time of polymerisation. Coombs and Knoll (1976) have shown that the size and shape of the spinning lens surface in the manufacture of the Soflens are controlled by three variables:-

1. Shape of the mould (Sagittal depth and diameter)
2. Value of injected monomers
3. Spin Speed

and three constants,

1. Surface tension of monomer
2. Material density
3. Gravity

Hence, the shape of the posterior surface of the lens will be a result of the interaction between all of the above factors.

Clements (1978) reported that surface tension acts to hold the liquid monomer mixture in an envelope within the mould aperture ; Centrifugal force acts to force liquid in the direction  $90^{\circ}$  from the axis of the mould rotation; and Gravity acts to force liquid down into the centre of the mould concavity. The simplest case of a spinning surface occurs when the effect of surface tension on the meniscus is ignored, in which case the surface will be a paraboloid and can be described in cylindrical coordinates (Z, r) by the equation,

$$Z = w^2 r^2 / 2g \qquad 1.9$$

where

$$w = 2\pi n$$

n spin speed in revolutions per second

g gravitational acceleration

The central radius of curvature of this surface is  $g/w^2$ , therefore by increasing the spin speed, shorter radius of curvature will be obtained, decreasing spin rate, produces flatter curves. Hence different posterior lens curvatures can be made by changing the spinning rate. For example if the spin speed is five revolutions per second the radius would be 10 mm.

In practice, spin casting is a combination of the static and spinning cases, whose equation can be given by adding LaPlace's formula Adam (1968) for a meniscus to equation 1.9,

$$z = \frac{w^2 r^2}{2g} + \frac{\sigma}{\rho g} \left( \frac{1}{R_o} + \frac{1}{R_m} \right) \quad 1.10$$

- where  $\sigma$  surface tension  
 $\rho$  density  
 $R_o$  radius of the osculatory sphere at (r, z)  
 $R_m$  " " " meridional " " "

It is important to take into consideration the relationship between the diameter of the stationary vessel, and the central radius of curvature of the meniscus when the mould is at rest. It was found that for the vessel of 8 mm diameter, the radius of curvature of the meniscus is approximately equal to the vessel diameter, whilst for a larger vessel of diameter 13 mm the radius would be 26 mm. Banko (1976)

reported the advantages of spin casting to be:-

1. Accurate reproducibility due to the use of the computer to control spin speed
2. Smooth surfaces especially the concave surface because of the free formed liquid surface
3. Homogeneous and complete cross-linking results from polymerisation in the spinning mould.
4. Ability to produce thin lenses

#### 1.5.2 Lathe Cutting

Hydrogel contact lenses may be fabricated in the same manner as conventional PMMA contact lenses. The method entails a dry (xerogel) button blank being mounted on a steel button with a resin-based wax. The button is then cut to the desired base curve and polished with a wax tool using an oil-based polish to prevent hydration during manufacturing. The same process is repeated to form the front surface. Then the removal of residual polish is achieved by paraffin or xylene. The finished dehydrated lens is hydrated in normal saline (0.9%).

## CHAPTER II

### METHODS OF MEASURING THE RADII OF CURVATURE OF OPTICAL SURFACES

#### 2.1 Introduction

The radius of curvature is the principal factor determining the vertex power of an optical lens, and requires to be calculated precisely.

This chapter is divided into three main sections,

1. Principles of accurate curve measurements
2. Measurements of corneal contact lenses
3. Measurements of soft hydrophilic lenses

The first section described the classical instrumentation for radius measurement:-

The spherometer, which can be classified into main categories; mechanical and optical. The mechanical spherometer is suitable for radii between 1 m and 2 cm, but there are many cases such as eye-piece lens, and microscope lens etc, where the diameter and radii of curvature are so small that a mechanical spherometer cannot be used satisfactorily, in such cases an optical

spherometer is required. The second section will discuss available methods for measuring radii of curvature for corneal contact lenses, where an accurate measurement is important to achieve a satisfactorily fitting relationship. The third section described the existing methods for measuring radii of soft hydrophilic lenses, where particular problems are encountered because of the flexibility and hydrophilicity of this type of lens.

## 2.2 Principles of accurate measurement of curvature

### 2.2.1 Mechanical spherometers

The theoretical concepts of spherometers are simple and the basic principle is to measure the sagittal height of surface over a known diameter. The general formula for the radius of curvature is given by Pythagorean theorem:-

$$R = \frac{d^2}{8h} + \frac{h}{2} \quad 2.1$$

where R radius of curvature of surface  
h sagittal height  
d chord diameter

Martin (1924) described currently available spherometers by Guild, Aldis, Steinheil and Abbe. Twyman (1952) suggested two principal sources of error in three-legged spherometers:-

- (a) The difficulty of determining the effective radius of the circle passing through the points of contact of the three legs
- (b) The exact location of the point of contact between the central screw and the test surface

Hence, Twyman suggested the use of ring instead of the conventional three legs in the construction of a mechanical spherometer. A sharp edge ring spherometer was introduced to increase accuracy but occasionally results in damage to the lens surface, and a serious error may result from the presence of slight burrs on the edges. Cooke (1964) suggested that radii of curvature can be measured accurately by a ring spherometer but there is an averaging effect due to the ring striking only the high spots. He therefore introduced the bar spherometer which in addition to spherical measurement astigmatic surfaces may also be detected on unpolished surfaces. Golod and Nikitin (1964) introduced a superposition spherometer type IZS-8 which was suitable for measuring convex and concave spherical surface radii in the range of 80 - 40000 mm. Bondarev (1965) has modified the use of superposition spherometer to measure radii in the range of 0.1 - 80 mm.

Guild (1918) employed Newton's rings in conventional spherometers (three legs or circular ring) to detect the exact point of contact of the screw with the surface under test.

However, the Guild spherometer was only suitable for measuring transparent objects.

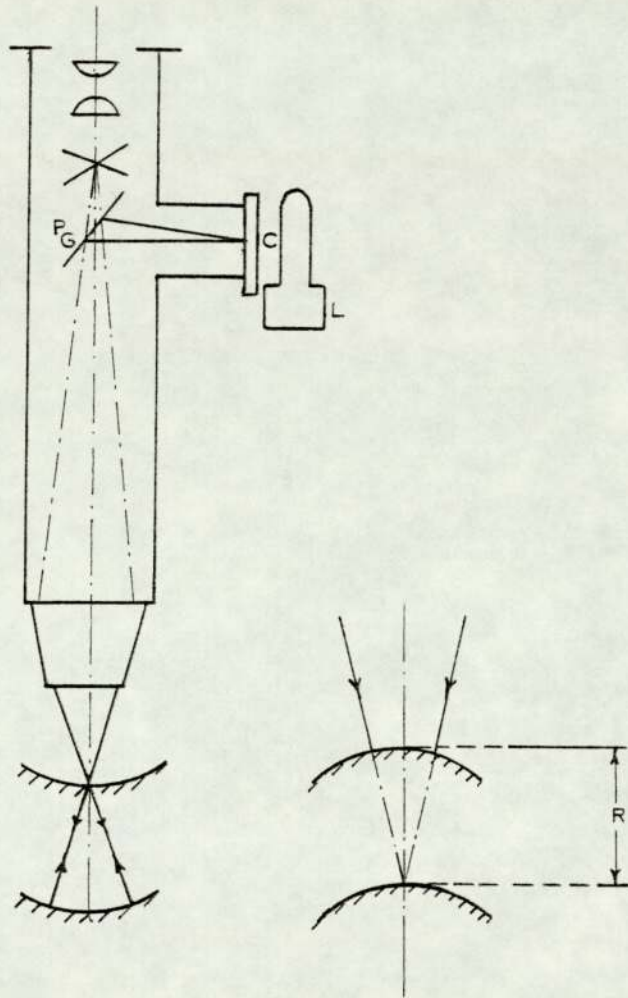
A modified model of the Guild spherometer was constructed by Speyer (1943) to eliminate the errors due to weight of lens since the optical setting could be achieved before mechanical contact.

### 2.2.2 Optical spherometers

Sarma (1970) classified optical spherometers into three types.

#### 2.2.2a Autocollimation method

Drysdale (1900-1901) suggested measuring the radius of curvature of an optical surface by allowing the light to retrace its path in two positions. In one position the incident rays strike the surface under test normally, and are reflected back. In the other position, the image is formed on the vertex of the surface. Hence the distance between these two positions is the radius of curvature of the surface under investigation. Johnson (1960) constructed an instrument which consists essentially of an autocollimating microscope and vertical illuminator (Figure 2.1). The device was used to measure optical surfaces of short radii and small diameter. It was similar to Drysdale's device but the illuminator carried a cross-line. Two precautions



- L illuminator
- C cross-line
- P<sub>G</sub> plane glass reflector
- R radius of curvature

Figure 2.1

Johnson's Instrument

were required when using the instruments; firstly, to avoid the reflection from the back surface of the lens, it was smeared with vaseline, and secondly the microscope objective has as small a depth of focus as the working distance and radius of the surface will allow. De Vany (1966) described an instrument called a universal tester which is like Johnson's but which incorporates a thin membrane of aluminized pellicles which was employed instead of a glass reflector.

#### 2.2.2b Microscope method

Guild (1923) reported a variety of methods for checking "miniature" optics such as microscope objectives. Rank (1946) criticised the autocollimating microscope, using a Gaussian eyepiece, due to the difficulty experienced in looking for one bright field on another bright field at the centre of curvature in the preliminary adjustment. He replaced the Gaussian eyepiece by an Abbe eyepiece which lead to a brilliant spot in a dark field at the centre of curvature, thus improving the adjustment. The short radius of curvature of concave spheres was precisely measured by this method using a 10X objective, and the accuracy achieved was  $\pm 0.025$  mm. Wilson (1956) described the application of a Guild spherometer for accurate measurement of small radii of curvature of the order of 5 mm. In order to obtain high accuracy, he improved the accuracy of determining the object

and image sizes which implied a departure from paraxial conditions. An accuracy of one part in 700 was claimed for the measurements of small radii of about 5 mm.

#### 2.2.2c Interference fringes methods

Guild (1923) employed Newton's rings in his spherometer to determine the exact amount of contact between a test surface and a glass sphere attached to the end of a micrometer screw. Sandhu and Friedmann (1965) described the use of a spherical reference surface instead of a plane one to determine the radius of curvature of an unknown spherical surface.

Kolmiisov and Egudkin (1962) described the use of an interferometer "IZK-57" for precision contactless measurements of ball diameters from 1 to 10 mm by comparing them with a reference ball diameter. The precision of this measurement was found of the order of  $\pm 0.1$  micron.

A method based on the moire technique for the evaluation of radius of curvature of irregual specimens was reported by Kumar (1976). The technique could be utilised for determination of the curvature of human cornea.

Biddles (1969) described an instrument which allowed the testing of deeply curved optical surfaces by interferometry. The prototype of a conventional Fizeau interferometer was

developed and the flat reference plate replaced by convex master surface with radius of curvature equal to that of the concave surface under test. The important feature of this method was that the surfaces were both illuminated and observed at normal incidence, hence fringes seen were fringes of constant separation of the surfaces. To examine a surface with a numerical aperture of more than 0.4, the master surface may be pivoted about a certain point by sliding it along the surface of an iron sphere. The disadvantage of this method was the requirement for a corrector lens to be added onto the other surface of the lens under investigation, when the surface under test was convex. The same instrument could be used as a precision spherometer but knowledge of the radius of the master surface was required.

## 2.3 Measurements of corneal contact lenses

### 2.3.1 Bier contact lens spherometer

In 1958 Bier produced an instrument which utilised the "Drysdale method" which was modified for contact lens measurement. This device can be claimed to measure the corneal radius of contact lenses accurately to  $\pm 0.01$  mm.

### 2.3.2 Radiuscope

A radiuscope based on the "Drysdale principle" is the most commonly used instrument designed to measure the radius of curvature of small spherical surfaces such as contact lenses. The radiuscope consists of a microscope with a dial gauge attached to read the position of the microscope. This instrument is capable of measuring the radii of curvature for negative and positive spherical surfaces. Focusing on the vertex of the surface will enable the observer to detect the flaws on the surface of the contact lens and the second focusing at the centre of curvature will show the irregularities or distortion of the surface. Most of the radiuscopes are calibrated to 0.01 mm. Tannehill and Sampson (1966) have suggested that the radiuscope reading for contact lenses should be taken centrally and also in two meridians. They have also suggested the use of the instrument to study the optical quality of the anterior surface of a contact lens.

Freeman (1965) substituted Drysdale's telescopic system for a microscope with a half-silvered mirror set at  $45^{\circ}$  in the beam above the objective, to measure contact lens radii of curvature. He claimed from the results a standard deviation of  $\pm 0.002$  mm.

2.3.3 Keratometer (associated with a special attachment)

The keratometer was designed to measure the radius of curvature of cornea. Its application was extended to measure the radius of curvature of concave surfaces such as the optical zone of contact lenses. Difficulties were encountered in mounting the contact lens in front of the instrument satisfactorily. Different types of holders with depression were made, and the contact lens attached to the depression by an adhesive substance such as plasticine. The problem with this arrangement was that any slight pressure on the contact lens may cause warping and distortion of the lens surface. Another type of attachment called the Con-Ta-check, made by a contact lens company, Inc. Chicago, consisted of a silver mirror set at  $45^{\circ}$  to the optical axis of the instrument and a holder to mount the lens with its convex side down in the horizontal position. Laycock (1957) suggested introducing a film of water between the holder and the contact lens, as this would allow the lens to stay in position utilising capillary attraction and also to minimize the reflection from the convex surface. Since the keratometer was designed to measure the convex surface of the cornea, errors will be present in the measurements of concave surfaces. Emsley (1963) reported that the average correction factor to be added to the concave radius of curvature measured by Bausch and Lomb keratometer was 0.03 mm. This conclusion was confirmed by Bennett (1966). Brezel (1959) introduced a

modified attachment called a contactometer. It was in principle similar to the "con-ta-check" but has a plastic carrier having two depressions, placed between a standard ball of 42.50 D for verifying the accuracy of the keratometer. The work reported by Bennett (1964) in which he applied Drysdale's principle to the keratometer was not novel and had originally be undertaken by Fincham (1925) and reported by Le Grand (1952). The advantages of using the keratometer for measuring the radii of curvature of contact lenses are: firstly, it is a convenient method because a keratometer is a standard piece of equipment in the practitioner's office, secondly it can be employed to detect the warpage and waves of the central optic zone, on the other hand, the keratometer is not as accurate a method as the instruments based on Drysdale's principle.

#### 2.3.4 Focimeter

Sarver and Kerr (1964) designed a radius of curvature measuring device (R-C device) which consisted of a holder and standard lens with a known front, back central optic radius, thickness and refractive index. A small amount of a fluid having a refractive index similar to the standard lens and the contact lens should be placed between them (Fig 2.2 a,b). The back radius of a standard lens was longer than the front radius for all powers of contact lenses in order to keep the

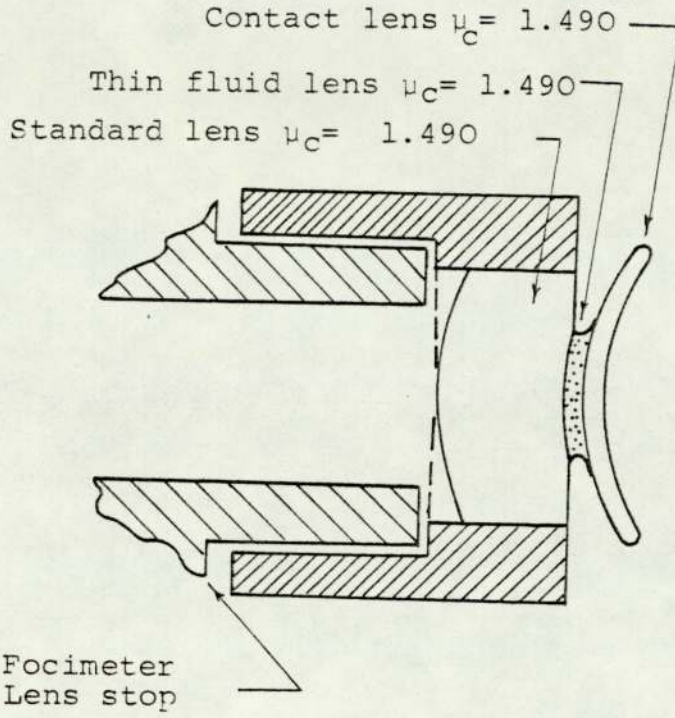


Figure 2.2a R-C device (after Saver and Kerr, 1964)

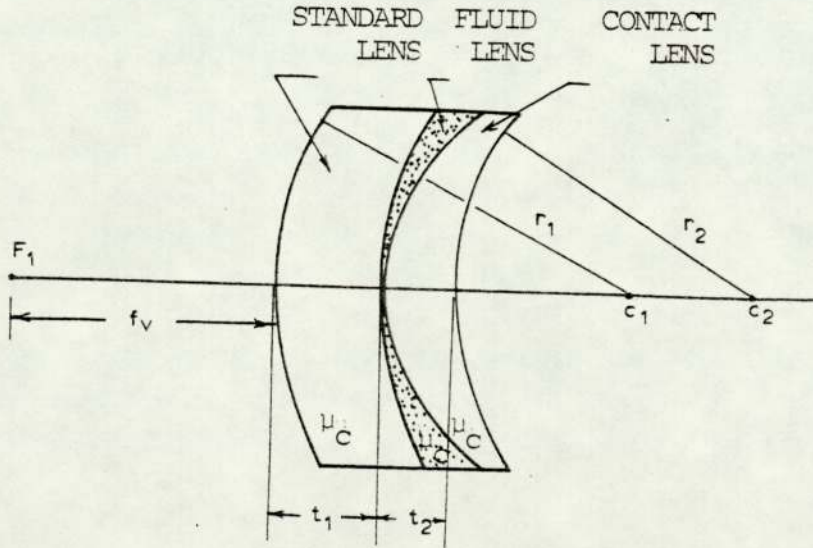


Figure 2.2b Optical components of the R-C device (after Saver and Kerr, 1964)

thickness of fluid lens to minimum. Since the thickness of fluid lens is nearly zero, the lens system can be treated as a thick lens of thickness  $t_1 + t_2$ . When the R-C device was adapted to a focimeter the front vertex power of the lens system could be given and the back central optic radius (B.C.O.R.) may be calculated by the Gaussian equation:-

$$R_2 = \frac{[1 - \frac{\mu}{C}] \left[ 1 + \frac{t_1 + t_2}{\mu} (F_V - F_1) \right]}{F_V - F_1} \quad 2.2$$

where,

- $F_1$  front surface power
- $F_V$  front vertex power
- $t_1$  standard lens thickness
- $t_2$  contact lens thickness
- $\frac{\mu}{C}$  refractive index
- $R_2$  back central optic radius of contact lens

The thickness of a contact lens may be measured by a contact lens thickness gauge. A computer program was compiled to solve equation 2.2. This instrument was reliable in measuring the B.C.O.R. within  $\pm 0.01$  mm, if the focimeter is read to the nearest 0.12D. Dickins (1966) used the R-C device for measuring 50 lenses.

She reported that, if there was insufficient liquid between the contact lens and device it was difficult to obtain the central image on the focimeter. He found in addition that a large quantity of liquid would cause an error in the measurement. The error in front vertex power was calculated for the value of the refractive index of the liquid being more than lens system by 0.001. The conclusion was that there was no significant error in the front vertex power for this small difference of refractive index. Fearn (1970) applied the same principle of using a focimeter to determine the B.C.O.R. but instead of using R-C device, he used lens "A" from his trial set of a known front central optic radius (F.C.O.R.). The procedure was to set the focimeter to the nearest vertical position and place the lens under test with convex side downward on the lens stop and lens "A" set on top of it. The power of the combined lens system was measured. Then a drop of fluid of known refractive index was introduced between the two lenses and another reading was taken, the difference giving the measured power of fluid lens. The B.C.O.R. of the fluid lens was equal to F.C.O.R. of lens "A" and because the thickness of fluid lens is approaching zero, the F.C.O.R. of fluid lens can be calculated, which is equal to the B.C.O.R. of lens under investigation. It was found that when the power of the fluid lens exceeded about  $\pm 1.75D$  the results were unreliable. Fearn pointed out that the advantage of this

principle over the radiuscope was that the scale of lensometer was firmly fixed to the slider carrying the moving lens, and hence was quite free from the "backlash" error. The accuracy achieved was in most cases in the order of  $\pm 0.01$  mm.

### 2.3.5 Toposcope

The toposcope was introduced as an instrument for measuring radii and diameters for spherical and aspherical corneal contact lenses by means of moire fringes. The toposcope is a microscope of variable low power magnification (4 to 20X). The target was a grid consisting of a series of straight parallel lines localised at the focal plane of the objective. The eyepiece of the microscope contains a second grid with similar lines at a slight angle to the target grid. The contact lens under test is placed in the field of view of the microscope with the surface of interest uppermost and bottom surface submerged in fluid. Hence, when the target grid was observed, reflected from the surface of contact lens, at a certain magnification straight parallel dark fringes (moire fringes) parallel to the horizontal index in the eyepiece will appear from edge to edge of the field of view. The radius was then read from the attached dial which had 0.01 mm divisions. The shape and orientation of fringes were a direct function of the relationship between the two sets of lines. Blackstone (1966) investigated the

toposcope and reported that precise measurements could be made for all areas of a contact lens. (Figure 2.3 a, b), shows the moire fringes in correct position for the measurement of central and peripheral curves of the spherical surfaces of a corneal contact lens. Also (Fig 2.4) illustrates the appearance derived from an aspheric surface. The advantages of this instrument may be summarised as:-

1. The edge to edge illumination in the contact lens gives measurements of the radii of curvature for central and peripheral curves for spherical surfaces
2. Rapid checking of the sphericity of the curves is possible
3. It is possible to investigate the condition of the surfaces and measure the amount of asphericity
4. Distorted areas can be located by the instrument
5. It is the only available device which can measure the radii of the haptic portion of a scleral lens

Ludlam and Kaye (1966) suggested further advantages to the toposcope:-

1. The radii of both negative and positive surfaces of contact lens can be measured
2. The instrument can be designed with the degree of accuracy required

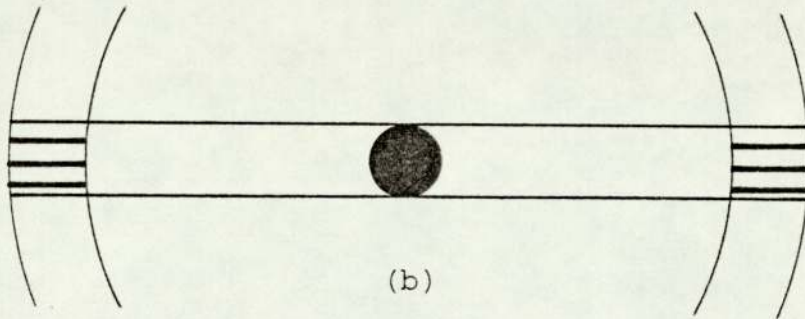
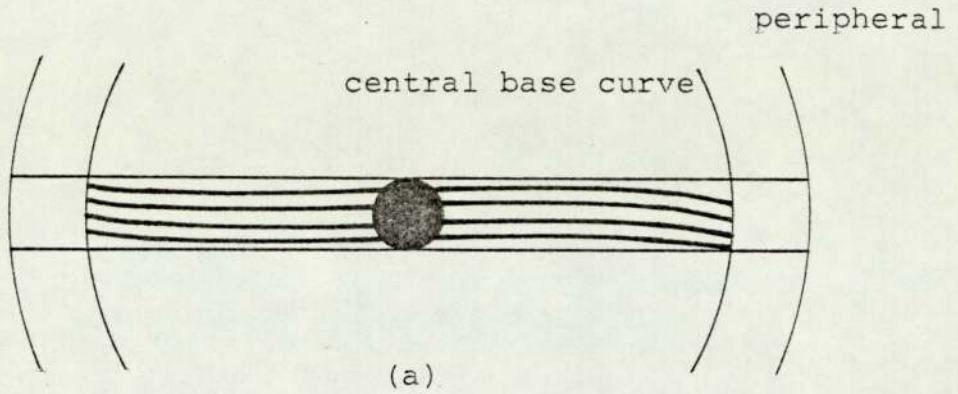


Figure 2.3 Moire fringes in focus,  
(a) central base curve  
(b) peripheral curve

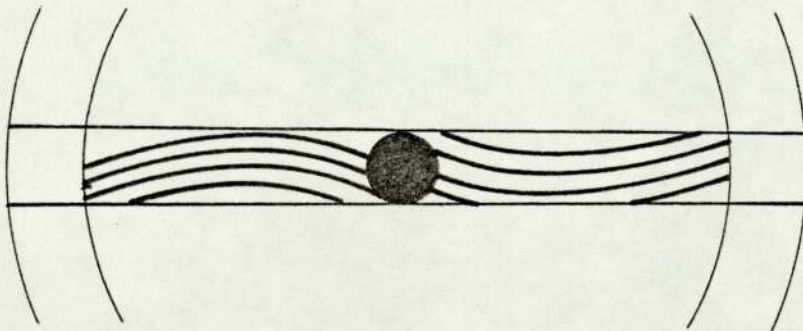


Figure 2.4 Moire fringes shows aspheric surface

3. Measurements so made were not subject to errors in focus, observer acuity or subjective differences between observers.

Storey (1969) examined the toposcope and concluded that the instrument has a poor accuracy particularly for peripheral radii.

#### 2.3.6 Newton's rings

Dickins and Fletcher (1964) compared seven different instruments for measuring B.C.O.R. of a set of test plates with concave surfaces and of radii covering the usual range of corneal contact lenses. The methods were ranked according to maximum absolute error which range from -0.01 mm to +0.04 mm. Newton's method was ranked fourth and it was suggested that Newton's method was not applicable to the measurement of thin contact lenses.

## 2.4 Measurement of soft hydrophilic lenses (hydrogel lenses)

Most current methods for measuring conventional hard contact lenses are not practical for measuring hydrogel lenses. The difficulty of measurements arises from the flexibility and hydrophilicity of hydrogel lenses, causing deformation and distortion across their surfaces and thus influencing the form of the lens. The methods of measuring the radii of curvature of hydrogel lenses are given as follows.

### 2.4.1 Hemispherical convex template: "Plastic radius gauge"

Brailsford (1972) measured the back radius of curvature of a series of hydrogel lenses by placing the lens on a number of spheres to check which sphere matches the lens. Harris et al (1973) used a series of five hemispherical convex templates with curvatures varying from 8.0 mm to 9.2 mm in 0.3 mm steps; having previously determined that it was impossible to distinguish differences in base curve of less than 0.3 mm. The templates were wetted with a drop of saline and the gel lens placed on top. If a bubble appeared between the template and lens, the radius of the lens is too steep, whilst a flat radius showed lens edge stand off. When the lens showed a proper fit, the base curve of the lens was the same as the curvature of the template. Measuring the base curve of a hydrogel lens in air may present problems due to surface deformation and shrinkage of material on dehydration. Hampson (1973) attributes inaccuracies of template method to

distortion of the lens during handling, and capillary attraction and stretching between the master sphere (template) and the hydrogel surface.

#### 2.4.2 Radiuscope

Brucker et al (1972) reported an attempt was made to read B.C.O.R. of a hydrogel lens with a radiuscope, the uneven surface of the water on the lens distorted the image. If the lens was partially dried, then there was a rapid reduction in the radius of curvature caused by evaporation. Koetting (1973) also reported attempts to measure the B.C.O.R. in air by means of radiuscope. The results were far from satisfactory for similar reasons to those reported by Brucker.

In order to overcome problems arising from the measurement of hydrogel lenses in air, a second trial was undertaken by placing the lens in a saline cell under the radiuscope. The lens was immersed in saline with the concave side uppermost, and potential lens movement was overcome by using a tapered cell with a concave resting surface as the base. This arrangement led to slight distortion of the lens but at least held it steady enough to bring the radiuscope into focus. A non-reflecting black background was used to increase the illumination. However, the technique was unsatisfactory due to the small difference between the refractive index of gel lens material and saline which was

insufficient to produce a usable surface reflection (the reflectance is 0.12 per cent for lens material of refractive index 1.43). Chamarro (1974) suggested using the radiuscope with an immersed objective but a similar problem of low reflectance was encountered. Nakajima et al (1974) used a radiuscope with extremely bright illumination. However, they were dissatisfied with the results, although the reasons for dissatisfaction were not stated. Steel (1977) utilised crossed polaroids in a radiuscope in an attempt to get a clear image from the surface of a hydrogel lens. The instrument was modified with a sheet of polaroid inserted in front of the target graticule and a second polaroid, set at ninety degrees to the first, set in the eyepiece. In addition, a retarder (a quarter-wave plate for the mean wavelength of the light used) was placed in front of the microscope objective with its axis at  $45^{\circ}$  to the direction of polarisation (Fig 2.5). A second retarder was also introduced between the hydrogel lens and surface of saline to avoid reflections from the saline surface. As a result the original state of polarisation was changed and some reflected light was passed through the second polariser to the eye giving a clear visible reflected image of the surface of hydrogel lens.

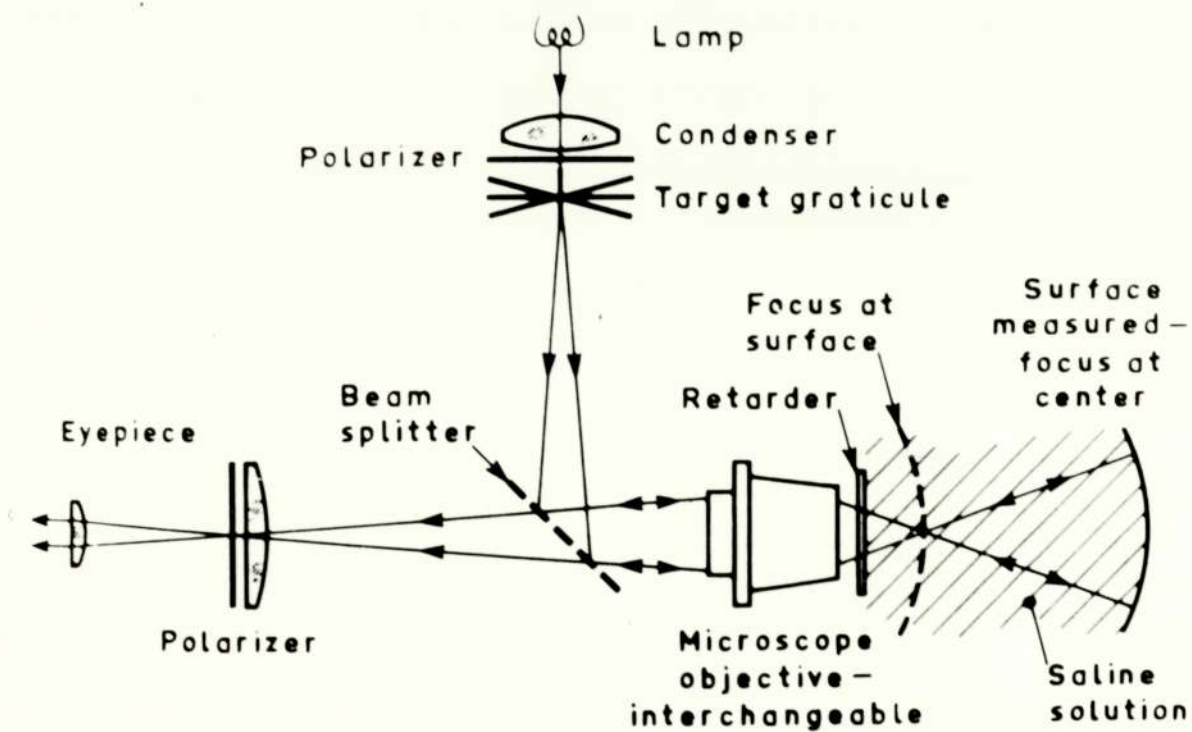


Figure 2.5 Optical diagram of autostigmatic microscope with two polarizers and retarder added (after steel & Noack)

### 2.4.3 Keratometry

Chaston (1973) designed an attachment to a keratometer for hydrogel lens measurements. The device consisted of a lens cell and a front surface silvered mirror. The lens cell was filled with saline, and hydrogel lens placed in the cell (Fig 2.6). The radius of curvature of hydrogel lenses was obtained by multiplying the measured value by the refractive index of the saline. The difficulties encountered with this system were reported by Holden (1975) to be:

1. The hydrogel lens always tends to adhere to the bottom of the container
2. Lenses having thin edges may "spread" producing a flatter estimate of radius of curvature
3. Care has to be taken to avoid entrapment of an air bubble.

In addition, Chaston also reported a further difficulty with this method when used with a Bausch and Lomb keratometer. The shortest measurable radius of curvature was found to be 8.70 mm and an auxilliary lens of +1.50D was required to be mounted in front of the observation telescope of the keratometer.

Forst (1974) has reported a slight variation of the 'Chaston' method using a deflecting prism instead of silvered mirror and measuring the hydrogel lens radii in a number of

meridians to obtain an average value. Holden (1975) modified Chaston's apparatus by redesigning the wet cell (Fig. 2.7). The lens was retained by a central annular ring 6-7 mm diameter with concave side uppermost. Various modifications were also made on the keratometers to improve the visibility of their mires, a 25W globe was used in a Bausch and Lomb keratometer and a replacement of the filters and globes was made in a Javal-Schiolz type. The use of a wet cell required individual calibration depending upon the keratometer employed.

#### 2.4.4 Profile projection technique

Sohngees (1974) employed a system comprising a 35 mm projector incorporating a cooling system and a high luminosity 24 volt/250 watt halogen lamp to project an intense beam onto a specially designed screen which was engraved with horizontal and vertical linear millimetre scales and a series of annular graduation from 7.2 mm to 9.50 mm radius. The lens cell was filled with normal saline, and a hydrogel lens centred convex side upward the cell was mounted into the adapted slide carrier of the projector. The lens profile was projected onto the graticules which were then adjusted vertically until alignment was achieved and the radius read from the scale. This instrument was calibrated by means of an 8.00 mm concave test plate.

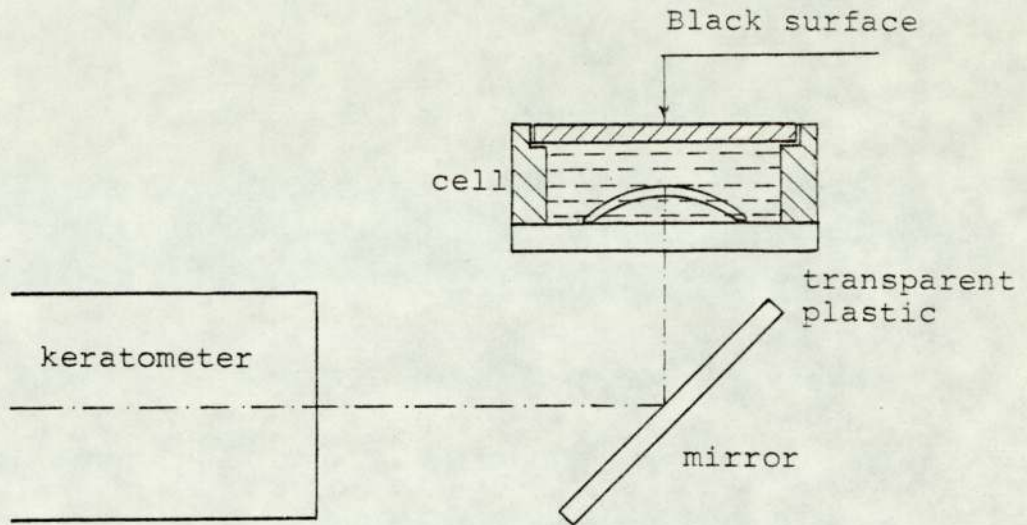


Figure 2.6 Principles of Chaston idea for measuring radius of curvature of hydrogel lenses

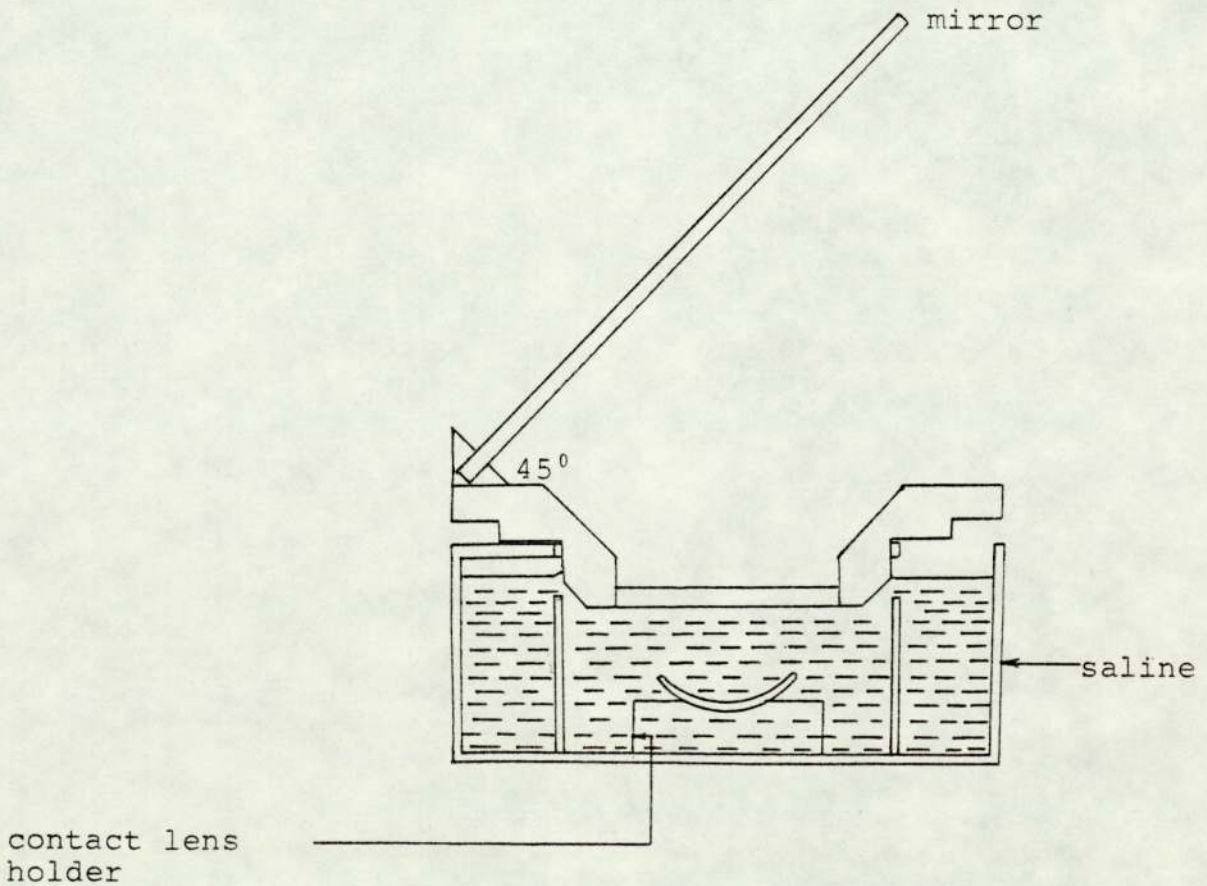


Figure 2.7 Design of wet cell (after Holden, 1975)

Loran (1974) fixed Sohnges projector on a rotating turntable to overcome the problems arising from a poorly centred lens, and claimed a reliability of  $\pm 0.1$  mm for this type of instrument. Koetting (1975) used Sohnges projector to study spun cast and lathe cut lenses. He found that the front surface could be read quite reliably, but in spite of the possibility of bringing the back surface into focus, the accuracy was in doubt. Similar work was undertaken by Padula et al (1974) using a conventional slide projector and a diffusing plate.

#### 2.4.5 Sagittal height: "Sagometer principle"

Brailsford (1972) demonstrated the use of a depth micrometer to measure sagittal height of a hydrogel lens in air. The rod of a micrometer was adjusted until it touched the inside surface of a hydrogel lens which gave the sagittal height "h", the cord diameter "d" was read from the base vernier. Hence, the radius of curvature of the base curve could be calculated from equation 2.1. NaKajima et al (1974) introduced an apparatus called a Basecope. This instrument was a modification of Abbe's spherometer. The base curve of a hydrogel lens was calculated from the measured sagittal depth of the hydrated lens in a special cuvette, filled with saline solution. With proper handling the instrument had a claimed accuracy of 0.05 mm. Another mechanical wet sagittal measuring device was the wet cell radius gauge made

by Goldberg (1975) and manufactured by Contact Lens Manufacturing Ltd (1976). The instrument consists of a monocular microscope and a detachable chamber filled with 0.9% saline which contained a cylindrical pointed probe. The probe may be raised or lowered by rotating a knob which was calibrated in radius of curvature (mm) until it touched the surface of the hydrogel lens. The position at which the probe touched the lens was observed with a microscope. This device used a concave mirror to reflect light from an external source for illumination. It was reported that this system had a tolerance of  $\pm 0.1$  mm. All methods described for sagitta measurement in air or even in saline, suffer from mechanical disturbance to the lens surface. In attempt to overcome this difficulty, Garner (1976) used a modified radiuscope to measure the sagittal height optically, to calculate the radius of curvature of the base curve of hydrogel lenses. Port (1976) also utilised ultrasound in measuring hydrogel lenses. It was known that ultrasound reflects when there is a change in refractive index. (Fig 2.8) shows three reflections represented by peaks which may be visualised on an oscilloscope screen. Using a time maker trace and a knowledge of the velocity of sound in saline, distances on the screen could be converted to millimetres. Hence, sagittal height and centre thickness may be measured. Another attempt to measure hydrogel lenses without disturbing their surface was undertaken by Kawabe and

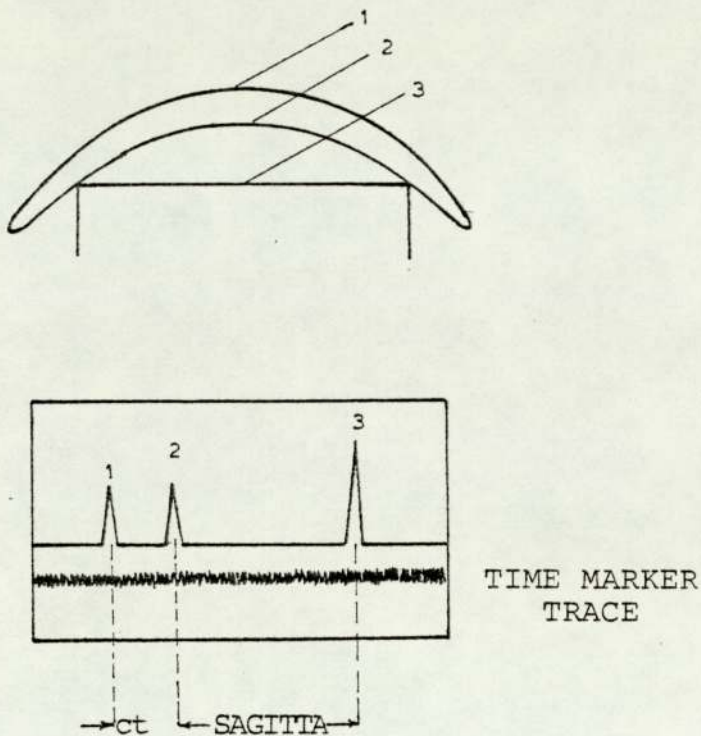


Figure 2.8 The three peaks: 1, from the front surface of the hydrogel lens: 2, from the back surface of the hydrogel lens: 3, from the support pillar (After Port, 1976)

Hamano (1977). The gel lens was placed in a cell containing 0.9% saline and mounted horizontally on a Nikon projection microscope. The image of the lens was obtained on the projector screen utilising a  $45^{\circ}$  prism. By adjusting the position of the lens relative to the orthogonal cross marks of the projection microscope, the optic diameter of the lens could be determined by the horizontal reading and sagittal height by a vertical reading. From these two measurements, the front and back radii of curvature could be calculated

from equation 2.1. Hamano and Kawabe (1978) measured the sagittal height of a hydrogel lens in air using an electro-conductive needle bar connected to a motor drive. When the needle bar comes into contact with the inner surface of hydrogel lens a current passes through the circuit.

The main difficulty with all methods of sagittal measurement is that the technique is only applicable to the spherical surfaces. It is not effective for the Bausch and Lomb Soflens which has an aspheric ocular surface or for any hydrogel lens made from an anisotropic gel material.

#### 2.4.6 Other methods (Laser, toolmaker microscope and moire fringes)

The lens radius device (LRD) was introduced by Sagan (1973).

A helium-neon laser (10 MW) was used as a source of illumination. The laser beam was directed by a beam splitter, so the reflected beam from back surface of hydrogel lens was focused on a viewing screen through a collimating lens. This focusing mechanism was linked to a dial which was calibrated to read the radius in millimetres. Sagan found that LRD was unreliable and totally unsatisfactory if a true and accurate measurement was required. He suggested that a refined focusing mechanism and imaging system would be needed to improve the results.

Bissell (1974) built an instrument from a combination of a toolmaker's microscope, and an auto-collimating eyepiece with a graticule similar to 'Adam Hilgers Angle Dekkor'. The hydrogel lens was measured in saline and the mathematics involved is similar to the Chaston method which has been previously described. Gilman (1976) was the first to suggest the use of interferometry for measuring hydrogel lenses (moire fringes). This method was employed to measure B.C.O.R. and its variation across the lens surface for the Bausch and Lomb lenses. The instrument was a standard Nikon binocular zoom microscope modified to measure the back surface of hydrogel lenses by moire fringes. The principle of operation was similar to that of the toposcope produced by Optical Methods Inc. The disadvantage of this method was that the measurement was done in air and the author reported a significant change in curvature, first flattening, then steeping across the lens as it dried out during measurements.

## CHAPTER 3

### Measurements of central optic radii and thickness of hydrogel lenses (SOFLENS<sup>R</sup>) by interferometry

#### 3.1 Introduction

The purpose of this study was to find an accurate method for measuring the F.C.O.R., B.C.O.R. and the thickness of hydrogel contact lenses, since the precision in contact lens manufacture depends to a great extent on the ability of the available methods to check the accuracy of the finished lenses.

As seen in chapter two, there is a lack of precision in existing hydrogel lens measurements. Interferometry arose as a preferred solution, since it has been used to study the topography of lenses for more than one hundred years, and it has been increasingly employed since the 1950's for the accurate measurement of geometrical form and micro-structure of surfaces in terms of the wavelength of light.

The principal problem with the use of this method was the production of an interference pattern when the difference in refractive index between the hydrogel lenses and surrounding medium was about 0.09. In addition, the short

radii of curvature of hydrogel lenses created difficulties.

### 3.2 Preliminary experiment

The first experiment was carried out to determine the feasibility of obtaining interference fringes (Newton's rings) from the hydrogel lens submerged in saline solution (0.9%).

The instrument used was the Universal Camera Microscope  $M_e F_2$  (c. Reichert Co. Austria) and the hydrogel lens was mounted in a cell with a base of very thin glass plate, filled with saline solution. The microscope was an inverted reflection type and had the advantage of high contrast between dark and bright fringes; also there was no difficulty in mounting the cell-lens system on the instrument. The microscope was illuminated with monochromatic light of wavelength  $5890\text{\AA}$  and the magnification and numerical aperture of the microscope objective was 16/0.25.

The interference pattern (Fig. 3.1) was seen as being the result of interference between the front surface of the hydrogel lens and the plane parallel plate. It was clear from the pattern that there were some fringes missing at the centre due to the flattening of the lens at this point. This trial showed that it was possible to

obtain an interference pattern with a small difference of refractive index in the lens-cell system.

A modified cell was designed to prevent the flattening of the hydrogel lens at the centre and several different approaches were tried in an attempt to illuminate the microscope with a mercury vapour lamp in conjunction with suitable filters; also a He-Ne laser was used, but it was not possible to generate an interference pattern from the back surface of the hydrogel lens. This attempt was abandoned for two reasons:- firstly, because the Newton's rings approach is really only acceptable for shallow surfaces and not for highly curved ones like hydrogel lenses; secondly, because of the failure to obtain interference fringes from the back surface of the lens.

In order to generate interference fringes from both surfaces, an interference microscope called Linnik micro-interferometer was used. This interferometer is based on the Michelson interferometer principle, the reference surface being fixed in the instrument.

### 3.3 Interference Microscopy

#### 3.3.1 Definition and classification

The interference microscope is a combination of two functions, interferometry and microscopy, into a single instrument.

As reported by Krug et al (1960) the term "Interference microscope" was first used by Sirks (1893); he termed it "Interferentiemicroscope".

A precise definition of an interference microscope was given by Krug et al (1960): "The interference microscope is a microscope in which part of the beam is split into two or more coherent beams with variable relations of phase and direction. These partial beams may be directed in three different ways:-

- (1) Only some of them come into contact with the object
- (2) All come into contact with the object, but the object or its image is placed differently with respect to each beam
- (3) All come into contact with the object, but with most of them the diffraction image is not essentially altered.

In an interference microscope the partial beams interfere with each other behind the object. The interference thus produced can be observed either in the object image, or in a spectroscope, or in the rear focal plane of the objective. It is possible to observe the shape of the wave-fronts directly influenced by the object; from this observation conclusions may be drawn about the thickness, refractive index and surface form of the object

and about the phase shift of the light on reflection; or about the product of the first two or the last two quantities. The structures to be studied must be sufficiently small to justify microscopic study; they should, however, lie sufficiently above the resolution limit of the microscope used, so that the values found can be satisfactorily related to the corresponding object structures".

There are about a hundred different interference microscopes described in the literature and with the extension of the ranges of application, it was necessary to classify them carefully according to their characteristic features in the following manner:-

- (1) Multiple beam or double beam interference microscopes
- (2) Microscopes intended for transmitted or incident light work
- (3) Microscopes where the reference wave front influenced or uninfluenced by object.
- (4) Types where the beam could be divided by different types of beam splitters, for example semi-transparent layers, double refraction, diffraction or stops (diaphragms) .

### 3.3.2 The Linnik Interference microscope

Linnik (1933) was the first person to describe the use of microscope objectives in each arm of the Michelson interferometer. This interferometer is a double-beam system for reflecting surfaces with incident illumination. Its principle is to present to the eye of the observer two superimposed fields of view. The first is the reference field which contains the image of the light source after reflection from the reference surface. The second is the image field containing a similar image which has been deformed after reflection at the object. These two fields are coherent with each other point-for-point, but light at any point in either field is as far as possible incoherent with light from any neighbouring point. Interference takes place between the two fields, yielding a pattern of fringes; the object stands revealed by its effect on this pattern as a consequence of the path differences it introduces (Dyson 1970). Hence the difficulty of bringing a reference surface sufficiently close to the surface under examination (as in the case of the Fizeau system) was resolved in the Linnik instrument.

The original Linnik interferometer was not free from some disadvantages, principally aberrational defects which affected performance. However, these were eliminated in the modified form of the instrument made by Kinder (1937).

The interference microscope as improved by Kinder was used by Rantsch (1944-1945) who suggested two modifications. Firstly, replacing the plate beam splitter with a cubic shape, and secondly by moving the objective in the reference ray-path parallel to the optical axis; hence, interference bands could be obtained without tilting the reference and object surfaces. This improvement could be obtained by inserting two plane parallel plates of equal thickness and equal tilt; one in the reference beam path, and the other in the object beam path.

The first commercial incident light interference microscope was manufactured by Carl Zeiss, Jena (1943), incorporating Linnik's principle and the improvements of Kinder and Rantsch.

A Russian version of Linnik's interferometer (The MII4) was also developed, in which the rays were parallel in the dividing cube, and the interference bands were adjusted by moving the objective (Sacharewski 1952, Egorow 1955). Carl Zeiss Oberkochen (1955) produced a double beam interference microscope for reflecting surfaces with incident illumination, the illuminating beam being divided by a cubic type of semitransparent layer and the reference wave front being uninfluenced by the specimen under investigation.

The reasons for choosing the Linnik micro-interferometer for studying the hydrogel lenses can be summarised as follows:-

- (1) The two-beam interferometry method may be used for highly curved surfaces, i.e. high wedge angles greater than  $5^{\circ}$ , since the multiple beam method by Tolansky (1948) was applicable only at low wedge angles (Mykura 1954).
- (2) There was no contact with the object under examination.
- (3) It was the only available interference microscope with changable reference mirrors of different reflectivity, this feature being useful for studying low reflecting surfaces (the reflection factor was 0.12 for the lens-saline system).
- (4) The compact design of the instrument gives extreme stability which was important where one was examining hydrogel lenses immersed in saline.
- (5) Because it was an inverted type there was enough space for the lens-cell system to be mounted on the microscope stage.

### 3.3.3 Description of the instrument

#### 3.3.3a General Construction

The instrument used was designed originally to check the quality of precision finish surfaces (flat, spherical, cylindrical) and to determine, for instance, the number and depth of scratches and machining traces. The instrument magnifies the test surface between 80X and 480X and reveals the surface structure by contour-line representation. The wavelengths of light used as the measuring standard remain unchanged so that the instrument always measures correctly, without ever needing calibration. The technical details are given in table 3.1.

The specimen to be investigated can be placed on a mechanical stage, so that the surface to be examined can be located above the opening of the stage insert. Then this mechanical stage can be tilted and shifted in two directions  $\pm 5$  mm in one direction and  $\pm 10$  mm in the other. The stage inserts are interchangeable and may be selected to suit the shape of the testpiece. The Thallium spectrum lamps ( $\lambda = 5350\text{Å}^0$ ) and 6V 5W filament lamp at the rear of the instrument are connected to the mains by means of a power supply unit. The magnification can be varied by revolving the objective mount on the right hand side of the instrument. The reference mirrors which are slipped onto the objectives in the revolving objective mount can be exchanged and adapted to suit the

Table 3.1      Technical Details (after Carl Zeiss Oberkochen)

Total magnification with 8X eyepiece/ field of view diameters on object side/ numerical aperture (N.A.)	80X/1.85mm/0.16 200X/0.72mm/0.32 480X/0.28mm/0.64
Reticule in eyepiece	graduated linearly 10mm in 100 intervals
Motion range of mechanical stage	one coordinate $\pm 5$ mm
Stage insert	two        " $\pm 10$ mm two        " $\pm 2.5$ mm height adjustment 5mm
Light source	Thallium spectrum lamp (Monochromatic light $\lambda/2 = 0.27\mu$ ) 6V 5W filament lamp (white light) in centering base
Refractive power of comparison mirrors	90%, 60% and 30%
Dimensions	Length                    270mm Width                     180mm Height                    190mm Weight with camera approx.        13.5 Kg

reflectivity of the testpiece. In this way, two objectives always lie opposite each other, one serving for imaging the sample, the other being terminated by the comparison mirror. Below the revolving objective mount is a mark which indicates the height position of the revolving objective mount. With the image selector various beams can be selectively stopped out to allow the observation of a testpiece or the comparison mirror or the interference bands separately.

Either a 35 mm camera attachment or a  $3\frac{1}{4}$  x  $4\frac{1}{4}$  polaroid attachment can be fitted below the inclined tube. The fine focusing knob and the beam path selector are on the front left hand side of the instrument.

### 3.3.3b Inner Construction

The path of the rays of the interference microscope is shown in perspective in (Figure 3.2). The path of rays passes either from the thallium lamp Th, across the lens  $L_1$  or from the incandescent lamp W, across the Lens  $L_2$  to the mirror  $S_1$ . From there the light arrives at prism  $P_1$  across the lens  $L_3$ , the aperture diaphragm  $B_1$ , the field of view diaphragm  $B_2$ , and the lens  $L_4$ , passing at the rear of prism  $P_2$ . In prism  $P_1$  a semipermeable reflecting layer is located, which splits the beam into two parts. One

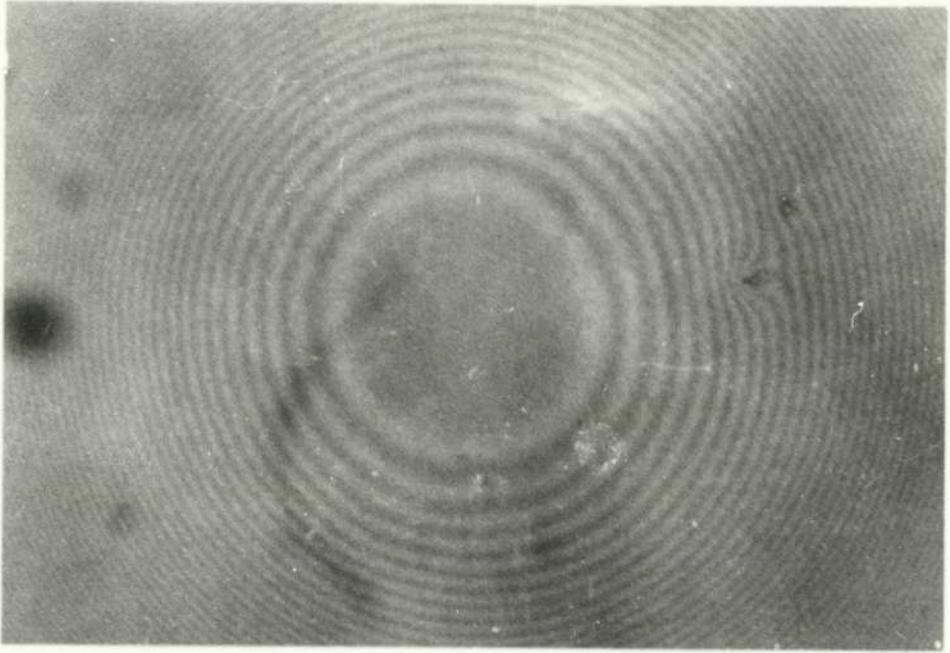


Figure 3.1 The first attempt to obtain interference fringes from a hydrogel lens immersed in saline solution

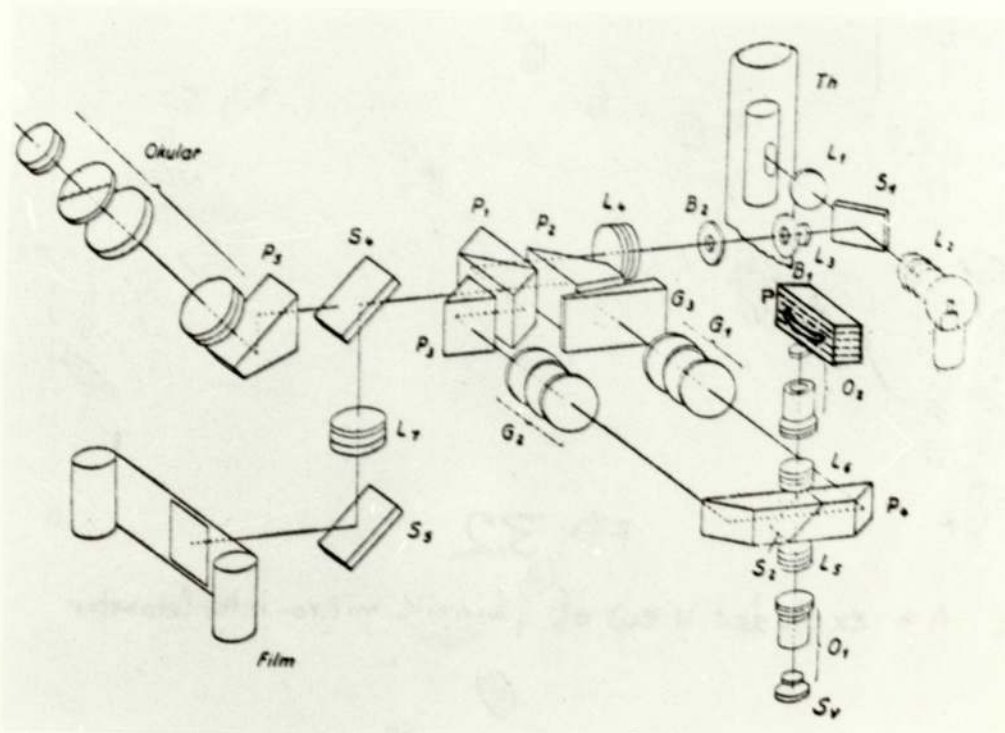


Figure 3.2 An exploded view of Linnik micro-interferometer



part passes across the deflecting prism  $P_2$ , the wedge plate  $G_3$ , and the set of plane plates  $G_1$  to the reflecting prism  $P_4$ ; it is deflected downwards by the mirror  $S_2$  and arrives across the lens  $L_5$  and the objective  $O_1$  at the comparison mirror  $S_V$ . Here the beam is reflected and takes the same way back to prism  $P_1$ . The other beam arrives from prism  $P_1$ , passes across prism  $P_3$ , plate set  $G_2$ , prism  $P_4$  at mirror  $S_2$ , is deflected upwards and passes through lens  $L_6$ , objective  $O_2$  to the test object  $P$ . From there it is reflected back on itself. With visual observation, both beams unite in prism  $P_1$  and arrive across prism  $P_5$  into the ocular. For photography the beam from mirror  $S_4$  is deflected and arrives across lens  $L_7$  and mirror  $S_5$  at the plane of the photographic film. Mirrors  $S_1$  and  $S_4$  are rotatable, as are the sets of plane plates  $G_1$  and  $G_2$ ; the size of the aperture diaphragm  $B_1$  is variable, and the objectives  $O_1$  and  $O_2$  are interchangeable simply by turning the revolving objective mount (Anon 1955).

### 3.3.3c Cell-lens design

In this method, it was desired to obtain an accurate measurement of lens curvature. One possible way of achieving this is to design a special cell as shown in (Fig. 3.3 ). The hydrogel lens has to be suspended in such a way that there is no pressure exerted on it, otherwise distortion of the surfaces may occur. Ideally the lens should float against an annular stop. Also it must be kept in normal saline solution to retain its correct shape.

Consequently, the cell was made of perspex, and consisted of two main parts. The first part was a column 'A' which carried the hydrogel lens, being designed to have a special cap 'B' at its end, with an annular hole of 7 mm diameter, the curvature of the inside surface being 8 mm. This column could be adjusted by means of a fine screw. In addition, it was designed to swing in an arc to permit measurement of the surface of the hydrogel lens at different positions. The movement was indicated by a pointer on a scale. The second part 'C' was a container to carry column 'A' and was filled with saline solution (0.9%). Since the test beam of the interferometer emerges vertically, the bottom of the container was made from a thin optically flat glass plate about 0.14 mm thick. A small electric heater and thermistor was fitted very close to the lens to keep the temperature constant at 21°C.

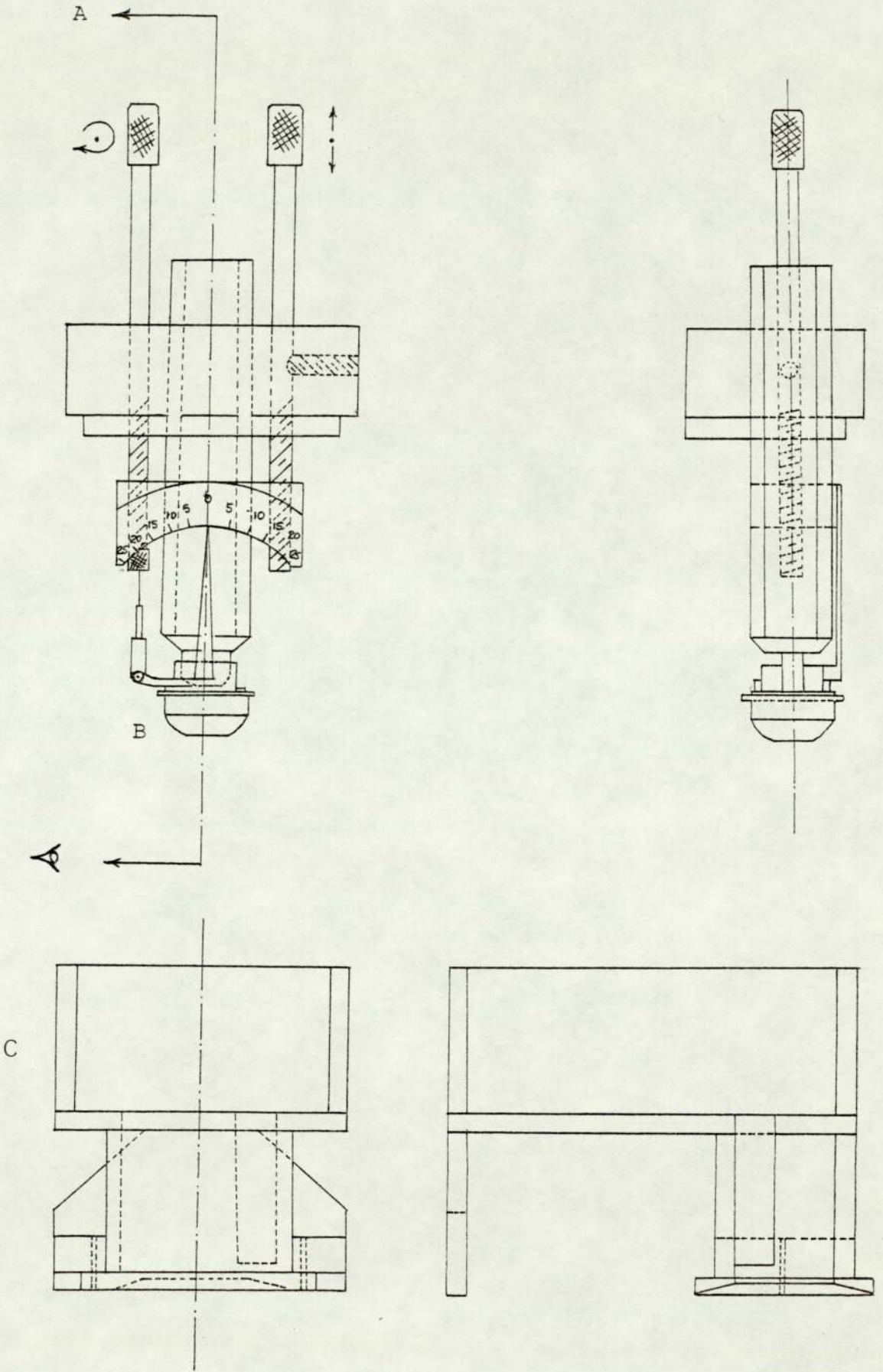


FIGURE 3.3

Line drawing of the cell-lens system in cross-section (scale 1:1)

### 3.4 Experimental procedure

#### 3.4.1 Calibration

The instrument was calibrated using ball bearings whose radii had been previously measured at the National Physical Laboratory, Teddington (U.K.). After connecting the mains and switching on the monochromatic light, the surface to be examined should lie perpendicular to the beam. For this purpose, the mechanical stage was set in its basic position. To study the spherical surface the instrument must be prepared by putting the band interval and the direction knob to its highest position. The summit of the sample was brought over the objective through displacement of the mechanical stage. The interference bands for the spherical surface appear circular in shape. The most suitable objective for this range of radii of curvature was found to be X25, a comparison mirror of the highest reflectivity 90% being used, since the ball bearings had high reflecting surfaces.

Fringe measurement was carried out by initially measuring a micrometer stage graticule with the aid of the microdensitometer print out from known graticule dimensions (Fig. 3.4).

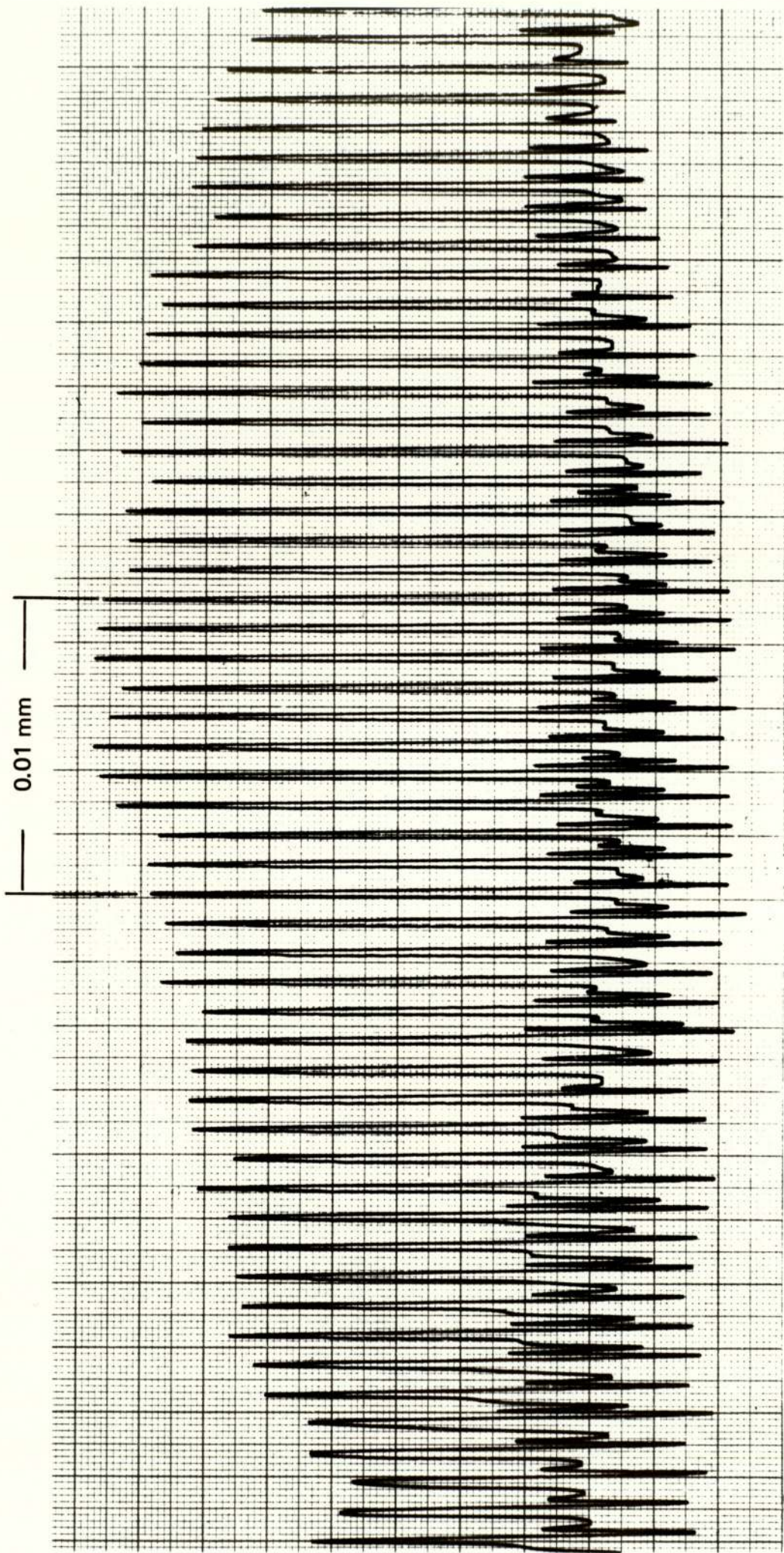


Figure 3.4 Microdensitometer print out of micrometer stage

### 3.4.2 Measurement of central optic radii of hydrogel lenses

The lens under investigation was mounted carefully in cap 'B' of column 'A' of the lens-cell system, the later being fixed at the top of the mechanical stage of the micro-interferometer (Fig. 3.5). Since the optical properties and performance of hydrogel lenses are subject to considerable variations, the change in temperature of the surrounding medium (saline) will change the percentage of the water content for the hydrogel material. This variation in the amount of water content will affect the lens dimensions and refractive index (Ng, 1974 and Mizutani 1974). Consequently, the temperature should be kept constant at 21°C during the experiment. The revolving objective mount was set on X25, experience showing this to be the optimum magnification.

The percentage of light reflected from a hydrogel lens is dependent upon the refractive indices of the two media involved, and is governed by the expression

$k = (\mu_2 - \mu_1)^2 / (\mu_2 + \mu_1)^2$  where 'k' is the reflection factor and  $\mu_1$ ,  $\mu_2$  are the two refractive indices. The

reflection factor can be as small as 0.12% assuming

$\mu_1 = 1.336$  (0.9% saline) and  $\mu_2 = 1.43$  (Poly HEMA).

So a comparison mirror with the lowest reflective power available (30% reflectivity) was set on the objective lying opposite the sample. The mechanical stage was then slowly

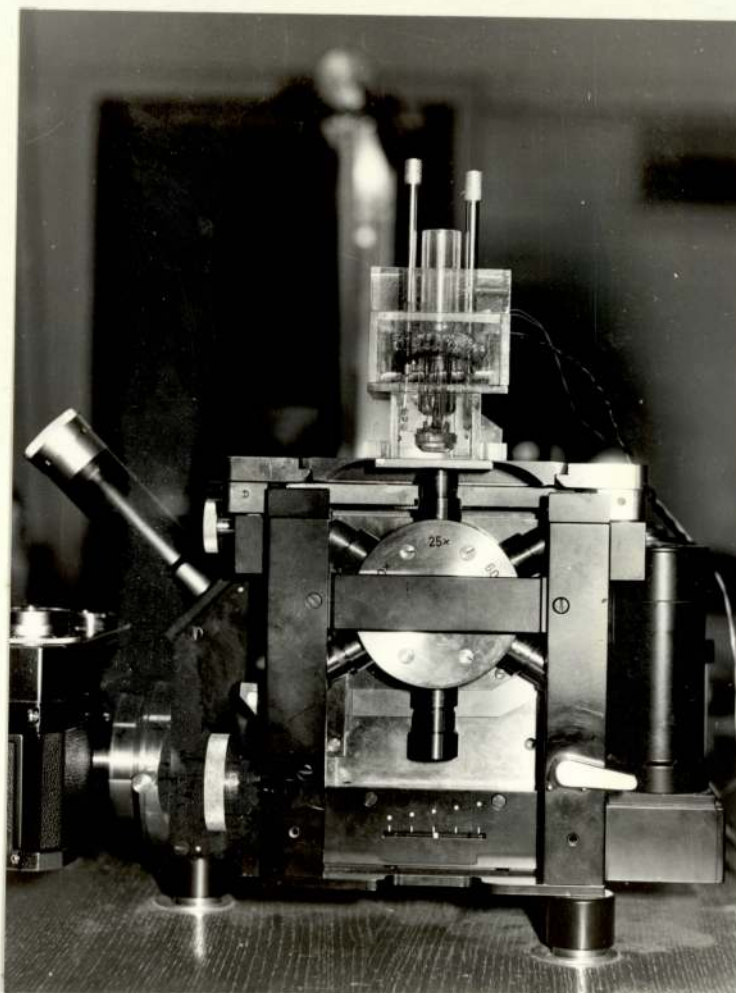


**Figure 3.5** Linnik micro-interferometer with the lens-cell system

displaced until the summit of the curvature of the hydrogel lens was lying approximately over the objective. The correct position was reached when the interference bands appear; sharp focus being obtained using the fine adjustment knob. The contrast of interference bands increased when the aperture diaphragm was closed; this adjustment was continued until photographs were then taken using a high speed, very fine grain film (Kodak TRI-X Pan ASA 400) with an exposure time of 35 sec.

#### 3.4.3. Measurement of central thickness

This instrument was not calibrated to measure lens thickness. To rectify this, a dial gauge was fitted to the objective lens and the fine adjustment knob was calibrated. The distance between sharply visible interference fringes for the front and back surfaces gave the thickness of the lens. Since the measurements were carried out in physiological saline, the real thickness of hydrogel lens was equal to the measured thickness multiplied by 1.07, assuming a refractive index 1.43 for polyHEMA and 1.336 for 0.9% saline.

### 3.5 Theoretical considerations

To interpret the interference pattern, it is expedient to consider the monochromatic beam split by a semi-reflecting beam splitter. One part of the plane wavefront will strike the surface of the hydrogel lens and will be distorted taking the shape of the lens surface, the other part will reflect on the optically perfect surface of the comparison mirror and its wave front will return back as a perfect plane wave (reference wave front). The wave front ' $\Sigma_2$ ', having been deformed by the surface of the lens, and the reference wave front ' $\Sigma$ ', recombine in the beam splitting ' $P_1$ ' (Fig. 3.6). The interference fringes may be regarded as contour lines at height intervals of a half a wave-length ( $\lambda/2$ ) of the monochromatic light used (Fig. 3.7) and may be viewed by means of an eyepiece and photographed.

In order to evaluate the radius of curvature of the lens surface, the least square method was utilised to fit a circle to the observed fringe positions, as measured by a microdensitometer from the photographs.

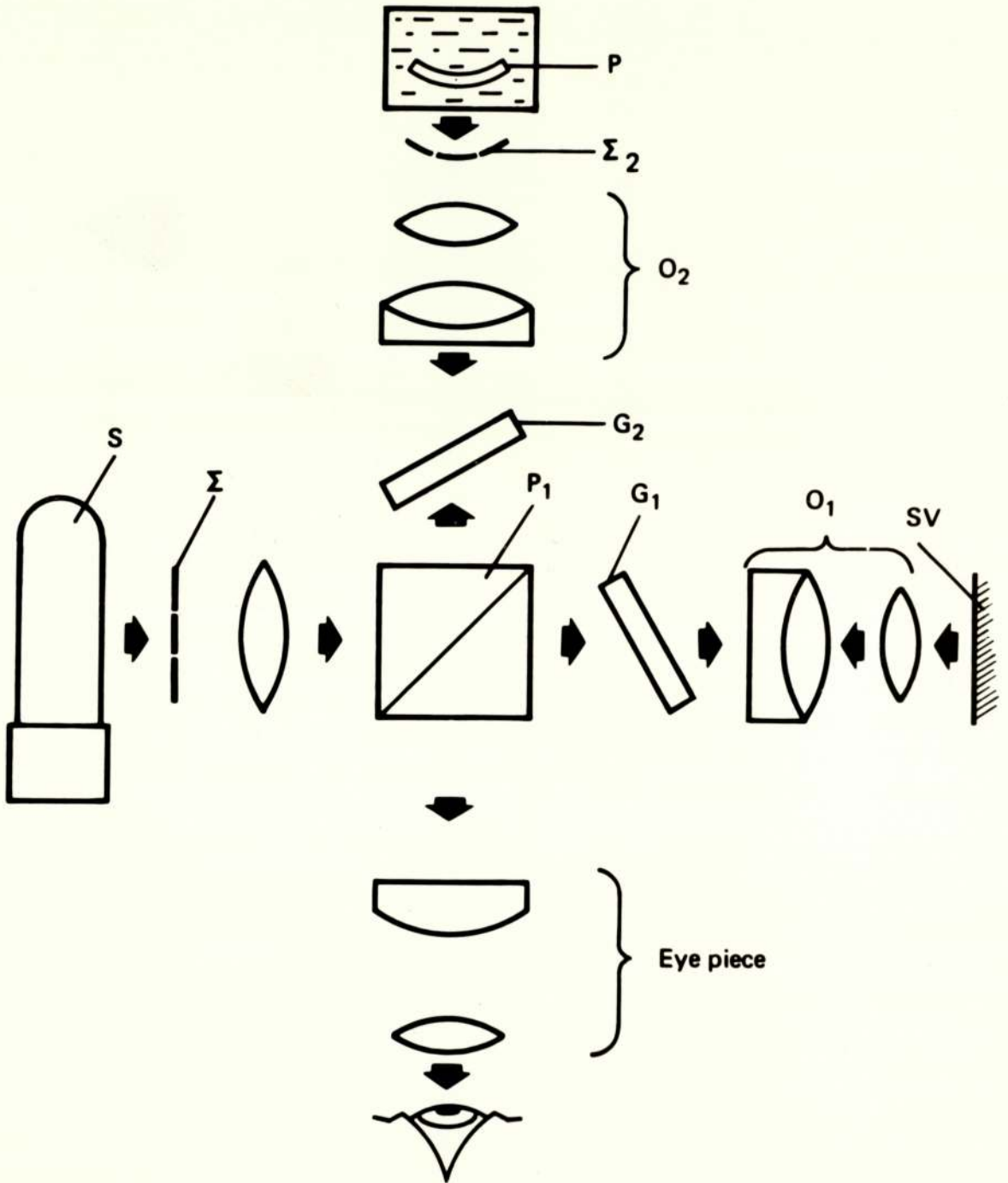


Figure 3.6 Principle of the linnik micro-interferometer

$\lambda$  = wavelength of monochromatic light

$D_i$  = diameter of fringe

P = surface of soft hydrophilic lens

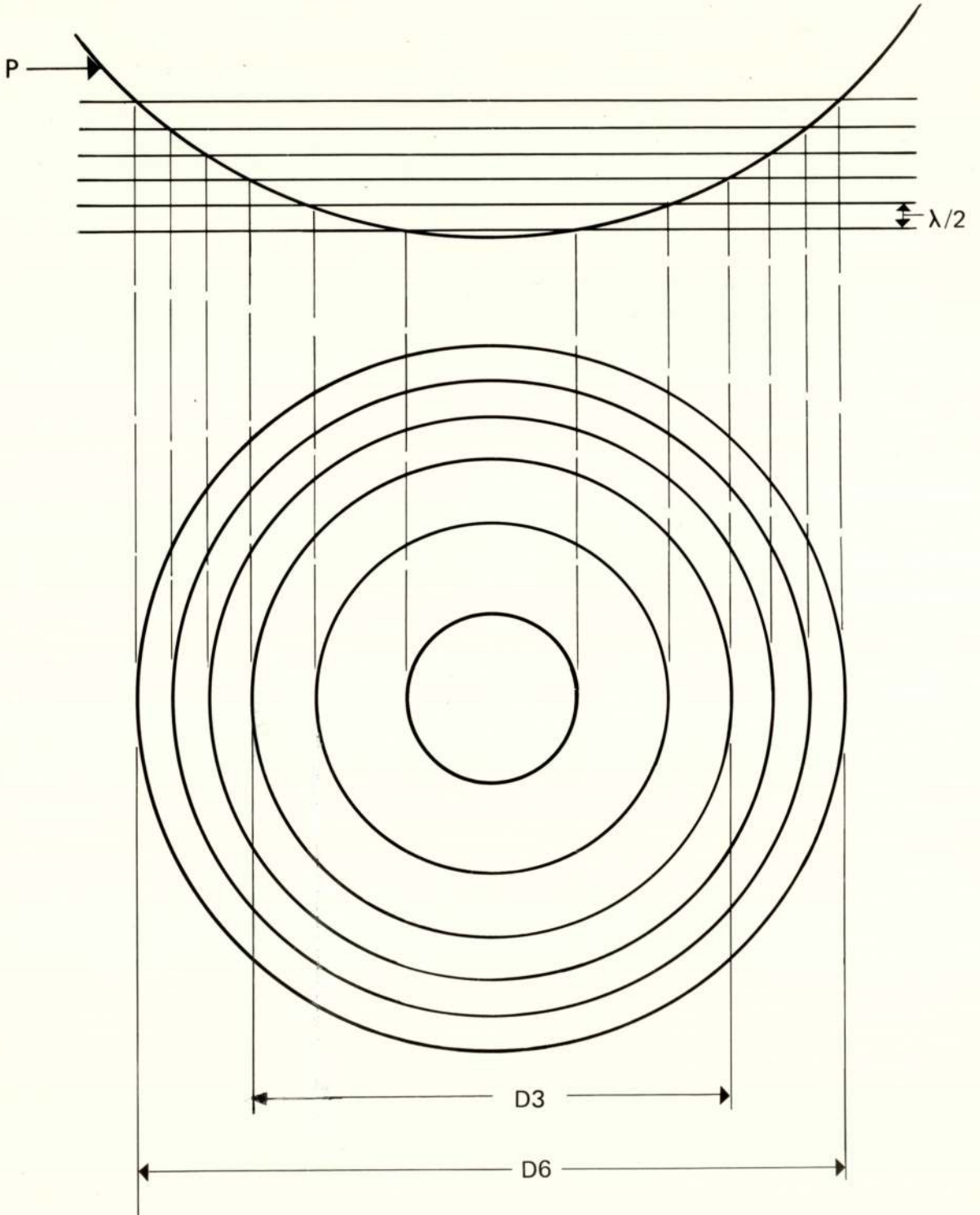


Figure 3.7 The formation of interference fringes

Let  $x_i$  and  $y_i$  represent the  $i^{\text{th}}$  observation of the radius of the fringe and multiples of half the wavelength respectively, and suppose that there are  $n$  such observations which should satisfy the relation,

$$(x - c_1)^2 + (y - c_2)^2 = c_3^2$$

where the  $c_j$  ( $j = 1, 2, 3$ ) are to be determined.

There are several possible methods of estimating  $c_j$ , all of which involve lengthy iterative processes. However, sufficiently accurate estimates can be obtained by minimising the function,

$$\phi(c_j, x_i, y_i) = \sum_{i=1}^n [(x_i - c_1)^2 + (y_i - c_2)^2 - c_3^2]^2$$

which has the advantage of considerably reducing the numerical computation.

For the function  $\phi(c_j, x_i, y_i)$  to be a minimum, we require

$$\frac{\partial \phi}{\partial c_j} = 0 \quad (j = 1, 2, 3)$$

giving,

$$\sum_{i=1}^n (x_i - c_1) \psi(c_j, x_i, y_i) = 0, \quad \sum_{i=1}^n (y_i - c_2) \psi(c_j, x_i, y_i) = 0$$

$$\sum_{i=1}^n \psi(c_j, x_i, y_i) = 0$$

wherein

$$\psi(c_j, x_i, y_i) = (x_i - c_1)^2 + (y_i - c_2)^2 - c_3^2$$

which reduce to

$$\sum_{i=1}^n x_i \psi(c_j, x_i, y_i) = 0$$

$$\sum_{i=1}^n y_i \psi(c_j, x_i, y_i) = 0$$

$$\sum_{i=1}^n \psi(c_j, x_i, y_i) = 0$$

On expanding the summations, the equations can be solved to give:

$$c_1 = \frac{q_2 r_1 - q_1 r_2}{2(p_1 q_2 - p_2 q_1)}, \quad c_2 = \frac{p_1 r_2 - p_2 r_1}{2(p_1 q_2 - p_2 q_1)}$$

where

$$\left[ \begin{array}{l} p_i = \alpha_i \beta_{i+1} - \alpha_{i+1} \beta_i \\ q_i = \alpha_i \gamma_{i+1} - \alpha_{i+1} \gamma_i \\ r_i = \alpha_i \delta_{i+1} - \alpha_{i+1} \delta_i \end{array} \right] \quad (i = 1, 2)$$

with

$$\alpha_1 = \Sigma x_i, \quad \beta_1 = \Sigma x_i^2, \quad \gamma_1 = \Sigma x_i y_i, \quad \delta_1 = \Sigma x_i (x_i^2 + y_i^2),$$

$$\alpha_2 = \Sigma y_i, \quad \beta_2 = \Sigma x_i y_i, \quad \gamma_2 = \Sigma y_i^2, \quad \delta_2 = \Sigma y_i (x_i^2 + y_i^2),$$

$$\alpha_3 = n, \quad \beta_3 = \Sigma x_i, \quad \gamma_3 = \Sigma y_i, \quad \delta_3 = \Sigma (x_i^2 + y_i^2)$$

the summations being from  $i = 1$  to  $n$ . The radius is found to be

$$c_3 = [c_1^2 + c_2^2 - 2c_1(\beta_3/\alpha_3) - 2c_2(\gamma_3/\alpha_3) + (\delta_3/\alpha_3)]^{\frac{1}{2}} \quad \dots 3.1$$

3.6 Experimental Results

The ball bearings measured in the National Physical Laboratory (NPL), Teddington (U.K.) were used to calibrate the micro-interferometer. The results in table 3.2 show that the measurements could be taken to a three decimal place.

Table 3.2            Comparison of the calibrated and measured radii of ball bearings

Radius of curvature of ball bearing measured at (NPL)	Radius of curvature of ball bearing measured by micro-interferometer
10.319 mm	10.318 mm
8.732 mm	8.734 mm
7.937 mm	7.935 mm
7.143 mm	7.141 mm
6.350 mm	6.351 mm

The hydrogel lenses used in this study were normal prescription lenses and were provided by the Softlens division of the Bausch and Lomb Corporation (U.K.). They were manufactured from 2-hydroxyethylmethacrylate known as poly-HEMA. The physical properties of the lenses are summarised in table 3.3.

Table 3.3            Physical properties of HEMA polymer

-Refractive index ( $N_D$ 20°C equilibrated in H <sub>2</sub> O)	1.43
-Softening point	120°C
-Visible light transmission sample thickness 0.75 mm	97%
-Water content by weight Equilibrated in H <sub>2</sub> O	41.7%
"            "    0.9% NaCl	38.6%
-Water content by volume equilibrated in H <sub>2</sub> O	47%
-Linear swell Equilibrated in 0.9% NaCl	18%

These lenses, commercially known as the SOFLENS<sup>R</sup> contact lenses, are produced by the spin-casting method. They are available in different series labelled as B, F, J and N (of overall diameter 12.5 mm) and B3, F3 and J3 (of 13.6 mm diameter). Each series has one F.C.O.R. and a variable B.C.O.R. which changes by an average of 0.05 mm to give 0.25D change in power. The SOFLENS'S<sup>R</sup> under investigation were of powers of -2.0, -4.0 and -6.0D in the ranges B, F, J, N, B3, F3 and J3. The power and range of lenses used in this study were selected to cover those most likely to be encountered in normal optometric practice. The front

surface of a SOFLENS<sup>R</sup> is a replica of the spherical surface of the mould in which it is polymerised and its value is constant for each series of lenses but the back surface is aspheric and is the product of the forces at play on the lens at the time of polymerisation.

Twenty one SOFLENS<sup>R</sup> were used to study F.C.O.R., B.C.O.R. and thickness, ten successive photographs being taken of each individual lens. (Fig. 3.8) shows the interferogram of the front and back surfaces for a -2.0D (F3) SOFLENS<sup>R</sup>. The fringes were observed to be sharp over the thirty order. An automatic recording microdensitometer model MK3C manufactured by Joyce Loebel was utilized to scan the microinterferograms. (Figs. 3.9 a,b) shows one of the microdensitometer print outs, each successive peak representing a bright or dark fringe. In order to give an equivalent curvature value for the lens, a circle was fitted to the values measured over the central 800 microns on each lens using equation 3.1. A total of 420 measurements at the centre of lens surface were carried out and the average value of radius of curvature for each surface is listed in table 3.4.

The highest difference between the average measured results and the published data was 0.130 mm and the lowest was 0.008 mm. The maximum value of the coefficient of variation was 2.0% and the minimum value was 0.6%. Table 3.5 gives

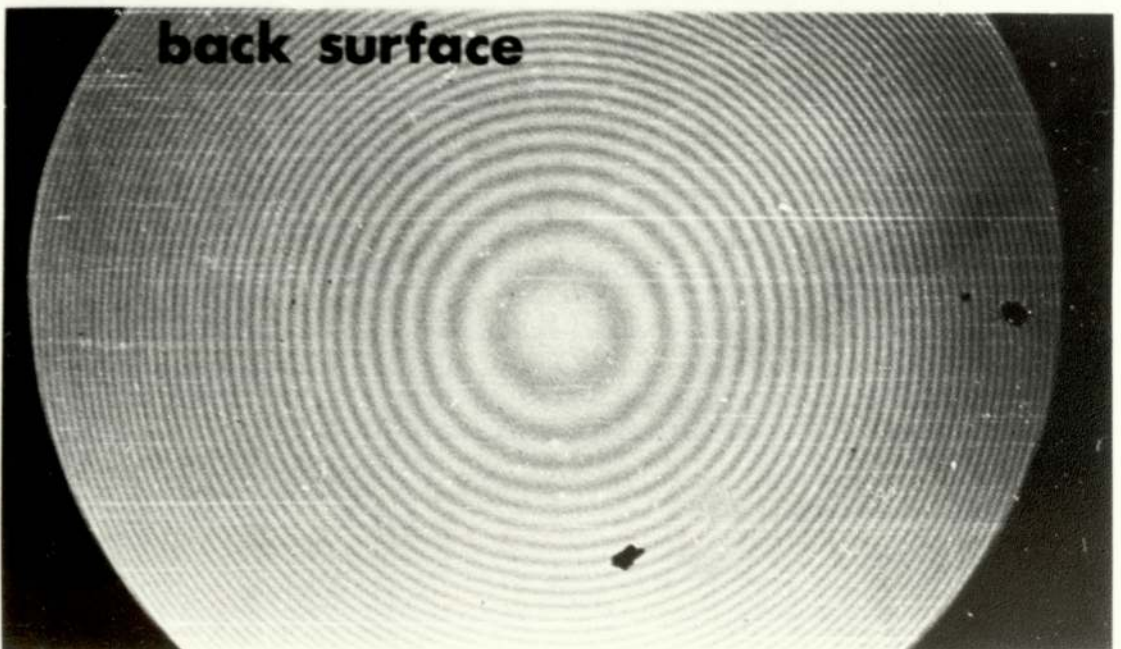
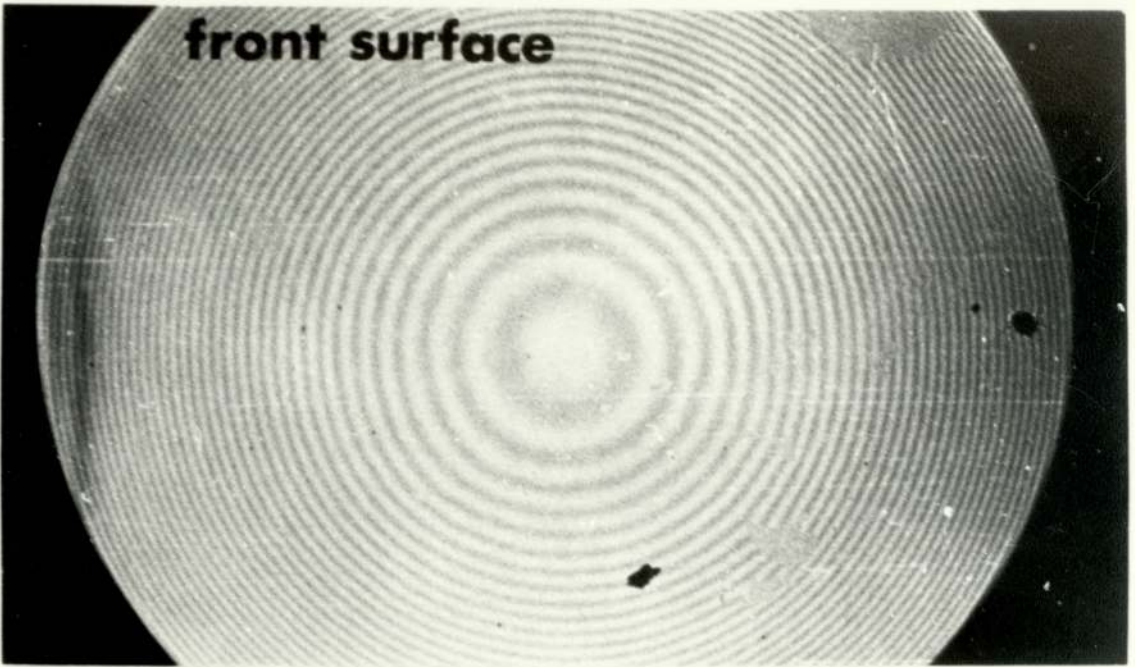


Figure 3.8 The interferogram of the front and back surface of a  $-3F3$  SOFLENS

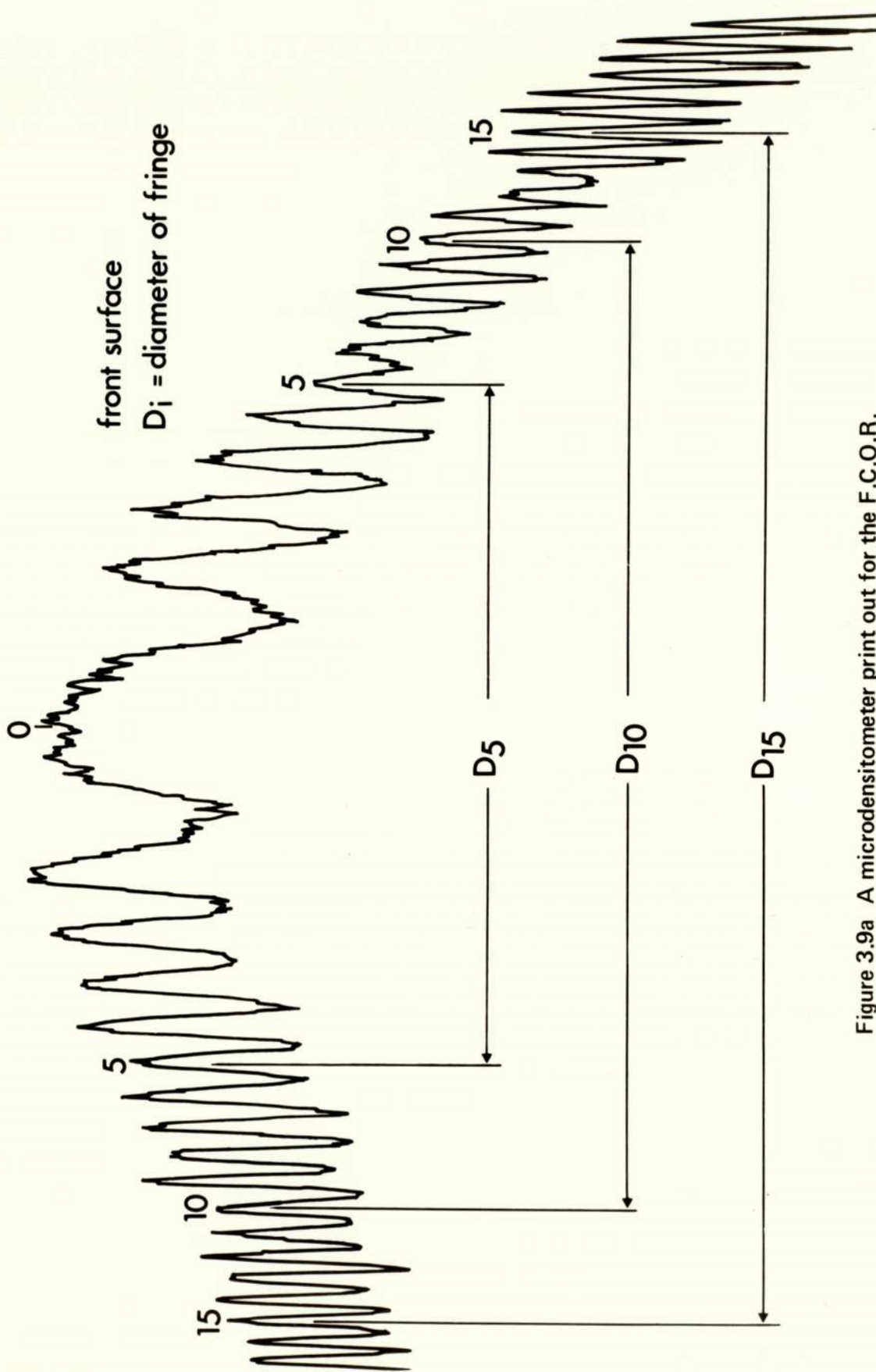


Figure 3.9a A microdensitometer print out for the F.C.O.R.

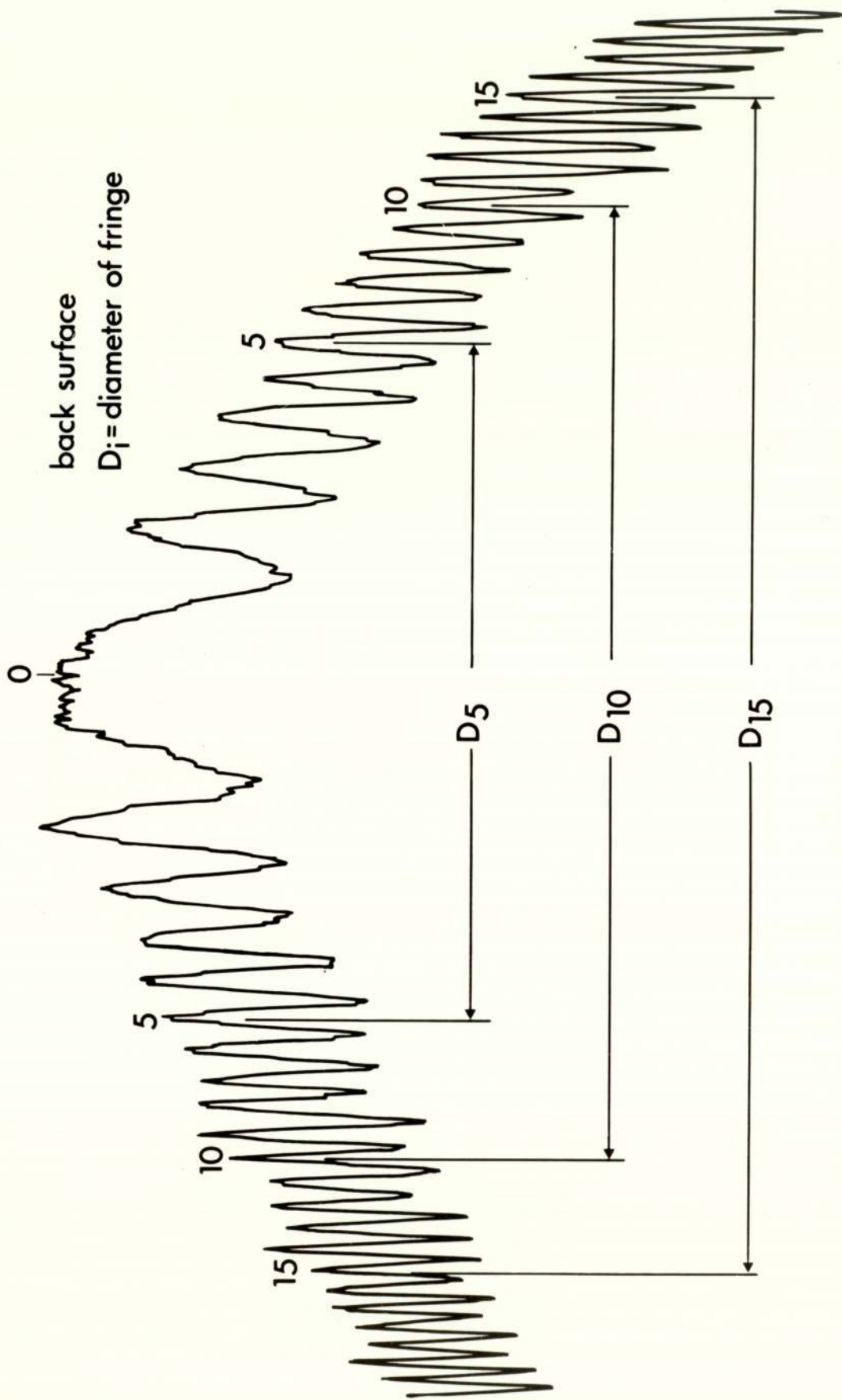


Figure 3.9b A microdensitometer print out for B.C.O.R.

the average of the measured centre thickness. The maximum difference between the published and measured data was 0.022 mm and the minimum value 0.001 mm (Fig. 3.10) illustrates the difference between the values for the F.C.O.R. published by the manufacturer and the values measured by interferometry. (Fig. 3.11) shows the difference between the theoretical data published by the manufacturer and the experimental results for B.C.O.R. A comparison of manufacturer-data and experimental results for centre thickness is given in (Fig. 3.12).

A computer program was written to calculate the central optic radius of hydrogel lenses depending on the equation 3.1. (Appendix I).

The computer print out shown in Appendix II shows a sample of a 90% confidence limits of the average taken for each radius of curvature, where ten readings were taken for each lens. The formula used for calculating the confidence intervals was based on  $\chi^2$ -test as follows,

$$\frac{\text{S.D.} \cdot \sqrt{n}}{\chi^2_{\frac{\alpha}{2}}(n-1)} < \bar{X} < \frac{\text{S.D.} \cdot \sqrt{n}}{\chi^2_{(1 - \frac{\alpha}{2})}(n-1)}$$

where,

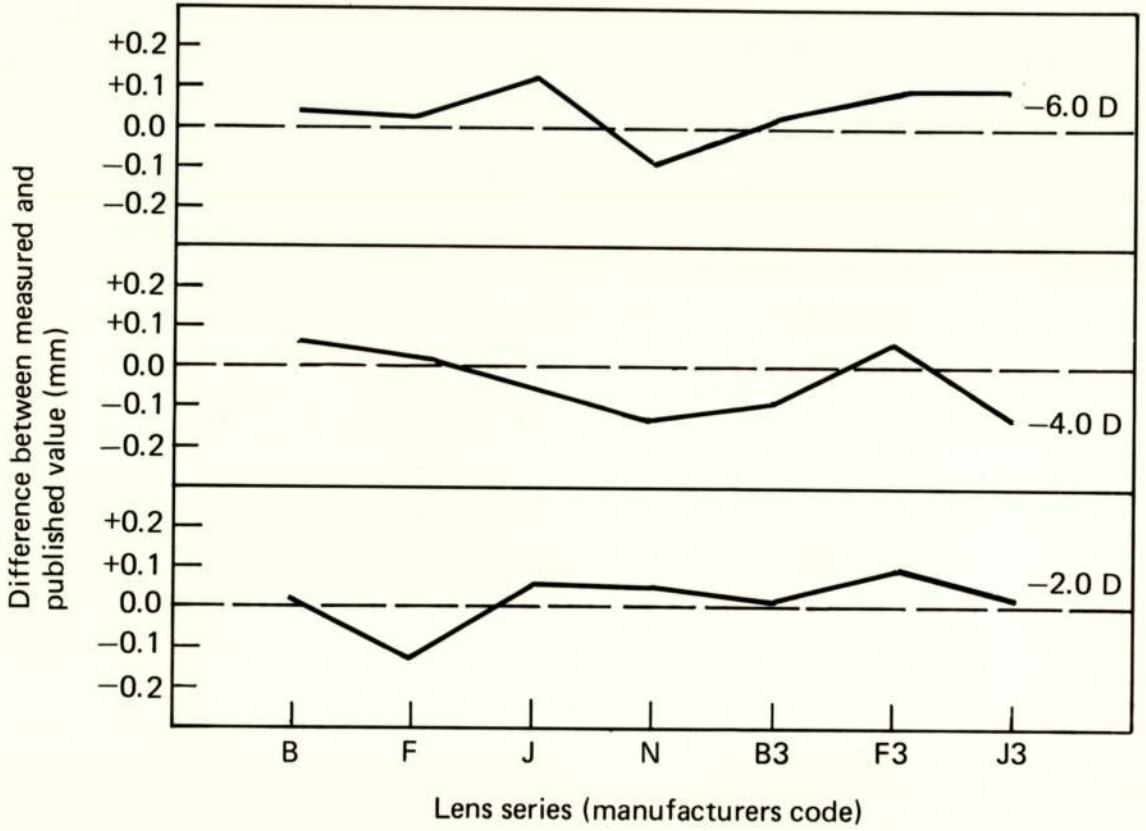


**Figure 3.10** Graphical representation illustrating the difference between the manufacturer's and measured values for the F.C.O.R. of SOFLEN®

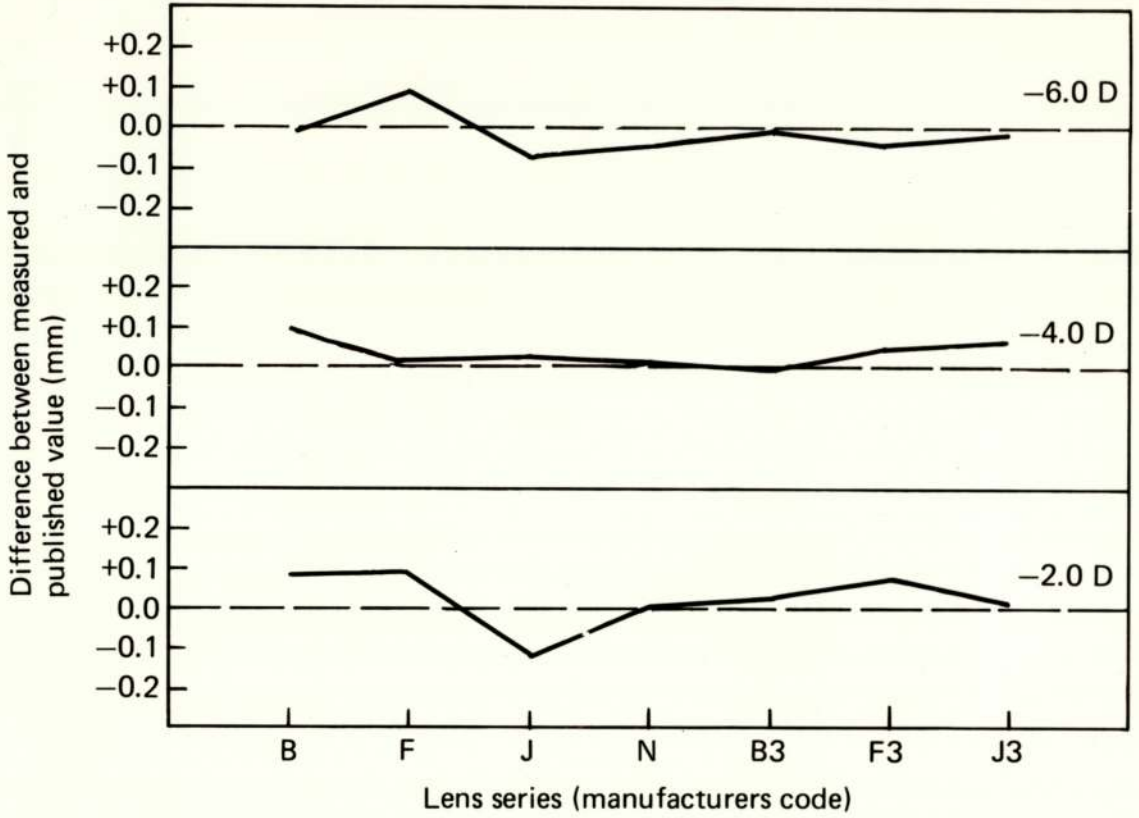
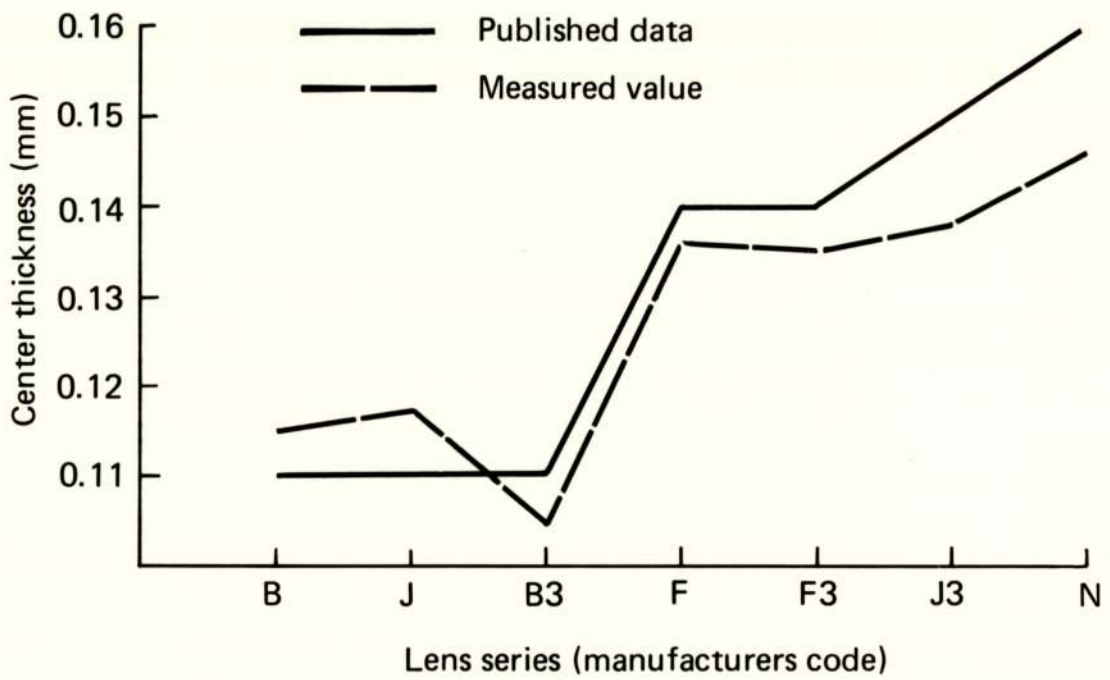


Figure 3.11 Graphical representation illustrating the difference between the manufacturer's and measured values for the B.C.O.R. of SOFTLENS<sup>®</sup>



**Figure 3.12 Comparison of the theoretical and measured central thickness of SOFTLENS<sup>®</sup>**

$\bar{X}$  is the average measured value for central optic radius

S.D. is the standard deviation

n is the number of readings

$\chi^2_{\frac{\alpha}{2}}$  and  $\chi^2_{1-\frac{\alpha}{2}}$  are the 0.05 and 0.95

confidence limits respectively

The measured  $X_1(K)$  and calculated ( $X_1EST$ ) values of  $i^{th}$  observation of the radius of the fringe are tabulated for F.C.O.R. and B.C.O.R. of each lens under investigation. Each sample shows that a high degree of correlation exists between the measured and calculated values.

### 3.7 Source of Errors

Several errors may arise in the interpretation of the interferograms and consequently effect the calculation of radii of curvature of hydrogel lenses. These errors include:-

### 3.7.1 Fringe spacing error

Tolmon and Wood (1956) reported that in order to achieve the high accuracy required in measurements using an interference microscope, it was necessary to evaluate the fringe spacing precisely since the fringes in the interference microscope were produced in strongly convergent light, whereas the fringes in gauge measuring interferometers are formed in collimated light. Therefore, where the incident light is normal or very nearly so, the fringe spacing is accepted as equivalent to half of the monochromatic light employed. Tolmon and Wood (1956) calibrated Linnik-Zeiss and Hilger and Watts interference microscopes in order to determine the correction factors for the microscopes, since it was considered that theoretical computation was not practicable. They showed for high-power interference microscopes (N.A. = 0.6) the fringe space is approximately 10% greater than half the wavelength.

However, Gates (1956) has made an attempt to calculate the correction factor theoretically. He considered a zone of illumination in a perfect optical system which is bounded by circles subtending angles  $\theta$  and  $\theta + d\theta$  with the optical axis. The flux in this annulus is proportional to  $\theta + d\theta$ . The fringe spacing may be averaged over the whole aperture by multiplying the fringe spacing  $\lambda/(2\cos\theta)$  by  $\theta d\theta$

as a weighting factor and integrating over the full cone of illumination  $\alpha$ . The result was normalized by dividing the integral of the weighting factor. The averaged fringe spacing is then:-

$$\int_0^\alpha (\lambda \theta/2 \cos\theta) d\theta / \int_0^\alpha \theta d\theta = \lambda/2 \left[ 1 + \frac{\alpha^2}{4} + \frac{5\alpha^4}{72} + \frac{61\alpha^6}{2880} + \dots \right]$$

$$+ \frac{E_n \alpha^{2n}}{(n+1)(2n)!} + \dots$$

.....3.2

Where  $E_n$  were Euler's numbers.

In practice the outer zones of the objective are slightly less effective than has been allowed for here. A weighting factor of  $\sin\theta d\theta$  instead of  $\theta d\theta$  will diminish the effect of the more oblique zones. The averaged fringe spacing is then given by:-

$$\int_0^\alpha (\lambda \sin \theta/2 \cos\theta) d\theta / \int_0^\alpha \sin\theta d\theta = (\frac{1}{2}\lambda) \ln \cos\alpha / (\cos\alpha - 1)$$

.....3.3

A summary of the results is given in table 3.6.

Label power	Series	Published F.C.O.R.	Average Measured F.C.O.R.	Coefficient of Variation	Published B.C.O.R.	Average Measured B.C.O.R.	Coefficient of Variation
Diopters		mm	mm	%	mm	mm	%
-2.0	B	9.08	9.104	1.3	8.70	8.785	1.1
-4.0			9.141	1.1	8.35	8.458	1.0
-6.0			9.130	1.2	8.05	8.062	1.8
-2.0	F	8.74	8.620	0.8	8.35	8.443	1.3
-4.0			8.763	1.0	8.05	8.060	1.7
-6.0			8.760	1.3	7.75	7.812	1.9
-2.0	J	8.44	8.510	1.1	8.10	7.986	1.4
-4.0			8.391	1.4	7.80	7.820	1.5
-6.0			8.553	1.3	7.55	7.482	1.3
-2.0	N	8.14	8.186	2.0	7.80	7.806	1.1
-4.0			8.010	1.3	7.55	7.561	1.6
-6.0			8.041	1.6	7.25	7.201	1.4
-2.0	B3	9.67	9.682	1.3	9.20	9.221	1.8
-4.0			9.598	1.4	8.85	8.840	1.5
-6.0			9.691	1.2	8.55	8.542	0.6
-2.0	F3	9.34	9.421	1.3	8.90	8.970	1.1
-4.0			9.412	1.0	8.55	8.587	1.3
-6.0			9.432	1.5	8.25	8.210	1.6
-2.0	J3	9.02	9.038	1.8	8.60	8.621	1.5
-4.0			8.913	1.2	8.25	8.312	1.9
-6.0			9.118	1.6	7.95	7.932	1.6

TABLE 3.4 The average measured values and coefficients of variation for front and back central optic radii of SOFLENS R contact lenses

Label power	Series	Published centre thickness	Average measured centre thickness	Series	Published centre thickness	Average measured centre thickness
Diopters		mm	mm		mm	mm
-2.0	B	0.11	0.112	B3	0.11	0.112
-4.0			0.118			0.108
-6.0			0.117			0.095
-2.0	F	0.14	0.134	F3	0.14	0.138
-4.0			0.142			0.132
-6.0			0.140			0.135
-2.0	J	0.11	0.123	J3	0.15	0.134
-4.0			0.120			0.138
-6.0			0.111			0.142
-2.0	N	0.16	0.148			
-4.0			0.151			
-6.0			0.138			

TABLE 3.5 A comparison between the theoretical and measured central thickness for SOFLENS R contact lenses

Table 3.6

Numerical aperture	0.3	0.6	0.65
Experimental factor (Tolmon & Wood)	1.03	1.09	1.12
Calculated from eqn. (Gates)	1.02	1.12	1.15
" " " "	1.02	1.12	1.14

All the fringe spacings in the experimental results were multiplied by the correction factor 1.03 since the numerical aperture used was 0.3

Corrections for changes in the value of  $\lambda$  due to the atmospheric conditions such as pressure, temperature and humidity may be made, but these are usually small and were neglected in the present work.

### 3.7.2 Errors due to wave front and spherical aberration

The plane wave front must pass through the front surface of the hydrogel lens in order to study the back surface; this plane wave front will be affected by spherical aberration, which may be expressed as a wave front aberration or as a seidel aberration. The wave front aberration and Seidel aberration errors for the series of SOFLENSES<sup>R</sup> were calculated for the central optic area of diameter 1 mm and the results are shown in (Fig. 3.13 a,b). It is obvious from the results that -6.0D(N) had the maximum value for both the wave front and Seidel aberration errors:-

$$\text{wave front aberration} = -2 \times 10^{-3} \mu$$

$$\text{Seidel aberration} = -16 \times 10^{-3} \mu$$

This means that maximum wave front aberration error represents only about  $0.004\lambda$  and for the Seidel aberration error  $0.03\lambda$ . Therefore, the effect of both wave front and Seidel aberration errors were ignored in the calculations.

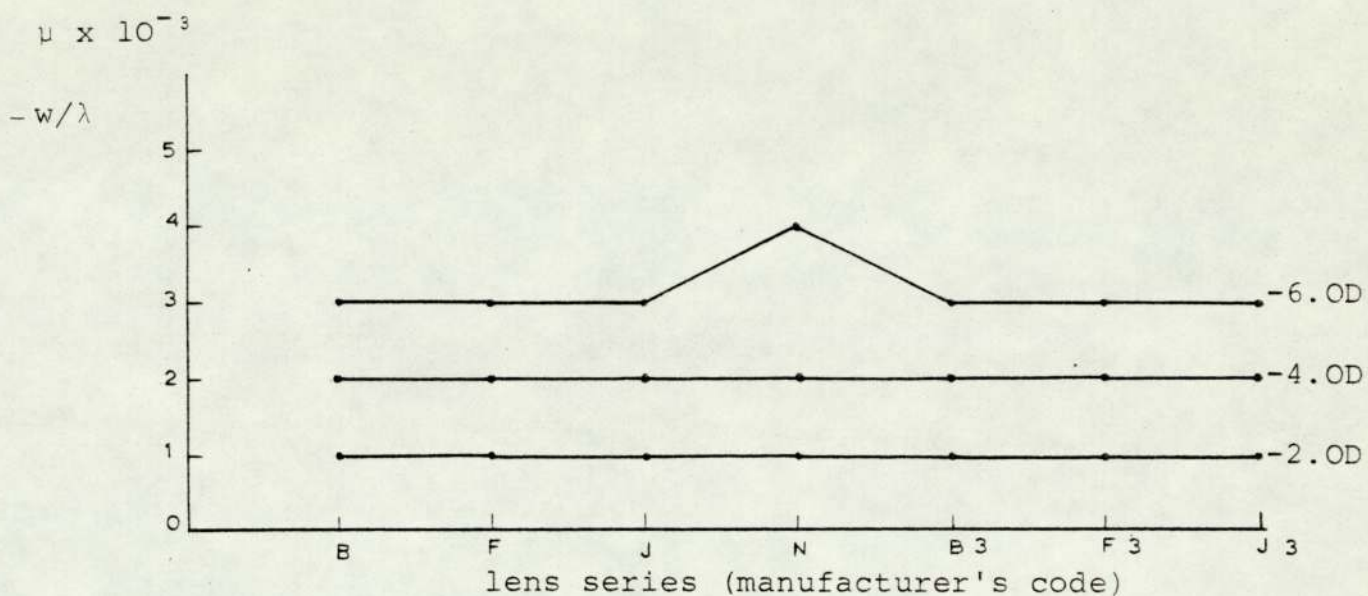


FIGURE 3.13a Relationship between SOFLENS<sup>R</sup> series and (wave front aberration)/λ

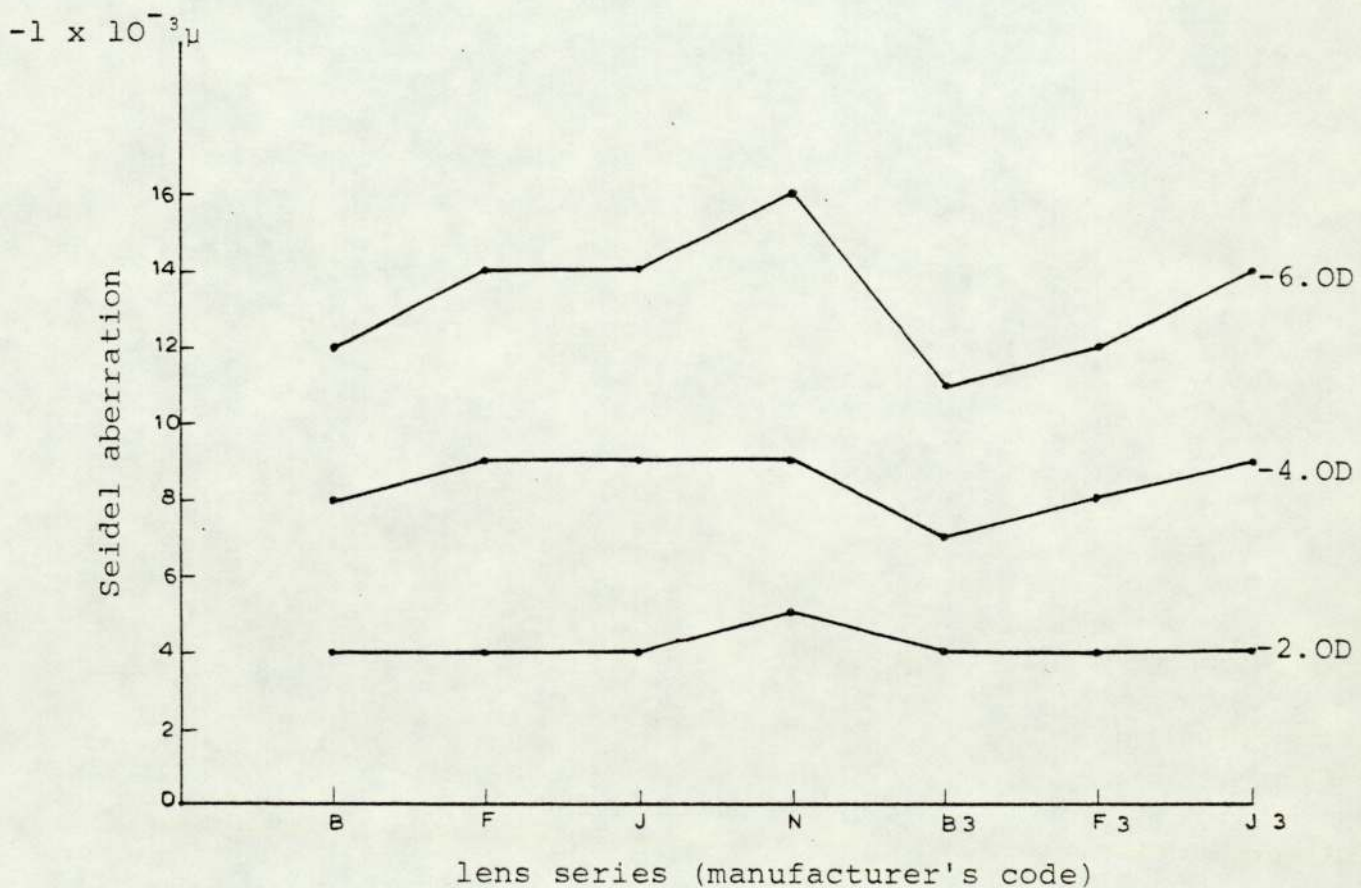


FIGURE 3.13b Relationship between SOFLENS<sup>R</sup> series and Seidel aberration

## CHAPTER 4

### Measurement of refractive index of the hydrogel material

#### 4.1 Introduction

The purpose of this study was to measure the refractive indices of hydrophilic hydrogel materials of different equilibrium water contents. The need to measure the refractive indices precisely was an important factor in the design of soft hydrophilic lenses. The linear swell and refractive index are important parameters in predicting the power of soft hydrophilic lenses after hydration.

Strachan (1973) has shown theoretically that for a -3.0D lens a change in refractive index of two hundredths gives a change of 0.12D, and for +3.0D lens a change of refractive index of two hundredths increases the plus power by 0.18D. He represented the theoretical calculation of refractive indices with equilibrium water content (Fig. 4.1) (assuming the refractive index of hydrogel material in dry state is 1.52).

Ng, (1974) employed the Abbe refractometer to measure a series of copolymer sheets by clamping the test sample between the two prisms of the refractometer, and by adjusting the position of the light source (sodium light) as well as the adjustment of the refractometer. He claimed a clear boundary

of contrast intensities at the intersection of the cross wires in the eyepiece. For those test samples which do not form a good contact with the prism surface, a drop of benzoylbenzoate ( $\mu_D = 1.568$  at  $20^\circ\text{C}$ ) was added on both sides of test sample before clamping the two prisms. The major sources of inaccuracy in measuring the refractive index by the Abbe refractometer were:-

- (a) A possible expulsion of a small amount of saline due to the pressure caused by clamping the hydrated hydrogel sheet between two prisms.
- (b) The uncertainty in reading the boundary would impose some degree of inaccuracy.

#### 4.2 Experiment 1: Apparatus and Methodology

This method was based on the total reflection refractometer first described by Pfund (1931).

A modified type of apparatus was set up which consisted of a plane parallel glass plate having dimensions 15 x 15 x 0.59 cm, the lower surface of this plate was coated with white paint and had concentric rings of diameters 1 to 10 cm in 1 cm steps to act as a scale. A He-Ne laser beam striking the glass-paint interface was used as a source. Light having an angle of emergence equal to or greater than, the critical angle was returned to the lower white surface, producing an illuminated area which has a black circular disc of diameter  $D_x$  at its centre (Fig. 4.2).

A thin layer of HEMA 1 mm thick in dehydrated state and of refractive index less than that of the glass plate was spread over the upper surface of glass plate, a second and larger circular ring of diameter  $D_G$  was then observed. It was evident that this ring was due to the rays which were totally reflected at the glass-HEMA interface. Hence the refractive index of dehydrated HEMA sheet ( $\mu_G$ ),

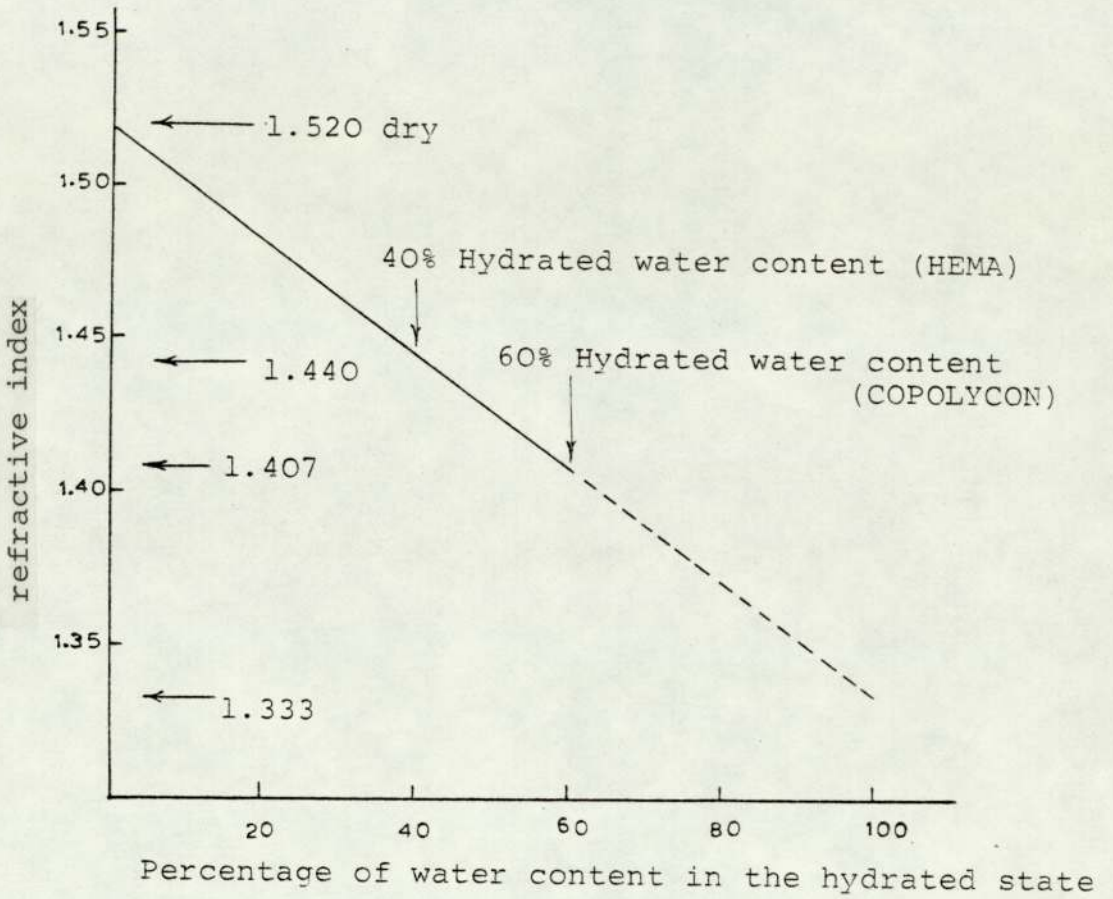


Figure 4.1 Theoretical relationship between the refractive index and the water content of hydrogel (after Strachan)

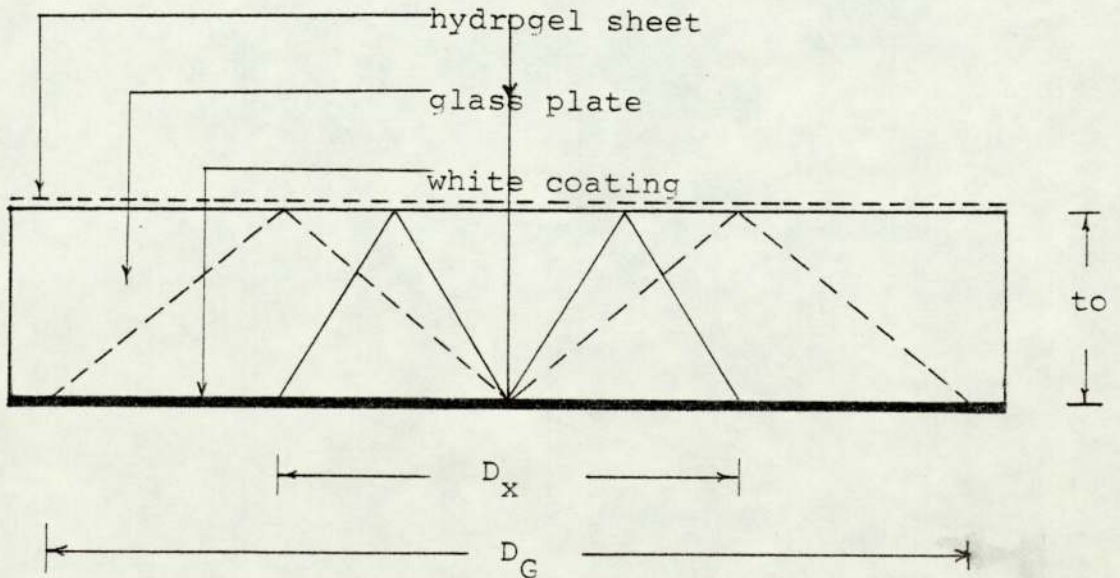


Figure 4.2 Geometry of the formation of rings

$$\mu_G = \mu_L \frac{D_G}{\sqrt{D_G^2 + 16t_0^2}}$$

where  $\mu_L$  refractive index of glass plate  
 $t_0$  thickness of glass plate (in cm)

$\mu_L$ ,  $D_G$ ,  $t_0$  are all measurable.

The HEMA sheet was partially hydrated in saline 15 min and the experimental procedure was repeated. Because of the presence of saline between the HEMA sheet and glass plate, the central ring became vague and after 48 hours, the HEMA sheet became fully hydrated, the dark central ring nearly disappeared, and it was impossible to measure the diameter of first white ring (Fig. 4.3 a,b).

Hence this method did not seem practical for measuring the refractive index of hydrogel materials.

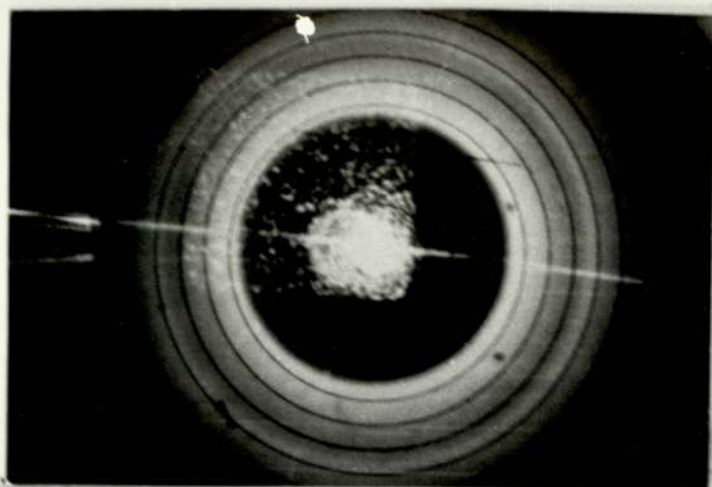


Figure 4.3a The appearance of the outer white ring due to the hydrogel sheet (dry state)

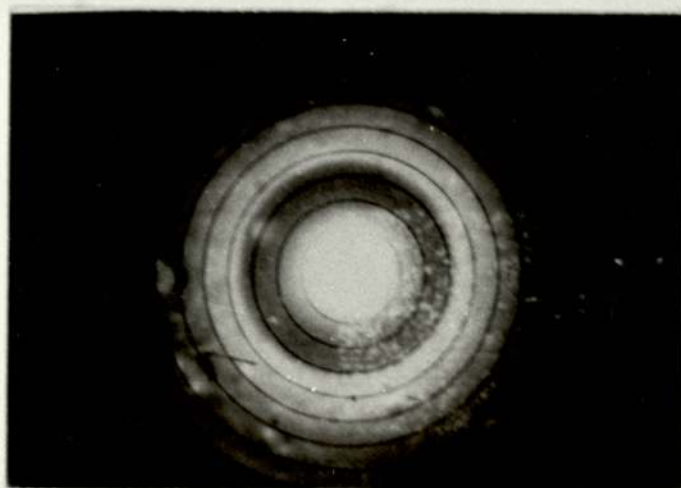


Figure 4.3b The disappearance of the outer white ring due to the saline film between a fully hydrated sheet and a glass plate

#### 4.3 Experiment 2:- Apparatus and Methodology

It was decided to submerge the hydrogel material in different liquids of different refractive indices which would not react or have any sort of effect which could change the water content of hydrogel material. The surface of material under investigation was illuminated with a He-Ne laser and by using a detector the amount of reflected light could be measured. The amount of reflection for each sample of hydrogel, and medium of known refractive index could be measured and a graph drawn. From the curve the zero reflection which would indicate the refractive index of hydrogel material under test could be determined.

The technique was found to be subject to a number of defects. In order to increase reflection the sample was prepared as a prism with one face painted black. The painted surface produced distortions in the hydrogel and the amount of reflected light was found to be very variable, the technique was, therefore, abandoned.

#### 4.4 Experiment 3: Apparatus and Methodology

The concluding section of work was the determination of refractive index of hydrogel material using a two-beam interference instrument which provides measurements of the path difference between two waves travelling along different optical paths. The micro-interferometer described in chapter three was slightly modified for this work.

The hydrogel materials used in this study were:-

Chemical type	Water Content (Equilibrated in 0.9%NaCl)	Manufacturer
HEMA	38%	Bausch & Lomb
HEMA	43%	Shiels Ltd. (Burton Parsons)
VP/MMA	55%	Contact lens manufacturer
VP/MMA	70%	"
VP/MMA	79%	"
VP/MMA	82.5%	"

All the samples were provided from the manufacturers in the form of buttons 10 mm diameter and approximately 5 mm thick. The surfaces were not polished in order to eliminate the risk of contamination by polishing agents. The buttons were soaked in sterile 0.9% saline solution for 2 weeks at 34°C. When hydrated, each button was placed onto a circular metal holder and frozen in a chamber, attached

to a cylinder of compressed carbon dioxide. The holder and frozen hydrogel button were then quickly transferred to the "Pearse" cold microtome cryostat manufactured by Slee Medical Equipment Ltd., at a temperature between -15 and -20°C.

After alignment of the frozen gel button with the edge of the microtome knife, sections were cut at thicknesses of 20 to 100 $\mu$  in steps of 10 $\mu$ . The sections produced were then transferred using cold feelers, to a reservoir within the cryostat, containing saline. After gently submerging the sections, five complete sections of each thickness were taken and stored in a small plastic pot containing saline bearing the sample number and section thickness.

It was intended that this technique would produce thin sections having plane parallel surfaces, although not necessarily of good optical quality. Most of the sections obtained were satisfactory with the exception of all the sections of different thickness for HEMA 38% which were difficult to cut and whose surfaces were full of ripples also. Similar defects were also noted in a few samples of the 55% VP/MMA material.

A hydrogel section of thickness " $t_G$ " was applied on to a

glass plate, whose other surface had been coated with a highly reflecting silver film. The hydrogel section was surrounded by a few drops of saline and covered with a thin sheet of glass of thickness 0.14 mm (Fig. 4.4a).

Two identical pieces of glass, each one having the same thickness as the thin glass plate which covers the hydrogel sections, were inserted in front of a reference mirror  $S_v$  of the micro-interferometer as a compensator (Fig. 4.4b).

Monochromatic light was used to locate the approximate position of the component parts of the interferometer and give fringes. Then with white light and further adjustments of the interferometer, including fine focusing the white light fringes were brought into view. These fringes were observed as a central dark fringe, i.e. corresponding to zero path difference, bordered on either side by 8 to 10 coloured fringes. The white light contained all wavelengths between 4000 and 6500  $\text{\AA}$ . By moving the mechanical stage the edge of the hydrogel section was brought into the middle of the field of view, the other half of the field of view shows a thin film of saline. The set of white fringes showed a displacement as a result of the optical path difference due to the difference between the refractive indices of the hydrogel section and saline.

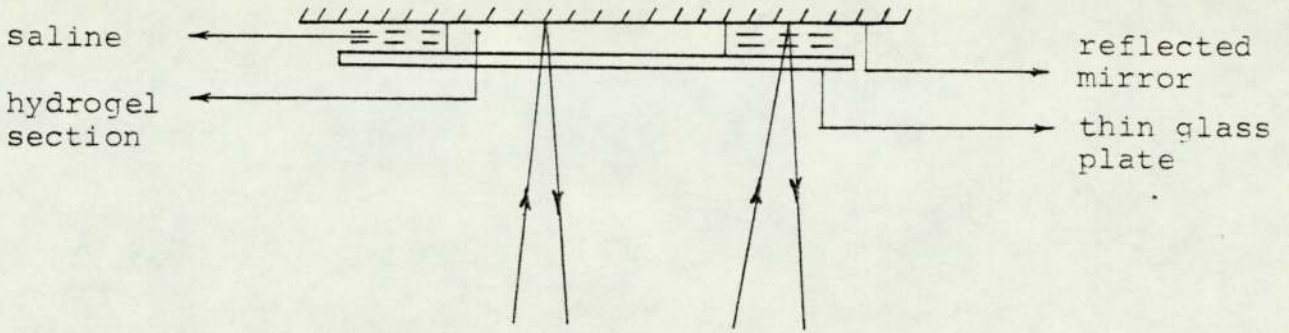


FIGURE 4.4a Hydrogel section covered with thin glass plate

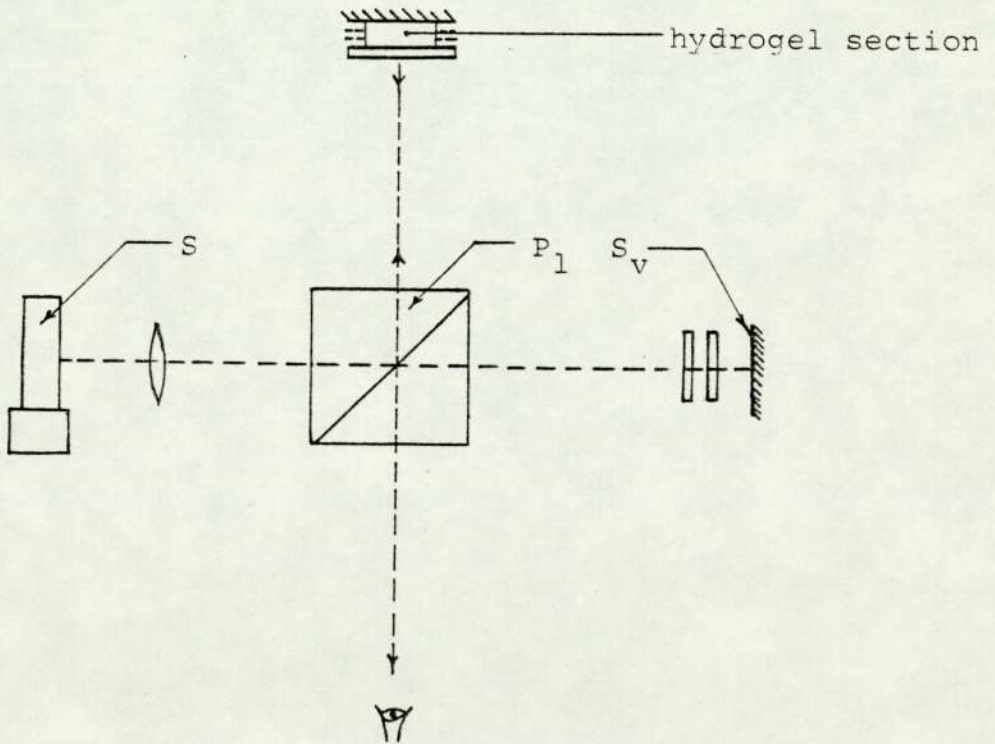


FIGURE 4.4b Modified micro-interferometer

$$\text{path difference} \quad n\lambda = 2t_G (\mu_G - \mu_S)$$

$\mu_G$  refractive index of hydrogel section

$\mu_S$  " " " saline ( $\mu_S = 1.336$ )

$t_G$  hydrogel section thickness in microns

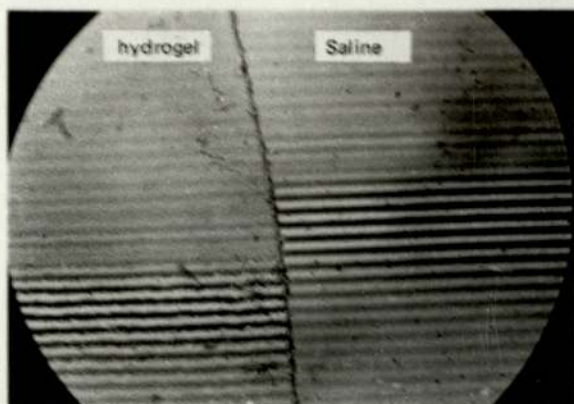
$\lambda$  wavelength of monochromatic light ( $\lambda = 0.5350 \mu$ )

The number of displaced fringes was initially determined with white light, and subsequently with a monochromatic source (Thallium 5350 A<sup>0</sup>) which allowed fringe displacement to be determined to the nearest half fringe.

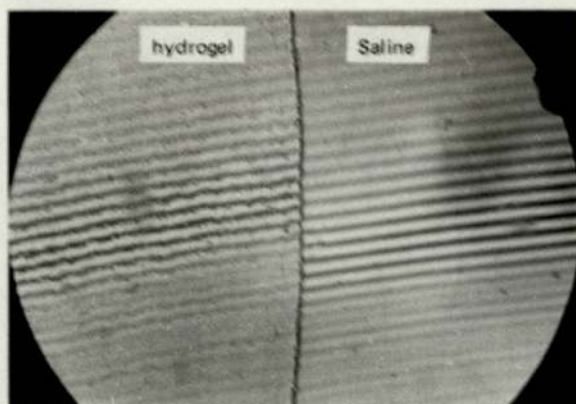
The measurements were carried out over ten minutes to avoid dehydration of the sample, after the evaporation of the surrounding saline. The film used was Kodak TRI-X Pan and the optimum exposure time was five seconds.

#### 4.5 Results and Conclusion

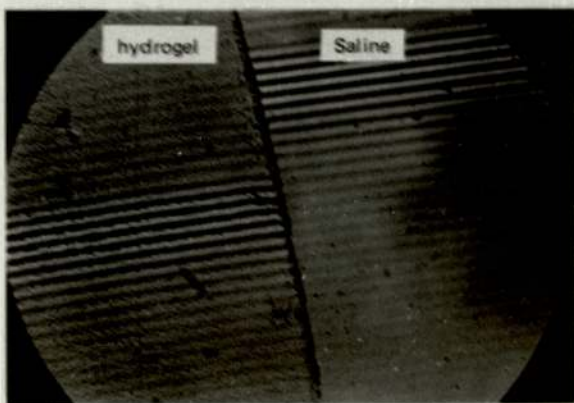
The above experimental procedure was carried out on all the previously mentioned materials. An example of the displacement of central dark fringe for different thicknesses (40, 60, 80, 100 $\mu$ ) of saufion 82% is shown in (Fig. 4.5). The relation between the thickness of the hydrogel section and number of fringes displaced for different hydrogel materials is shown in (Fig. 4.6).



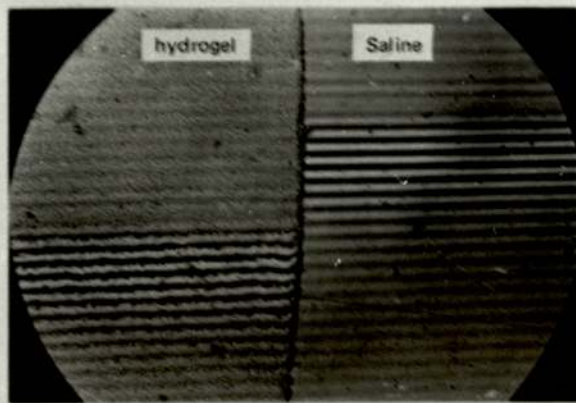
Thickness of hydrogel section 60µ



Thickness of hydrogel section 40µ



Thickness of hydrogel section 100µ



Thickness of hydrogel section 80µ

**Figure 4.5** The displacement of white light fringes due to the difference in refractive index between hydrogel material and saline solution for different thicknesses

The average value of refractive index for each hydrogel section was plotted against its water content value (Fig. 4.7) shows that the refractive index decreases as water content increases.

The reason for the small difference between the measured and theoretical results may be due to the assumption of a value for the refractive index, for the dry gel which as 1.52 is not correct for all materials. The results are in closer agreement with the theoretical values than those of Strachan (1975) whose tests were carried out on fully hydrated lenses which gave figures of 1.393 for a 60% water content material and 1.42 for a 42% water content material (B & L Soflens 1.43).

This method was suitable for high water content materials for two reasons, firstly it was easy to mount and cut the sample using microtome and secondly, the number of displaced fringes was small; ten for a thickness of a 100 micron, with a 82% water content hydrogel material. The fringes were readily observed in the field of view and could be easily counted without error.

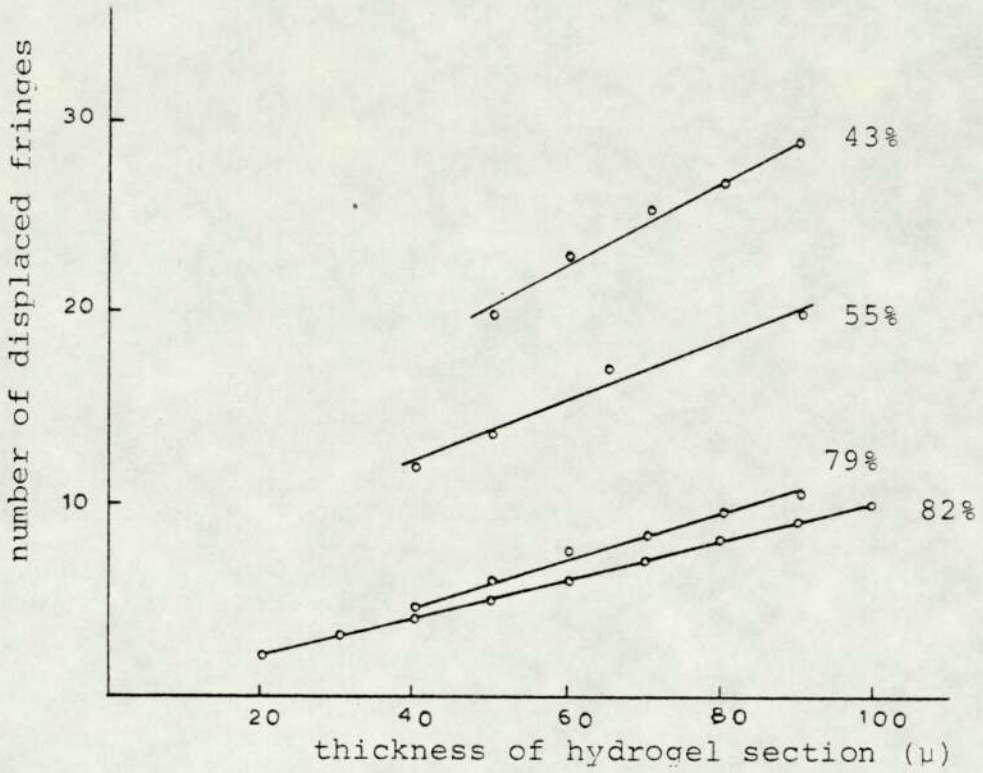


FIGURE 4.6 Shows the number of the displaced fringes as a function of the hydrogel thickness

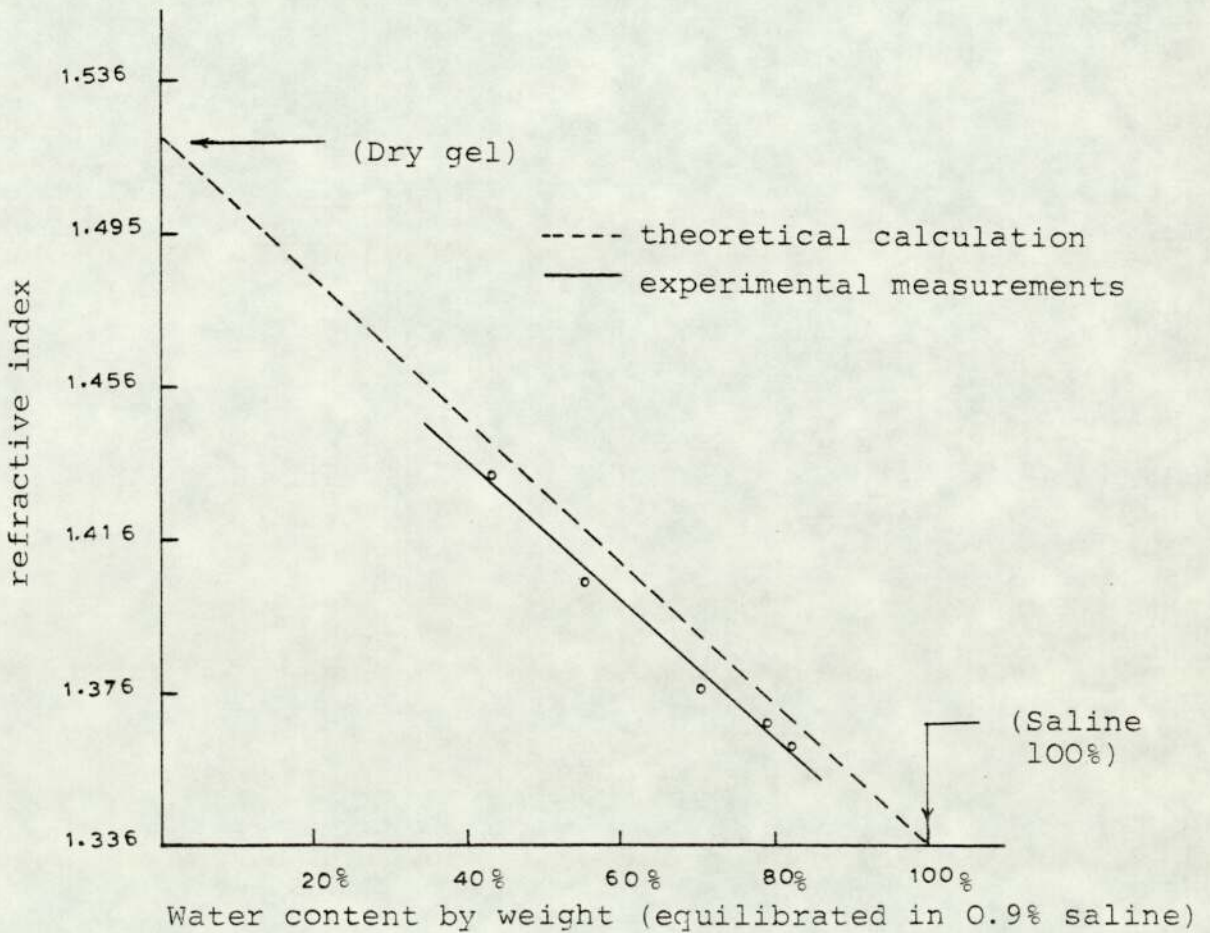


FIGURE 4.7 illustrates the relationship between refractive index and water content for hydrogel materials

## CHAPTER 5

### The evaluation of spherical aberration and change in the parameters for the hydrogel lenses on the human eye

#### 5.1 Introduction

The spherical aberration and shape change of hydrogel lenses were examined in air and in situ on the human eye. From the collected data the shape constant of the cornea and of the and of the hydrogel lens was calculated and the likely effects at both ambient and low luminance levels are discussed.

#### 5.2 Spherical aberration of the human eye

The presence of spherical aberration in the human eye was first described and measured, using an optometer, by Young (1801). The main disadvantage of his method was the uncertainty of the accommodative state of the observer.

In 1898, Tscherning devised an "aberrascopes" for investigating the effects of accommodation upon spherical aberration. He suggested that during accommodation the aberration was over-corrected. Gullstrand (1909) criticised Tscherning's method, declaring that "subjective stigmatoscopy, employed as a scientific method, demonstrates a positive aberration inside

the optical zone even with the most powerful accommodation".

Ames and Proctor (1921) attempted to measure spherical aberration along two meridians in the relaxed eye. Using three subjects they found that from the centre of the pupil, to a radius of about 1.5 mm, the eye showed positive aberration (under corrected spherical aberration). This aberration decreased from 1.5 mm to the pupil margin, tending to become zero at the edge. The average amount of aberration was rather more than half a dioptre.

Pi (1925) divided the pupil area of the homotropinized eye into a central zone and four peripheral quadrants and by using the skiascopic method, he investigated the spherical aberration of fifty patients. He showed that most of his subjects had under-corrected spherical aberration ranging from 0.25 to 5.00 D depending on the subject and upon the quadrants studied. The peripheral quadrant was 1.0 to 1.5 D myopic relative to the centre.

A similar investigation was reported by Stine (1930) who studied 277 normal eyes. He found that the type and degree of aberration was not dependent on the type or amount of refractive error. Positive aberration was the most frequent, especially in adults, but negative aberration and mixed

aberration (scissor movement) were detected in more than 40% of children. Also he pointed out that the crystalline lens was a most important factor in producing the aberration of the eye.

In 1945, an investigation of the spherical aberration of 30 eyes was undertaken by Von Bahr. He used an aberrometer constructed on Scheiner's principle. The study was carried out along the horizontal and vertical meridians of the pupil. The investigation showed the most eyes exhibited positive spherical aberration, the zones of the pupil becoming gradually more myopic from the centre of the pupil outward.

Ivanoff (1947, 1953) measured the spherical aberration using the direct method, based on a principle suggested by Le Grand. He measured the spherical aberration out to 2.0 mm from the centre of pupil. The results showed that along a single meridian the outer zones of the average eye exhibited approximately 0.9 D of positive spherical aberration in the relaxed state, and 1.25 D of negative spherical aberration when accommodated by 3.0 D. However, there was practically no aberration present when the eye was accommodated by 1.5 D.

Wertheimer (1955) and Koomen et al (1949) criticised the interpretation of Ivanoff's experimental results. In 1956, Ivanoff rectified his previous data which then became compatible with other spherical aberration measurements.

Jenkins (1963) investigated the spherical aberration of 164 eyes. He concluded that the spherical aberration of the human eye differs from one person to another and from meridian to meridian. Spherical aberration was also dependent upon age. In subjects aged between 5 and 60 years, 75% showed positive spherical aberration whilst in subjects less than 5 years old, 80% showed negative spherical aberration. In addition, subjective measurements showed that spherical aberration at a point more than 1.5 mm from the centre of the cornea was much less than calculated from the theoretical eye.

Schober et al (1968) proposed the term monochromatic aberration, as they noticed that the different methods of measuring spherical aberration not only worked with varying degrees of accuracy, but could also supply markedly different results for one and the same eye.

Knowledge of the high order aberrations of the eye is still very limited but has been studied by Howland and Howland (1976, 1977). They designed an aberroscope similar to Tscherning's instrument, but with a strong  $\pm 5$  D crossed cylinder lens used to defocus the source. The analysis of the data revealed a wide variety of type and severity of monochromatic aberrations of normal eyes. They found that spherical aberration was often dominant about one meridian, a feature they termed 'cylindrical aberration'. In addition, the third order (coma-like) aberration plays a predominant role in wave aberrations at all pupil sizes.

### 5.3 Effect of contact lenses on the spherical aberration of the human eye

As described in Chapter 1, Westheimer (1961) has observed that spherical aberration is the most important aberration in contact lens wear, since contact lenses have a relatively high curvature over a relatively small entrance pupil.

Millodot (1969) investigated the variation of visual acuity with corneal contact lenses. He reported that at low luminance the visual acuity decreases, since the spherical aberration increases as the pupil size increases.

In 1974, Kerns fitted 20 patients with corneal contact lenses having an aspheric front surface. The analysis of the data indicated that there was a mean increase of 6.54 percent Snell-Sterling visual efficiency. This improvement in visual acuity was attributed to the reduction in the size of the circle of least confusion, due to the spherical aberration.

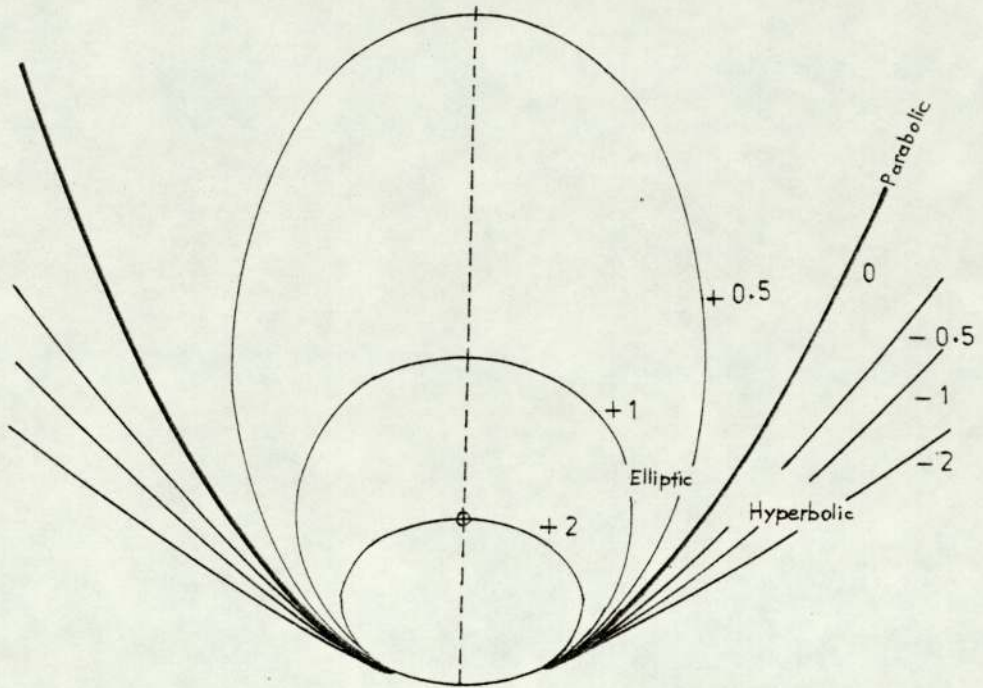
Following the introduction of hydrogel lenses, Wichterle (1967) described the aberration phenomena in fitting such contact lenses. He suggested that the first step in the elimination of spherical aberration lay in the theoretical treatment of the interaction between the lens and the corneal surface. Also, he reported that the shape constant

(shape constant  $S = 1 - e^2$  where  $e^2$  is the shape factor and  $e$  is the eccentricity) of the normal human eye is about  $0.75 \pm 0.20$ . Thus the optical zone of the cornea is spherical with a small elliptic deviation; therefore, the normal eye is subject to spherical or more correctly, elliptic aberration. To compensate for this aberration, the fitted hydrogel lens must have an anterior surface of a parabolic or at least a spherical shape to result in a shape constant of 0.0 or at least 1.0. Figure 5.1 illustrates types of curves as characterised by the shape constant  $S$ .

Millodot (1975) pointed out that the corneal contact lenses has spherical front surface, therefore, the effect of the spherical aberration is significant at low levels of luminance, but the flexible nature of hydrogel lenses permits the aspherical nature of the cornea to reassume its role in reducing the spherical aberration.

Woo and Sivak (1976) tried to measure the effect of corneal and hydrogel contact lenses on the spherical aberration of the human eye. The analysis of their data showed that there was very little difference in the value of spherical aberration whether corneal or hydrogel contact lenses were worn.

Wechsler (1978) studied the visual acuity in corneal and hydrogel contact lens wearers. The conclusion to be drawn from his data that the percentage of hydrogel lenses wearers



surface with  $S < 1$  has a greater rate of flattening at the periphery

surface with  $S = 1$  almost no peripheral flattening

surface with  $S > 1$  is steeper in the peripheral region

FIGURE 5.1

Diagram illustrating types of curves as characterized by the shape constant  $S$  (after Wichterle 1967)

having decrease in the visual acuity were more than those wearing corneal contact lenses. He attributed this decrease in visual acuity to the spherical aberration and lens surface defects.

#### 5.4 Apparatus

Measurements of the curvature and shape constant of the cornea and front surface of hydrogel lenses in situ on the human eye poses at least two problems:

- (1) The instrument should give data at many points simultaneously
- (2) The data should be available in both absolute and relative values

An apparatus which satisfies these two conditions is a photoelectric keratoscope, the "PEK", System 2000, manufactured by the Wesley-Jessen Co. of Chicago was available and was therefore used in the present study. This instrument was designed to study corneal topography, and give a measure of both the curvature and the shape constant of the cornea in two principal meridians.

The PEK consists of seven concentric rings arranged to provide a flat image plane. These rings approximate to an ellipsoidal surface with diameters 3 to 9 mm in 1 mm steps.

The four points in the central ring are used for the measurement of central corneal curvature. The system is attached to a polaroid camera. The photokeratogram may be analysed by a computer which maps the corneal profile in two meridians. Each meridian could be analysed for the exact location of the reflection points corresponding to each of the seven target rings. This information is computed in terms of sagittal depths and semi-chord lengths up to a maximum of 14 points per meridian.

#### 5.5 Experimental procedure

The PEK was calibrated by measuring the radius of curvature of five standard ball bearings of diameters 7.937, 7.143, 6.349, 5.550 and 4.760 mm.

To measure the curvature and shape constant of the human cornea and front surface of hydrogel lenses, five male myopic subjects were selected for this experiment with less than 1.4 D ocular astigmatism. Their ages were between 25-30 years. Each subject was fitted with a Bausch and Lomb SOFLENS in accordance with the B & L fitting manual. All lenses were fitted flatter than the flattest meridian of the cornea, and a good fit was judged when 1mm lag of lens movement was obtained on blinking.

After each subject had fully adapted to his lenses by two months of comfortable all day wear, the front surface of

each SOFLENS was photographed in situ on the eye using the PEK. The SOFLENS was then removed and the corneal profile was photographed, again with the aid of the PEK.

#### 5.6 Calculation of the spherical aberration of the SOFLENS<sup>R</sup> in air

A computer program was obtained (Kidger 1978) to calculate the spherical aberration of spherical surfaces which may be expressed as a wave front aberration or as a Seidel aberration.

This program was modified to suit Aston University's ICL 19045 mainframe, and was used to calculate the aberration of SOFLENS in air before fitting, and then on the ten myopic eyes.

As described in chapter 1, the back surface of a SOFLENS is aspheric. This study will assume the back surface of a SOFLENS is spherical over the central 3 mm. The calculation of aberrations obtained by ray tracing procedure for three position heights of incidence (Y) from the optical axis of lens 0.5, 1.0 and 1.5 mm and the maximum value of wave front aberration (W) at Y = 1.5 mm for different SOFLENS employed in the investigation is given in table 5.1.

TABLE 5.1

Wave front aberration of SOFLENSES<sup>R</sup> (in air) at Y = 1.5 mm

vial label	W( $\mu$ )
-7.50 B3	-0.159
-6.50 B3	-0.135
-3.00 F	-0.065
-3.50 F	-0.082
-1.75 F3	-0.033
-0.50 J3	-0.007
-2.00 F3	-0.038
-2.50 F3	-0.049
-1.75 F3	-0.032
-1.75 J3	-0.035

5.7 Calculation of the spherical aberration of SOFLENSES<sup>R</sup> in situ on human eye

Due to the flexibility and hydrophilicity of hydrogel lenses (especially thin lenses, of central thickness  $< 0.15$  mm) such lenses tend to mould themselves to the eye. It should be noted that the tear film between the hydrogel lens and the cornea will be ignored, since the tear volume under a hydrogel lens is 1/10 the tear volume under a corneal contact lens, Polse (1979). Therefore, the back surface of hydrogel contact lens will be a replica of the front surface of the cornea.

As described in 5.5, the PEK was employed to photograph the corneas of ten eyes. The measurement of radii of curvature and shape constant in two meridians of the front surface of the cornea under test was considered as a complete representation of the back surface of SOFLENSES in situ. In addition, the front surface of the SOFLENSES fitted were photographed by PEK. The corresponding photokeratograms are shown in (Fig.5.2a,b) these were analysed by the computer, the scanning having been carried out for the seven rings. The printout of the topography of front surfaces for corneas and SOFLENSES are listed in appendix III.

Townsley (1970) suggested that corneal contour might quite accurately be represented by a conic section. So, in general the front and back surfaces of SOFLENSES in situ could be carried as aspherical surfaces.

The previous computer program was slightly modified to make it suitable for the calculation of aberrations in two meridians for the aspheric surfaces. The same procedure was repeated and the results of wave front aberrations of SOFLENSES in situ at height of incidence 0.5 mm to 4.0 mm in 0.5 mm steps are summarized in (Table 5.2) for the horizontal meridian and in (Table 5.3) for the vertical meridian.

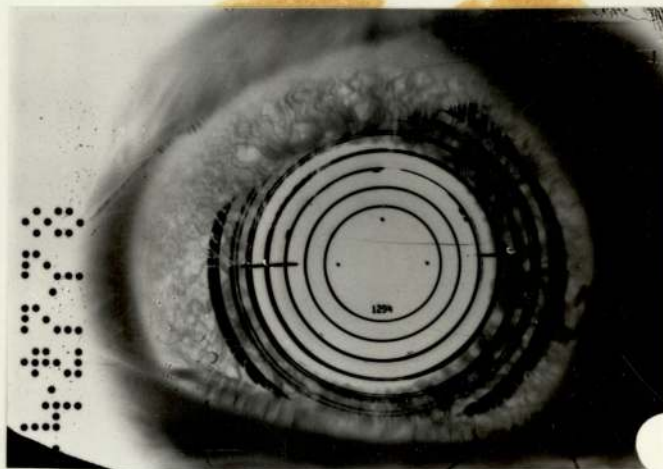


Figure 5.2a Photokeratogram of the Cornea for subject 7

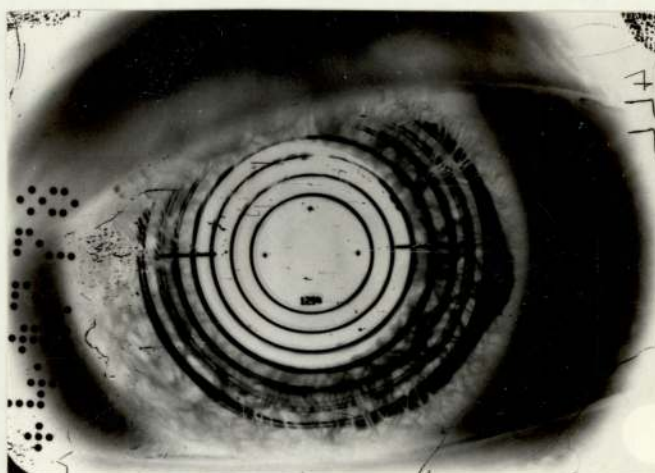


Figure 5.2b Photokeratogram of the front surface of the SOFLENS in situ for subject 7

Y (mm)	W(1)	W(2)	W(3)	W(4)	W(5)	W(6)	W(7)	W(8)	W(9)	W(10)
0.5	0.001	0.000	-0.001	-0.001	0.000	0.000	0.000	0.000	0.001	0.002
1.0	0.017	0.007	-0.018	-0.017	0.000	0.006	0.004	0.005	0.016	0.040
1.5	0.086	0.039	-0.093	-0.085	0.002	0.032	0.021	0.024	0.084	0.204
2.0	0.279	0.126	-0.299	-0.270	0.006	0.102	0.069	0.077	0.269	0.653
2.5	0.708	0.322	-0.744	-0.671	0.016	0.255	0.176	0.196	0.666	1.628
3.0	1.538	0.703	-1.579	-1.418	0.037	0.543	0.383	0.427	1.405	3.463
3.5	3.017	1.387	-3.008	-2.688	0.078	1.042	0.754	0.839	2.660	6.630
4.0	5.518	2.574	-5.303	-4.710	0.155	1.854	1.380	1.534	4.657	11.776

W(i) is the wave front aberration of sample number (i) and it is in microns

TABLE 5.2 illustrates the wave front aberration (W) of SOFLENSE<sup>R</sup> in situ for the horizontal meridian at height of incidence (Y) 0.5 mm to 4.0 mm.

Y (mm)	W(1)	W(2)	W(3)	W(4)	W(5)	W(6)	W(7)	W(8)	W(9)	W(10)
0.5	0.000	0.000	0.001	0.002	0.001	-0.001	-0.001	0.002	0.001	0.001
1.0	-0.002	0.000	0.021	0.033	0.014	-0.011	-0.016	0.025	0.021	0.014
1.5	-0.010	0.000	0.109	0.172	0.074	-0.057	-0.081	0.127	0.106	0.069
2.0	-0.030	0.001	0.356	0.559	0.024	-0.185	-0.259	0.411	0.340	0.223
2.5	-0.068	0.013	0.907	1.419	0.612	-0.465	-0.648	1.041	0.848	0.556
3.0	-0.124	0.055	1.983	3.090	1.330	-0.997	-1.384	2.259	1.809	1.180
3.5	-0.187	0.170	3.925	6.088	2.610	-1.925	-2.657	4.430	3.472	2.262
4.0	-0.222	0.445	7.267	11.214	4.780	-3.451	-4.726	8.108	6.182	4.022

W(i) is the wave front aberration of sample number (i) and it is in microns

TABLE 5.3 illustrates the wave front aberration (W) of SOFLENSES<sup>R</sup> in situ for the vertical meridian at height of incidence (Y) 0.5 mm to 4.0 mm

5.8 Calculation of the changes in SOFLENS parameters  
in situ on the human eye

The following information was obtained from the photo-keratogram printout as shown in appendix III and is listed fully in (Tables 5.4, 5.5).

- 1) The front and back central optic radii of lenses in air are " $R_1$ " and " $R_2$ "
- 2) The front and back central optic radii of lenses in situ are " $R_{1E}$ " and " $R_{2E}$ "
- 3) The shape constant of the front and back surfaces of lenses in situ are " $S_{1E}$ " and " $S_{2E}$ "
- 4) The labeled and calculated back vertex power of lenses in air (BVP)
- 5) The calculated values of the back vertex power of lenses in situ (BVPE)
- 6) The warp factor "C"

where  $C_{1E} = R_1/R_{1E}$  and  $C_{2E} = R_2/R_{2E}$

The suffix H and V will stand for horizontal and vertical meridian respectively.

Subject no.	Vial Label (D)	BVP (D)	R <sub>1</sub> (mm)	R <sub>2</sub> (mm)	S <sub>1HE</sub>	R <sub>1HE</sub> (mm)	C <sub>1HE</sub>	S <sub>2HE</sub>	R <sub>2HE</sub> (mm)	C <sub>2HE</sub>	BVPE (D)
1	-7.50B3	-7.50	9.67	8.25	1.18	8.62	1.12	0.79	7.85	1.05	-4.71
2	-6.50B3	-6.57	9.67	8.40	1.02	8.60	1.12	0.73	7.75	1.08	-5.26
3	-3.00F	-3.00	8.74	8.20	0.71	8.11	1.08	0.78	7.63	1.07	-2.98
4	-3.50F	-3.65	8.74	8.10	0.56	8.02	1.09	0.66	7.67	1.06	-2.73
5	-1.75F3	-1.80	9.34	8.95	0.81	8.03	1.16	0.76	7.78	1.15	-1.46
6	-0.50J3	-0.420	9.02	8.90	0.77	7.73	1.17	0.73	7.74	1.15	+0.39
7	-2.00F3	-2.07	9.34	8.90	0.92	8.04	1.16	0.81	7.72	1.15	-1.98
8	-2.50F3	-2.62	9.34	8.80	0.93	8.06	1.28	0.85	7.72	1.16	-2.07
9	-1.75F3	-1.80	9.34	8.95	0.65	8.38	1.11	0.44	8.04	1.11	-1.93
10	-1.75J3	-1.82	9.02	8.65	0.91	8.17	1.10	0.48	7.87	1.10	-1.72

TABLE 5.4 SOFLENSE parameters in air and in situ (Horizontal meridian)

Subject no.	Vial label (D)	BVP (D)	R <sub>1</sub> (mm)	R <sub>2</sub> (mm)	S <sub>1HE</sub>	R <sub>1HE</sub> (mm)	C <sub>1HE</sub>	S <sub>2HE</sub>	R <sub>2HE</sub> (mm)	C <sub>2HE</sub>	BVPE (D)
1	-7.50B3	-7.50	9.67	8.25	1.18	8.52	1.13	0.94	7.71	1.07	-5.16
2	-6.50B3	-6.57	9.67	8.40	1.25	8.41	1.15	0.99	7.64	1.10	-4.96
3	-3.00F	-3.00	8.74	8.20	1.17	7.84	1.12	0.87	7.40	1.11	-2.91
4	-3.50F	-3.65	8.74	8.10	1.27	8.12	1.08	0.82	7.61	1.06	-3.34
5	-1.75F3	-1.80	9.34	8.95	1.10	8.02	1.16	0.89	7.71	1.16	-1.87
6	-0.50J3	-0.42	9.02	8.90	0.77	7.68	1.17	0.88	7.69	1.16	+0.41
7	-2.00F3	-2.07	9.34	8.90	0.80	7.97	1.17	0.88	7.68	1.16	-1.81
8	-2.50F3	-2.62	9.34	8.80	1.12	7.94	1.18	0.83	7.64	1.15	-1.84
9	-1.75F3	-1.80	9.34	8.95	0.86	8.16	1.14	0.61	7.85	1.14	-1.81
10	-1.75J3	-1.82	9.02	8.65	0.79	8.02	1.12	0.63	7.79	1.11	-1.31

TABLE 5.5 SOFLENSE parameters in air and in situ (Vertical meridian)

The changes in lens parameters occurring on bending were investigated from the results in tables 5.4, 5.5.

The theoretical studies of the parameter changes of hydrogel lenses reported in the literature suggest two hypothesis.

#### 5.8.1 Equal change hypothesis

Kaplan (1966) has treated the problem using an oversimplified model, that is assuming that as the back surface of hydrogel lens bends, the front surface remains completely parallel to it. For example, if a lens of  $R_1 = 9.10$  mm,  $R_2 = 8.50$  mm and  $BVP = -3.0$  (centre thickness 0.17 mm, refractive index 1.44) steepened to become  $R_{2E} = 7.8$  mm the front radius should be  $R_{1E} = 8.4$  mm and  $BVPE = -3.53$ .

#### 5.8.2 Percentage change hypothesis

Strachan (1973) assumed that when a thin hydrogel lens bend or warped on the cornea, the percentage bend occurring on the back surface would be the same on the front surface if the refractive index and central thickness remained constant. Therefore, the warp factor  $C_{1E} = C_{2E}$ . For example, a hydrogel lens with radii of curvature  $R_1 = 9.10$  mm,  $R_2 = 8.50$  mm when bent with a warp factor 1.09, the front and back radii becomes  $R_{1E} = 8.35$  mm,  $R_{2E} = 7.80$  mm and  $BVPE = -3.23$ .

Holden et al (1976) investigated in an empirical manner the optical effects of bending hydrogel lenses. The study was carried out on 84 thin (0.18 mm) spherical minus powered lenses. The lenses were fitted on average 0.7 mm flatter than  $K_c$ . The mean fitting (warp) factor was  $1.090 \pm 0.043$ , BVPE was estimated clinically. The data was used to derive an empirical equation which relates the change in FCOR and change in BCOR.

$$\Delta\text{FCOR} = 1.133 + \Delta\text{BCOR} + 0.018$$

The correlation coefficient was 0.94

The equation relating the percentage change was,

$$\% \text{FCOR} = 0.997 \times \% \text{BCOR} + 0.547$$

The correlation coefficient was 0.947

5.9 Analysis of the results

- (1) The accuracy of the PEK for measuring radii of curvature is claimed as  $\pm 0.02$  mm
- (2) The shape constant  $S_{2E}$  of the ten eyes under investigation has a minimum value of 0.44 and maximum of 0.81 for the horizontal meridian. However, for the vertical meridian, the maximum value was 0.99 whilst the minimum value was 0.61. Hence all the surfaces of the corneas under test tend towards an elliptic shape with a prolate side. The horizontal meridian is flatter at the periphery than the vertical meridian (Fig. 5.3a)
- (3) The shape constant  $S_{1E}$  of the front surface of the SOFLENSES in situ tend to have values more than those of the corneal surfaces in most cases in both the horizontal and vertical meridians (tables 5.4, 5.5 and Fig. 5.3b)
- (4) The wave front aberration for the horizontal and vertical meridians of SOFLENSES in situ and in air at height of incidence 1.5 mm (which represents an average pupil diameter 3 mm at ambient luminance) is less than  $\pm \lambda/4$ , except in the case of subject number ten horizontal and subject number four vertical (Fig. 5.4). According to Rayleigh's Criterion, wave front aberration of less than  $\lambda/4$  may be neglected.

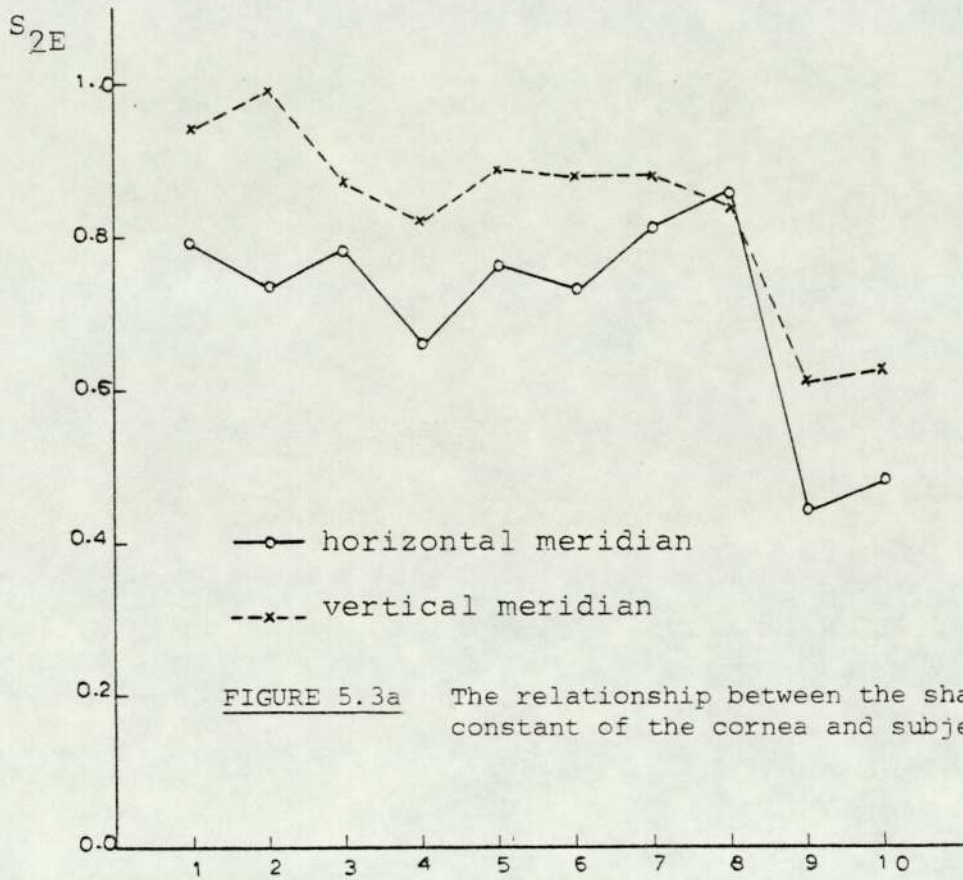


FIGURE 5.3a The relationship between the shape constant of the cornea and subject number

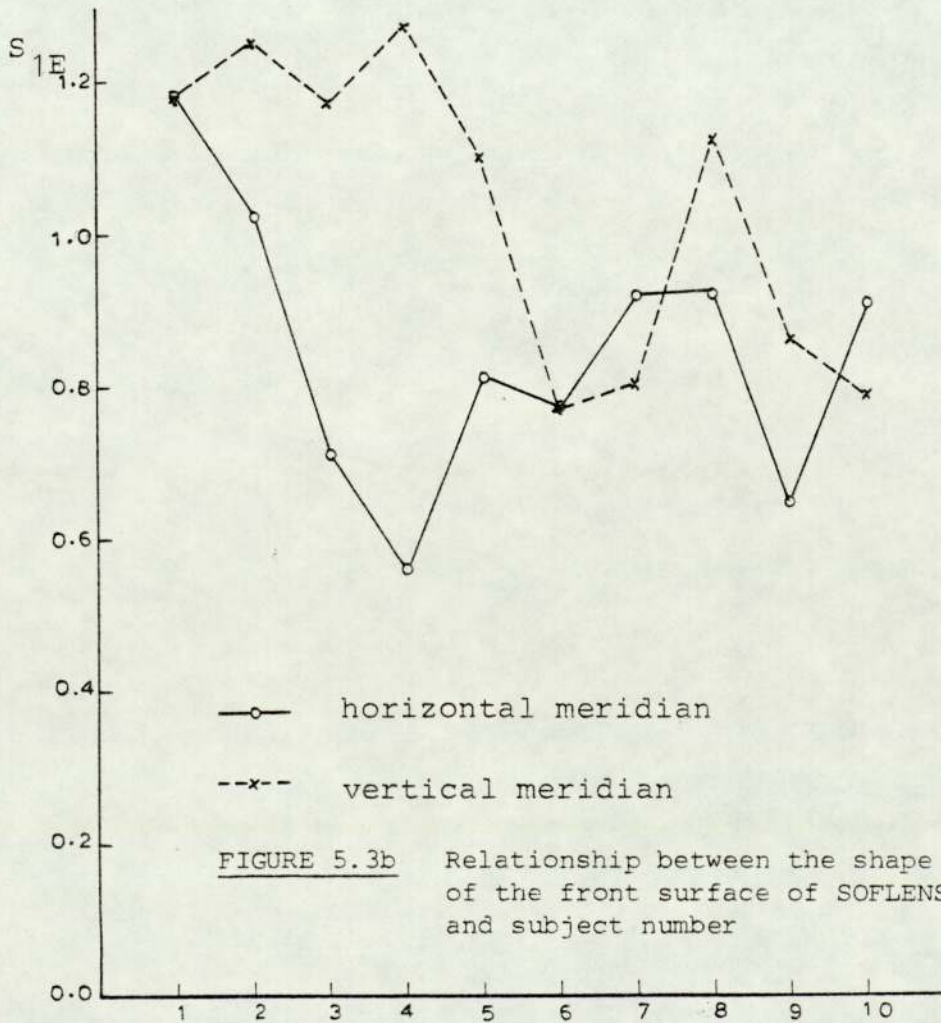
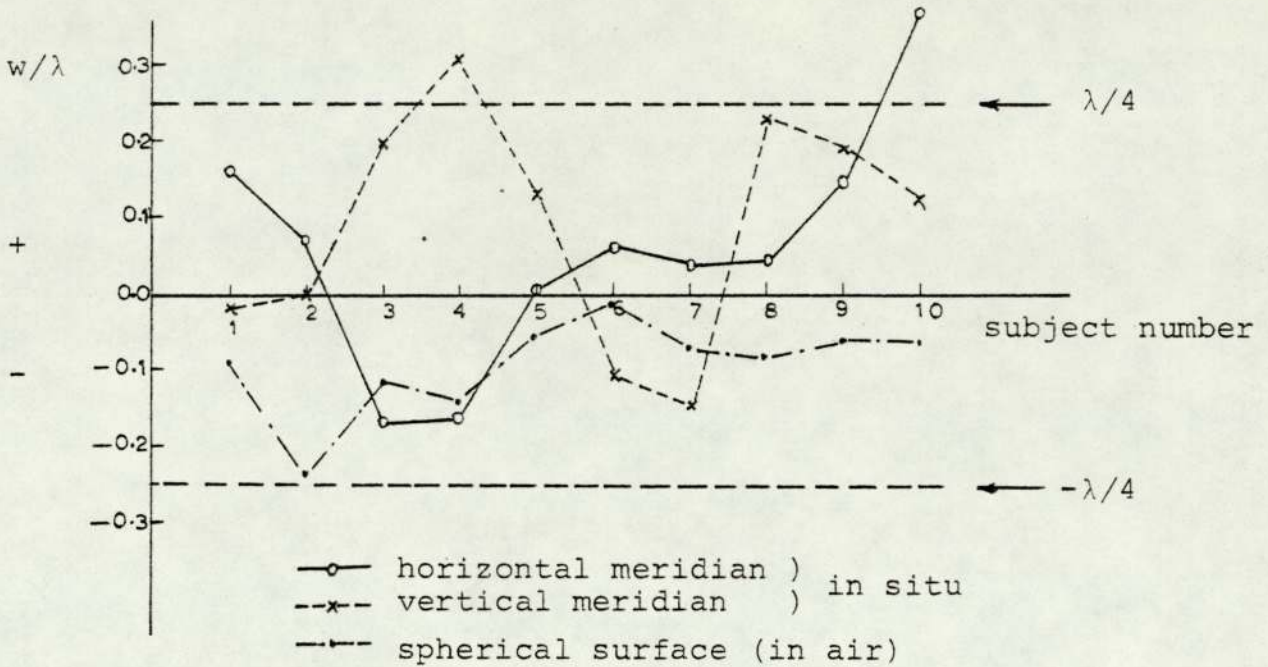


FIGURE 5.3b Relationship between the shape constant of the front surface of SOFLENSES <sup>R</sup> and subject number

Figure 5.4



At low luminance the pupil diameter may increase up to 8 mm or more. (Fig. 5.5) shows the calculated spherical aberration at height of incidence  $Y = 4$  mm, which suggests that the spherical aberration has a high effect which could not be ignored.

- (5) The change in Front Central optic radii of the SOFLENSES in situ is more than the change in the back central optic radii. Consequently all the minus powered lenses showed a decrease in lens power except in the vertical meridian for two subjects (number 5 and 9) and one subject (number 9) in the horizontal meridian (tables 5.4 & 5.5)



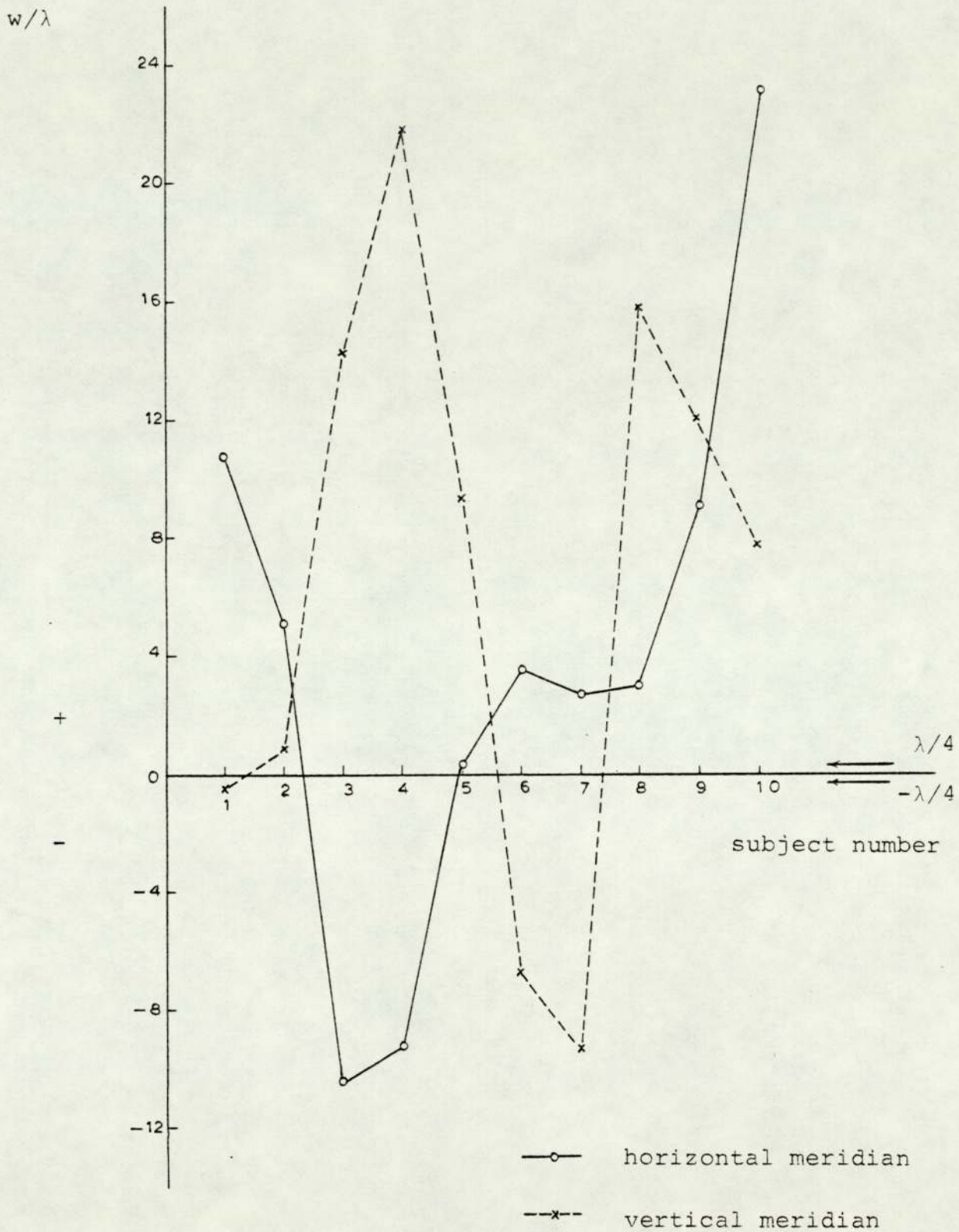


FIGURE 5.5

Illustrates the relationship between (the wave front aberration)/ $\lambda$  and subject number at a pupil diameter of 8 mm.

## CHAPTER 6

### Conclusion

#### 6.1 General discussion and conclusion

##### Curve measurement:

The importance of measuring hydrogel lens radii of curvature, and in particular the back central optic radius has promoted a considerable amount of research interest. The methods and instruments reported in the literature, and the commercially available apparatus, can be classified into three major groups assuming that the measurements are carried out in saline.

1. Sagittal height
2. Profile projection
3. Keratometry

With the first technique the problems are due to:

- i. Disturbance of the back surface of the hydrogel lens as soon as the probe touches the inside surface.
- ii. It is applicable only to the spherical surfaces. Unfortunately lathe cut hydrogel lenses are not usually spherical due to inhomogeneity in the hydrogel material which results in an aspheric back surface (Holden 1977). Also, in the case of spun cast lenses

the nature of the manufacturers process results in an aspheric back surface.

Profile projection also suffers from the problems of the asphericity of the lens surfaces, and in addition there is considerable difficulty in defining the back surface of the lens.

Keratometry presents difficulties in low power lenses where the mire images are close together. The keratometer is designed to measure the convex surface of the cornea, so errors will be present in the measurement of concave surfaces.

Having considered the difficulties of the existing measurement techniques this study was concerned with the development of a technique based upon interferometry. The problem to be solved was complicated by the following factors:-

1. The hydrogel contact lens has highly curved surfaces
2. The low reflection factor due to the small difference in refractive indices of hydrogel lens and saline
3. The instability of the hydrogel lens in saline

In order to overcome these difficulties, the Linnik micro-interferometer was used in conjunction with a novel cell-lens system. This two beam interferometer may be used for highly curved surfaces (Mukura, 1954). The instrument has a series of reference mirrors which allow samples of low reflection factor to be examined. Finally, the special cap in the cell-lens system minimises the distortion occurring on the lens surface.

The measured parameters Front and back central optic radii of curvature and central thickness of SOFLENSES showed close agreement with the manufacturer's published results. The accuracy achieved by this method was  $\pm 0.001$  mm (El-Nashar et al, 1979).

Refractive index measurement:

The inaccuracy of measuring the refractive index of hydrogel materials using an Abbe refractometer led to the use of the Linnik micro-interferometer. The experimental results show a closer agreement to the theoretical data than those reported by Strachan (1975).

Spherical aberration:

This preliminary investigation showed that the effect of spherical aberration with hydrogel lens wear is important and is significant at low luminance. It is necessary to define and evaluate the amount of spherical aberration of the human eye, and then design a hydrogel lens with the suitable curvature and shape constant which will eliminate the spherical aberration introduced by the human eye.

This work could possibly examine one of the factors which causes a decrease in the visual acuity at low levels of luminance when the pupil is dilated.

The experimental results of changes in hydrogel lens curvature in situ, on the eye, is not in agreement with the theoretical predictions, based on the equal change or equal percentage hypotheses. But the results are in agreement with the experimental results of Holden et al (1976). Consequently, most of the minus powered lenses showed a decrease in lens power because the warp factor (flexure) of the front surface is more than that of the back surface.

6.2 Suggestions for further work

Curvature measurement:

1. A comparison mirror (reference mirror) with a very low refractive power, of about 10% reflectivity, could be manufactured to allow hydrogel lenses of high water content to be measured with the Linnik micro-interferometer.
2. The limited accuracy of  $\pm 0.001$  may be increased by improving the measurement of the diameter of the fringes on the interferogram.
3. A simplified interferometer with a calibrated eyepiece could be designed to count the number of rings in the interference pattern visible in the limited field of view.
4. The measurements of back central optic radius of the hydrogel lens could be carried out at different positions to determine the correct shape of the back surface of the lens.

Refractive index:

This experiment could be further improved by using a more suitable solution of known refractive index which did not interact with the hydrogel material. A solution of high refractive index would decrease the displacement between the two groups of interference fringes; this would be of particular benefit in the measurement of low water content materials.

Spherical aberration:

It is very important to continue this study on a different group of patients, in order to establish the relationship of the human eye - hydrogel contact lens system. This work could attempt to evaluate a precise design for the front surface of hydrogel lenses which would give the correct and desirable refractive power and eliminate the spherical aberration of the human eye.

APPENDIX I

```
0012 TRACE 1
0000 MASTER MAIN
0001 REAL LEAST SQ
0002 REAL M ST DEV
0003 CAL. RAD. OF CURVATURE OF SOFT CONTACT LENSES, CORR. COEFF.
0004 DIMENSION X11(17), Y1(17), XI(17), Z(17)
0005 DATA Y1/-.0002728, -.0005457, -.0008185, -.001091, -.001364, -.001637, -.0019,
0006 1-.002183, -.002457, -.002728, -.003001, -.003274, -.003547, -.003820, -.004093,
0007 1-.004366, -.004638/
0008 ALPHA3=17
0009 SX=0.0
0010 SY=0.0
0011 SX2=0.0
0012 SXY=0.0
0013 SY2=0.0
0014 DELTA1=0.0
0015 DELTA2=0.0
0016 DELTA3=0.0
0017 WRITE (6,65)
0018 65 FORMAT (5X, 'C1', 13X, 'C2', 11X, 'C3', 12X, 'RAD', /)
0019 C DO LOOP TO READ THE DATA POINTS
0020 DO 10 I=1, 17
0021 10 READ (5, 15) X11(I)
0022 DO 70 I=1, 16
0023 Z(I+1)=X11(I+1)-X11(I)
0024 70 CONTINUE
0025 80 FORMAT(F10.5)
0026 READ(5, 11) CSEST
0027 11 FORMAT(F0.0)
0028 15 FORMAT (2F8.4)
0029 C DO LOOP TO FORM THE VARIOUS SUMS
0030 DO 20 J=1, 17
0031 XI(J)=X11(J)*(0.0021739/2.0)
0032 SX=SX+XI(J)
0033 SY=SY+YI(J)
0034 SX2=SX2+XI(J)**2
0035 SY2=SY2+YI(J)**2
```

```

0036  SXY=SXY+XI(J)*YI(J)
0037  DELTA1=DELTA1+XI(J)*(XI(J)**2+YI(J)**2)
0038  DELTA2=DELTA2+YI(J)*(XI(J)**2+YI(J)**2)
0039  DELTA3=DELTA3+(XI(J)**2+YI(J)**2)
0040  CONTINUE
0041  ALPHA1= SX
0042  ALPHA2= SY
0043  BETA1= SX2
0044  BETA2= SXY
0045  BETA3= ALPHA1
0046  GAMA1= BETA2
0047  GAMA2= SY2
0048  GAMA3= ALPHA2
0049  P1=2.0*(ALPHA1*BETA2-ALPHA2*BETA1)
0050  P2=2.0*(ALPHA2*BETA3-ALPHA3*BETA2)
0051  Q1=2.0*(ALPHA1*GAMA2-ALPHA2*GAMA1)
0052  Q2=2.0*(ALPHA2*GAMA3-ALPHA3*GAMA2)
0053  R1=ALPHA2*DELTA1-ALPHA1*DELTA2
0054  R2=ALPHA3*DELTA2-ALPHA2*DELTA3
0055  C1=(Q1*R2-Q2*R1)/(P1*Q2-P2*Q1)
0056  C2=(P2*R1-P1*R2)/(P1*Q2-P2*Q1)
0057  C3=SQRT(C1**2+C2**2-(2.0/ALPHA3)*C1+BETA3-(2.0/ALPHA3)*C2+GAMA3+
0058  1 DELTA3/ALPHA3)
0059  RAD=C3*1.735
0060  C32=C3**2
0061  XBAR=SX/ALPHA3
0062  WRITE (6,30)C1,C2,C3,RAD
0063  FORMAT (3X,F6.3,8X,F6.3,8X,F6.3,8X,F6.3//)
0064  DO LOOP CAL-XES,ST ERROR,K,LEAST S9,ST DEV,COPR,COEFF.
0065  WRITE (6,35)
0066  FORMAT(4X,'XEST',12X,'XI(K)',11X,'X1EST',12X,'12X','7')
0067  DELTA2=(X-XEST)**2
0068  ANUM=0.0
0069  DEN=0.0
0070  T=0.0

```

```

0071 V=0.0
0072 DO 40 K=1,17
0073 XEST=SQRT(2.0*YI(K)*CZEST-YI(K)**2.0)
0074 X1EST=XEST*(2.0/0.0621739)
0075 ANUM1=(XEST-XBAR)**2
0076 DEN1=(XI(K)-XEST)**2+(XEST-XBAR)**2
0077 C=(XI(K)-XEST)
0078 DDM=X1I(K)-X1EST
0079 DELTA2=(XI(K)-XEST)**2
0080 T1=(YI(K)-XEST)**2
0081 V1=(XI(K)-XBAR)**2
0082 ANUM=ANUM+ANUM1
0083 DEN=DEN+DEN1
0084 T=T+T1
0085 V=V+V1
0086 WRITE (6,50)XEST,XI(K), X1EST,X1I(K),Z(K)
0087 50 FORMAT (1X,F8.3,8Y,F8.3,8X,F9.3,8Y,F9.1,8X,F8.3)
0088 60 CONTINUE
0089 WRITE (6,45)
0090 45 FORMAT (//5X,'ST ERR',12X,'ST DEV',12X,'CORR COEFF')
0091 ST ERR=SQRT(T/ALPHA3)
0092 ST DEV=SQRT(V/ALPHA3)
0093 AB=SQRT(ALPHA3/(ALPHAS-2))
0094 M ST DEV=AB*ST ERR
0095 CORR COEFF=SQRT(ANUM/DEN)
0096 WRITE (6,60)ST ERR,ST DEV,CORR COEFF
0097 60 FORMAT(3X,F10.6,8X,F10.6,8X,F10.6////)
0098 STOP
0099 END

```

Rad Radius of curvature in air (mm)  
C3 Radius of curvature in saline (mm)  
XEST Theoretical diameter of interference rings  
X1(K) Measured diameter of interference rings  
X1EST Apparent theoretical diameter of interference rings  
X1I(K) Apparent measured diameter of interference rings

APPENIDX II

DOCUMENT RES-BZF

C1 0.000 C2 5.320 C3 6.320 RA0 9.104

XEST	XI(K)	XIEST	XI(K)	Z
0-061	0-059	50-041	54-2	0-000
0-086	0-086	79-261	79-5	25-300
0-106	0-106	97-071	97-5	13-000
0-122	0-122	112-069	112-1	14-600
0-136	0-136	125-308	124-7	12-600
0-149	0-149	137-275	137-0	12-300
0-161	0-161	147-290	142-5	11-500
0-172	0-172	158-520	158-2	9-700
0-183	0-183	168-173	168-0	9-800
0-193	0-193	177-203	177-5	9-500
0-202	0-202	185-856	185-6	8-100
0-211	0-211	194-124	194-2	8-600
0-220	0-220	202-053	202-0	7-800
0-228	0-228	209-683	209-6	7-600
0-236	0-236	217-044	217-5	7-900
0-244	0-244	224-163	224-5	7-000
0-251	0-251	231-038	231-3	6-800

ST ERR 0.000592 ST DEV 0.055770 CORR COEFF 0.999742



DOCUMENT RES-E4F

C1	C2	C3	RAD	XI(K)	Z
0-003	6-034	6-014	9-123		
XEST	XI(K)	XIEST		XI(K)	Z
0-061	0-059	56-041		54-7	9-999
0-086	0-087	79-261		80-3	25-550
0-106	0-107	97-071		98-5	18-180
0-122	0-123	112-069		113-2	14-750
0-136	0-137	125-308		125-0	12-730
0-149	0-150	137-275		138-4	12-420
0-161	0-163	147-890		150-0	11-610
0-172	0-174	159-520		159-3	9-900
0-183	0-184	163-173		169-7	9-900
0-193	0-195	177-203		179-3	9-590
0-202	0-204	185-855		187-5	8-190
0-211	0-213	194-124		196-1	8-680
0-220	0-222	202-053		204-0	7-830
0-228	0-230	209-885		211-7	7-680
0-236	0-239	217-044		219-7	7-970
0-244	0-245	224-163		225-7	6-030
0-251	0-254	231-038		235-5	7-610

ST ERR 0-001848  
 ST DEV 0-056219  
 CORR COEFF 0-009446

DOCUMENT RES-94B

C1	C2	C3	RAD	X1I(K)	Z
0.003	6.363	6.363	3.501		
XEST	XI(K)	XTEST			
0.052	0.052	53.723		47.4	0.000
0.083	0.079	75.982		72.5	25.120
0.101	0.098	93.055		90.5	17.850
0.117	0.116	107.433		106.6	16.120
0.131	0.130	120.124		119.8	13.260
0.143	0.143	131.596		131.9	12.030
0.154	0.155	141.772		142.3	10.920
0.165	0.166	151.962		153.0	10.200
0.175	0.177	161.215		162.7	9.690
0.185	0.185	169.371		170.6	7.870
0.194	0.195	178.167		179.5	3.960
0.202	0.204	186.092		187.7	8.160
0.211	0.212	193.693		194.3	7.160
0.218	0.219	201.007		201.7	6.850
0.226	0.229	208.063		210.8	9.140
0.234	0.237	214.883		217.8	6.940
0.241	0.244	221.473		224.1	6.330

ST EWR 0.002532  
 ST DEV 0.055507  
 CORR COEFF 0.998869

DOCUMENT RES-86F

C1	C2	C3	RAD	XI(K)	XIEST	XII(K)	Z
0.000	6.845	6.145	9.133	0.064	50.041	58.6	0.000
0.061	0.090			0.070	79.261	82.6	23.930
0.086	0.109			0.109	97.071	99.9	17.360
0.106	0.124			0.124	112.059	114.0	14.080
0.122	0.138			0.138	125.308	126.8	12.770
0.136	0.151			0.151	137.275	138.7	11.900
0.149	0.163			0.163	147.890	150.0	11.270
0.161	0.174			0.174	158.520	160.0	10.040
0.172	0.185			0.185	168.173	169.8	9.850
0.183	0.194			0.194	177.293	178.6	8.750
0.193	0.204			0.204	185.856	187.3	8.710
0.202	0.213			0.213	194.124	195.7	8.440
0.211	0.222			0.222	202.053	204.0	8.260
0.220	0.230			0.230	209.633	211.4	7.410
0.228	0.239			0.239	217.044	219.6	8.130
0.236	0.246			0.246	224.163	225.9	6.520
0.244	0.252			0.252	231.038	232.0	6.140

ST EIR      ST DEV      CORR COEFF  
0.002159      0.055104      0.999245

DOCUMENT RES-B6B

C1	C2	C3	RAD	XI(K)	XIEST	XI(K)	Z
-0.001	6.120	6.120	3.170				
				XI(K)	XIEST	XI(K)	Z
				0.056	52.769	51.5	0.000
				0.080	74.533	73.6	22.130
				0.099	91.403	90.8	17.140
				0.114	105.525	104.9	14.080
				0.127	117.990	117.3	12.440
				0.140	129.258	128.9	11.630
				0.151	139.254	139.2	10.300
				0.162	149.263	148.7	9.490
				0.172	158.352	158.1	9.380
				0.181	166.854	166.5	8.360
				0.190	175.002	175.0	8.570
				0.199	182.787	183.1	8.060
				0.209	190.253	192.6	9.490
				0.215	197.436	197.6	4.990
				0.222	204.367	204.5	6.940
				0.230	211.070	211.4	6.940
				0.237	217.543	218.0	6.520

ST ERR 0.000849      ST DEV 0.052856      CORR COEFF 0.999568

DOCUMENT RES-F2F

C1	C2	C3	RAD	X1(K)	X1EST	X11(K)	Z
0.001	6.472	6.472	0.639				
XEST	XI(K)	XIEST		X1(K)			Z
0.060	0.056	54.785		51.2			0.000
0.065	0.062	77.767		75.5			24.280
0.104	0.101	95.241		92.8			17.340
0.120	0.117	109.956		107.5			14.690
0.134	0.132	122.965		121.4			13.870
0.146	0.144	134.686		132.8			11.420
0.158	0.156	145.101		143.5			10.710
0.169	0.167	155.531		153.7			10.200
0.179	0.177	165.002		162.0			9.080
0.189	0.187	173.862		171.9			9.080
0.198	0.196	182.352		180.1			8.260
0.207	0.205	190.463		188.7			8.770
0.215	0.214	198.243		197.1			8.160
0.224	0.223	205.729		204.7			7.650
0.231	0.230	212.951		211.8			7.140
0.239	0.237	219.936		218.3			6.430
0.246	0.244	226.681		224.2			5.920

ST ERR 0.002238 ST DEV 0.054899 CORR COEFF 0.999153

DOCUMENT RES-F2B

C1	C2	C3	RAD	XI(K)	YI(K)	Z
0-002	6-363	6-363	3-495	0-046	53-745	0-000
0-058	0-077	76-013		0-077	76-013	26-720
0-083	0-096	93-092		0-096	93-092	18-160
0-101	0-113	107-476		0-113	107-476	15-500
0-117	0-128	120-172		0-128	120-172	13-880
0-131	0-141	131-648		0-141	131-648	11-520
0-143	0-153	141-823		0-153	141-823	11-120
0-154	0-164	152-025		0-164	152-025	10-100
0-165	0-174	161-279		0-174	161-279	9-590
0-175	0-185	169-539		0-185	169-539	9-380
0-185	0-194	178-235		0-194	178-235	8-670
0-194	0-202	186-167		0-202	186-167	7-750
0-202	0-211	193-771		0-211	193-771	7-750
0-211	0-219	201-087		0-219	201-087	7-250
0-219	0-227	208-146		0-227	208-146	7-550
0-226	0-235	214-974		0-235	214-974	7-240
0-234	0-242	221-566		0-242	221-566	6-200
0-241						

ST ERR 0-003640 ST DEV 0-055963 CORR COEFF 0-907810

DOCUMENT RES-F4F

C1	C2	C3	RAD	XI(K)	XIEST	XII(K)	Z
0.001	6.571	6.571	8.772				
XEST	XI(K)	XIEST	XII(K)	Z			
0.060	0.066	54.985	60.6	6.060			
0.085	0.089	77.767	81.6	21.010			
0.104	0.107	95.241	98.3	16.730			
0.120	0.123	109.956	113.2	14.890			
0.134	0.137	122.945	125.7	12.440			
0.146	0.150	134.686	137.7	12.040			
0.158	0.161	145.101	147.9	10.200			
0.169	0.172	155.531	158.3	10.400			
0.179	0.182	165.002	167.5	9.920			
0.189	0.192	175.862	176.5	9.180			
0.198	0.202	182.352	185.6	9.160			
0.207	0.210	190.463	193.0	7.340			
0.215	0.219	198.243	201.3	8.370			
0.224	0.226	205.729	208.1	6.730			
0.231	0.234	212.951	215.6	7.550			
0.239	0.243	219.936	223.4	7.750			
0.246	0.248	226.681	228.3	4.920			

ST ERR 0.003078 ST DIV 0.053362 CORR COEFF 0.998107

DOCUMENT RES-F4B

C1	C2	C3	RAD	XI(K)	XIEST	XII(K)	Z
0.003	6.053	6.053	6.081				
XEST	XI(K)	XIEST	XII(K)	Z			
0.057	0.056	52.769	51.0	0.000			
0.081	0.081	74.633	75.0	23.150			
0.099	0.100	91.403	92.3	17.340			
0.115	0.115	105.525	106.1	13.770			
0.128	0.129	117.990	119.1	13.060			
0.140	0.142	129.258	130.2	11.110			
0.151	0.153	139.254	140.3	10.100			
0.162	0.164	149.263	150.6	10.200			
0.172	0.174	158.352	160.1	9.590			
0.181	0.183	166.354	168.3	8.160			
0.190	0.192	173.002	177.1	6.770			
0.199	0.201	182.787	184.8	7.750			
0.207	0.209	190.253	192.5	7.650			
0.215	0.217	197.436	199.5	7.040			
0.222	0.225	204.367	206.8	7.240			
0.229	0.232	211.070	213.6	6.630			
0.236	0.238	217.543	218.9	5.480			

ST ERR                    ST DEV                    ST CORP COEFF  
 0.001728                    0.055053                    0.999454



DOCUMENT RES-F65

C1 0-004 C2 5-907 C3 5-907 RAD 7-886

XEST	XI(K)	XIEST	XII(K)	Z
0-056	0-051	51-775	46-9	0-090
0-080	0-077	75-227	71-0	24-070
0-097	0-096	89-691	88-4	17-440
0-113	0-115	103-538	103-6	15-200
0-126	0-127	115-768	116-5	12-850
0-138	0-139	126-324	127-7	11-220
0-149	0-151	136-651	138-7	11-020
0-159	0-161	146-451	148-0	9-280
0-169	0-171	155-369	157-6	9-590
0-178	0-180	163-711	165-9	8-360
0-187	0-189	171-705	174-1	8-160
0-195	0-198	179-563	182-1	7-960
0-203	0-206	186-668	189-3	7-240
0-211	0-214	193-717	196-9	7-550
0-218	0-221	200-517	203-7	6-830
0-225	0-229	207-094	210-6	6-940
0-232	0-235	213-445	216-5	5-890

ST ERR C-002765 ST DEV 0-053509 CORR COEFF 0-998546

DOCUMENT RES-J2F

C1	C2	C3	RAD
-0.000	6.333	6.333	6.322

XEST	XI(K)	XIEST	X1I(K)	Z
0.059	0.056	54.052	51.2	0.000
0.083	0.080	75.419	74.0	22.750
0.102	0.100	93.590	91.8	17.850
0.117	0.116	108.050	106.9	15.100
0.131	0.130	120.814	119.8	12.950
0.144	0.143	132.352	131.6	11.730
0.155	0.154	142.586	141.8	10.200
0.166	0.165	152.335	152.0	10.200
0.176	0.175	162.141	161.2	9.180
0.186	0.186	170.847	170.8	9.690
0.195	0.195	179.190	179.0	8.160
0.203	0.203	187.161	186.7	7.650
0.212	0.212	194.806	195.0	8.360
0.220	0.220	202.162	202.4	7.350
0.227	0.228	209.259	209.7	7.340
0.235	0.235	216.122	216.2	6.530
0.242	0.242	222.750	222.4	6.140

ST ERR	ST DEV	CORR COEFF
0.001271	0.054405	0.999715

DOCUMENT RES-J2B

C1	C2	C3	RAD	X1(K)	X1E2	X1I(K)	Z
0.001	6.028	6.028	8.047				
YEST	X1(K)	X1E2		X1I(K)			
0.053	0.052	52.931		48.1		0.000	
0.081	0.079	74.862		72.9		24.790	
0.100	0.098	91.603		90.3		17.340	
0.115	0.113	105.849		104.2		13.970	
0.129	0.127	118.352		117.3		13.060	
0.141	0.139	129.654		128.3		11.020	
0.152	0.151	139.680		138.7		10.400	
0.163	0.162	149.720		148.9		10.200	
0.173	0.171	158.837		157.6		8.670	
0.182	0.181	167.365		166.5		8.870	
0.191	0.190	175.538		174.9		8.470	
0.199	0.198	183.347		182.6		7.650	
0.207	0.206	190.836		189.9		7.340	
0.215	0.215	198.041		197.4		7.450	
0.223	0.222	204.993		204.5		7.140	
0.230	0.230	211.717		211.4		6.940	
0.237	0.236	218.210		217.4		5.970	

ST ERR 0.001694      ST DEV 0.055241      CORR COEFF 0.999479

DOCUMENT RES-J4F

C1	C2	C3	RAD	XI(K)	XIEST	XII(K)	Z
0.003	6.294	6.294	1.402				
XEST	XI(K)	XIEST	XII(K)	Z			
0.059	0.059	54.032	54.1	0.000			
0.083	0.083	76.619	76.7	22.640			
0.102	0.103	93.509	94.9	13.160			
0.117	0.118	106.050	108.6	13.770			
0.131	0.132	120.814	121.4	12.750			
0.144	0.145	132.352	133.5	12.440			
0.155	0.157	142.586	144.3	10.510			
0.166	0.168	152.835	154.5	10.200			
0.176	0.178	162.141	164.0	9.490			
0.186	0.187	170.847	171.7	7.650			
0.195	0.196	179.190	180.3	8.670			
0.203	0.205	187.161	188.3	7.950			
0.212	0.213	194.806	196.3	8.060			
0.220	0.221	202.162	203.7	7.340			
0.227	0.229	209.259	210.6	6.940			
0.235	0.236	216.122	217.5	6.830			
0.242	0.244	222.750	224.5	7.040			

CORR COEFF  
0.999652

ST DEV  
0.053292

ST ERR  
0.001412

DOCUMENT RES-J4E

C1	C2	C3	PAD	XI(K)	XIEST	Z
-0.003	5.900	5.900	7.876			
XEST	XI(K)	XIEST	XI(K)	Z		
0.056	0.056	51.943	52.0	0.000		
0.080	0.079	73.667	72.7	20.720		
0.098	0.097	89.974	89.6	16.360		
0.113	0.111	103.876	102.5	12.910		
0.126	0.125	116.146	115.3	12.820		
0.138	0.137	127.238	126.2	10.900		
0.149	0.143	137.077	136.1	9.880		
0.160	0.159	146.930	146.0	9.910		
0.169	0.168	155.876	154.7	8.700		
0.179	0.178	164.246	163.5	8.810		
0.187	0.186	172.266	171.0	7.530		
0.196	0.194	179.929	178.1	7.110		
0.204	0.202	187.279	185.5	7.370		
0.211	0.209	194.350	192.6	7.100		
0.219	0.217	201.172	199.2	6.640		
0.226	0.225	207.771	206.8	7.580		
0.233	0.232	214.142	213.8	6.990		

ST ERR                    ST DEV                    CORR COEFF  
 0.001298                    0.051117                    0.999502

DOCUMENT RES-J6F

C1 0.003 C2 6.427 C3 6.427 RAD 8.580

XEST	XI(K)	XTEST	X1I(K)	Z
0.059	0.063	54.032	58.3	0.000
0.083	0.087	76.419	79.2	21.420
0.102	0.106	93.590	97.2	17.470
0.117	0.121	108.050	111.6	14.430
0.131	0.135	120.814	124.4	12.850
0.144	0.148	132.352	136.3	11.830
0.155	0.160	142.586	147.2	10.920
0.166	0.171	152.035	157.1	9.890
0.176	0.180	162.141	165.9	8.870
0.186	0.190	170.847	175.1	9.180
0.195	0.199	179.190	183.2	8.060
0.203	0.208	187.161	191.3	8.160
0.212	0.217	194.806	199.3	7.960
0.220	0.225	202.162	206.8	7.440
0.227	0.232	209.259	213.9	7.140
0.235	0.240	216.122	220.8	6.940
0.242	0.247	222.750	227.0	6.180

ST ERR 8.004506 ST DEV 0.053795 CORR COEFF 0.996495

DOCUMENT RES-J6B

C1 0.003 C2 5.666 C3 5.666 RAD 7.564

XEST	XI(K)	XIEST	XII(K)	Z
0-056	0-042	51.102	38.2	0-000
0-079	0-071	72.275	65.5	27-230
0-096	0-091	88.515	83.3	17-850
0-111	0-107	102.191	98.4	15-100
0-124	0-120	114.262	110.7	12-240
0-136	0-133	125.174	122.4	11-730
0-147	0-144	134.853	132.6	10-200
0-157	0-155	144.546	142.4	9-790
0-167	0-165	153.348	152.0	9-590
0-176	0-174	161.581	160.3	8-360
0-184	0-183	169.472	158.3	7-960
0-192	0-191	177.010	176.1	7-750
0-200	0-200	184.240	183.6	7-550
0-208	0-208	191.197	190.9	7-340
0-215	0-215	197.908	197.4	6-430
0-222	0-222	204.399	204.0	6-630
0-229	0-228	210.668	210.2	6-150

ST ERR 0.004486 ST DEV 0.053608 CORR COEFF 0.996105

DOCUMENT RES-NZF

C1	C2	C3	RAD	X11(K)	Z
-0.001	6.232	6.232	8.320		
XEST	XI(K)	XIEST			
0.058	0.052	53.062		48.1	0.000
0.082	0.079	75.047		73.0	24.886
0.100	0.098	91.909		90.3	17.240
0.115	0.114	106.110		104.5	14.280
0.129	0.128	118.644		117.6	13.060
0.141	0.140	129.975		128.7	11.110
0.152	0.152	140.025		139.6	11.120
0.163	0.162	150.090		149.4	9.590
0.173	0.173	159.229		159.1	9.690
0.182	0.182	167.779		167.3	8.160
0.191	0.191	175.972		175.6	8.360
0.200	0.200	183.800		183.9	8.270
0.208	0.208	191.307		191.8	7.850
0.216	0.217	198.530		199.4	7.650
0.223	0.224	205.500		206.2	6.830
0.231	0.232	212.240		213.1	6.840
0.238	0.238	218.749		219.2	6.120

ST ERR 0.001653      ST DEV 0.055914      CORR COEFF 0.904516

DOCUMENT RES-N2B

C1  
 0.001  
 C2 5.895  
 C3 5.895  
 RAD 7.870

XEST	XI(K)	XIEST	X1I(K)	Z
0.056	0.055	51.945	50.2	0.000
0.080	0.079	73.667	72.4	22.240
0.098	0.096	89.974	88.7	16.320
0.113	0.112	103.876	103.2	14.480
0.126	0.126	116.146	116.1	12.860
0.138	0.138	127.232	126.9	10.810
0.149	0.150	137.977	137.9	11.010
0.160	0.160	146.930	146.0	8.920
0.169	0.170	155.876	156.3	9.320
0.179	0.179	164.245	164.8	8.570
0.187	0.188	172.265	172.9	8.060
0.196	0.196	179.929	180.5	7.650
0.204	0.205	187.279	188.7	8.160
0.211	0.212	194.350	195.3	6.630
0.219	0.220	201.172	202.3	6.940
0.226	0.227	207.771	208.9	6.630
0.233	0.233	214.142	214.6	5.740

ST ERR 0.000984  
 ST DEV 0.052315  
 CORR COEFF 0.999117

DOCUMENT RES-N4F

C1 -0.001 C2 6.028 C3 6.028 RAD 3.048

XEST	XI(K)	YTEST	XI(K)	Z
0.058	0.352	55.042	55.0	0.000
0.082	0.081	75.047	74.3	21.220
0.100	0.099	91.909	90.9	16.620
0.115	0.114	106.110	104.5	15.670
0.129	0.127	113.644	116.8	12.240
0.141	0.139	129.975	128.1	11.320
0.152	0.151	140.025	139.2	11.120
0.163	0.161	150.090	148.4	9.130
0.173	0.171	159.229	157.4	8.950
0.182	0.180	167.779	165.7	8.260
0.191	0.189	175.972	173.9	8.260
0.200	0.198	183.800	182.2	8.260
0.208	0.206	191.307	189.4	7.240
0.216	0.214	198.530	196.4	7.040
0.223	0.221	205.500	203.2	6.730
0.231	0.228	212.240	210.0	6.820
0.238	0.235	218.749	216.5	6.520

ST ERR 0.001912 ST DEV 0.051974 CORR COEFF 0.989339

DOCUMENT RES-N4B

C1	C2	C3	RAD	YI(K)	YIEST	XI(K)	Z
-0.005	5.728	5.728	7.647				
YEST	YI(K)	YIEST	XI(K)	Z			
0.056	0.054	51.102	54.6	0.000			
0.079	0.060	72.275	73.7	19.130			
0.096	0.097	88.515	89.2	15.550			
0.111	0.113	102.191	103.5	14.280			
0.124	0.124	114.252	114.4	10.910			
0.136	0.135	125.174	124.6	10.200			
0.147	0.145	134.253	133.1	8.470			
0.157	0.155	144.546	142.4	9.280			
0.167	0.165	153.348	152.0	9.590			
0.176	0.175	161.581	160.8	8.870			
0.184	0.183	169.472	168.2	7.960			
0.192	0.191	177.010	176.2	7.340			
0.200	0.199	184.240	183.1	6.940			
0.208	0.206	191.197	189.9	6.830			
0.215	0.214	197.903	197.1	7.140			
0.222	0.221	204.399	203.2	6.120			
0.229	0.227	210.668	208.8	5.620			

ST ERR 0.001595 ST DEV 0.049355 CORR COEFF 0.999503

DOCUMENT RES-N6F

C1 0.001 C2 6.065 C3 6.066 PAD 0.076

TEST	XI(K)	XIEST	XII(K)	Z
0.058	0.043	53.062	44.1	0.000
0.082	0.076	75.047	69.3	25.500
0.100	0.094	91.909	86.5	16.940
0.115	0.110	106.110	101.5	14.999
0.129	0.124	112.644	114.3	12.850
0.141	0.137	129.975	126.1	11.730
0.152	0.149	140.025	137.2	11.120
0.163	0.160	150.090	147.3	10.100
0.173	0.170	159.229	156.3	9.020
0.182	0.179	167.779	164.9	8.620
0.191	0.189	175.972	173.7	8.790
0.200	0.198	183.800	182.0	8.260
0.208	0.206	191.307	189.2	7.240
0.216	0.214	198.530	196.6	7.340
0.223	0.221	205.500	203.5	6.940
0.231	0.228	212.240	210.1	6.630
0.238	0.235	218.749	216.1	5.980

ST ERR 0.004254 ST DEV 0.056305 CORR COEFF 0.996755

DOCUMENT RES-N6B

C1 -0.001 C2 5.399 C3 5.399 RAD 7.200

XEST	XI(K)	XIEST	XII(K)	Z
0.054	0.054	50.080	49.5	0.070
0.077	0.076	70.322	70.2	20.780
0.094	0.093	86.744	85.3	15.040
0.109	0.108	100.147	99.1	13.810
0.122	0.120	111.976	110.7	11.580
0.133	0.132	122.670	121.5	10.810
0.144	0.144	132.153	132.1	10.640
0.154	0.152	141.654	140.2	8.140
0.163	0.162	150.279	148.9	8.610
0.172	0.170	158.348	156.2	7.300
0.181	0.178	166.080	164.3	8.010
0.189	0.187	173.468	171.8	7.590
0.196	0.195	180.553	179.8	8.090
0.204	0.202	187.370	186.5	6.450
0.211	0.209	193.948	192.3	6.010
0.218	0.216	200.309	198.5	6.040
0.224	0.223	206.451	205.3	6.980

ST ERR 0.001500 ST DEV 0.040323 CORR COEFF 0.999343

DOCUMENT RES-B3F2

C1 -0.005 C2 7.260 C3 7.260 RAD 9.692

XEST	XI(K)	XIEST	XII(K)	Z
0-063	0-052	57-334	47-5	0-000
0-059	0-079	51-796	72-4	26-950
0-109	0-100	100-176	92-4	20-000
0-126	0-112	115-654	103-0	10-600
0-141	0-133	129-316	122-7	19-700
0-154	0-146	141-666	134-6	11-910
0-166	0-159	152-621	146-3	11-720
0-178	0-170	165-591	156-6	10-200
0-189	0-181	173-552	166-7	10-100
0-199	0-191	182-871	175-9	9-290
0-208	0-202	191-802	185-5	9-600
0-218	0-210	200-334	193-4	7-870
0-227	0-220	208-517	202-0	8-590
0-235	0-228	216-391	210-1	8-080
0-243	0-237	223-988	217-7	7-580
0-251	0-245	231-335	225-5	7-870
0-259	0-252	238-430	232-3	6-770

ST ERR 0.008225 ST DEV 0.038647 CORR COEFF 0.990333

DOCUMENT RES-B5E2

C1 -0.003 C2 6.216 C3 6.216 RAD 9.233

XEST	XI(K)	XIEST	X1I(K)	Z
0.061	0.058	56.417	52.9	0.000
0.037	0.063	79.778	76.8	23.840
0.106	0.102	97.704	94.1	17.370
0.123	0.119	112.800	109.6	15.450
0.137	0.134	126.125	123.7	14.140
0.150	0.147	138.170	135.3	11.620
0.162	0.159	148.854	146.4	11.110
0.173	0.170	159.554	156.7	10.300
0.184	0.181	169.270	166.7	9.990
0.194	0.191	178.352	175.7	9.090
0.203	0.200	187.059	184.3	8.580
0.212	0.210	195.390	192.6	8.590
0.221	0.218	203.371	200.5	7.570
0.229	0.227	211.051	208.7	8.190
0.237	0.235	218.460	216.1	7.470
0.245	0.243	225.625	223.2	7.070
0.253	0.250	232.545	230.1	6.890

ST ERR 0.003011 ST DEV 0.056165 CORR COEFF 0.998554

DOCUMENT RES-B3F4

C1	C2	C3	RAD	XI(K)	XI(K)	XI(K)	XI(K)	Z
0.003	7.182	7.182	9.533	57.834	54.5	80.8	100.0	0.000
				81.796	80.8	100.0	115.1	26.260
				100.176	100.0	115.1	128.0	19.190
				115.654	115.1	128.0	141.5	15.150
				129.316	128.0	141.5	153.0	12.830
				141.666	141.5	153.0	163.5	13.630
				152.621	153.0	163.5	173.2	11.410
				163.591	163.5	173.2	183.1	10.310
				173.552	173.2	183.1	192.1	9.890
				182.871	183.1	192.1	200.6	9.900
				191.802	192.1	200.6	208.9	8.490
				200.334	200.6	208.9	217.2	8.280
				208.517	208.9	217.2	223.9	8.280
				216.391	217.2	223.9	231.6	6.770
				225.938	223.9	231.6	238.6	7.670
				231.355	231.6	238.6		6.970
				238.450	238.6			

ST ERR 0.001031      ST DEV 0.03801      CORR COEFF 0.999033

DOCUMENT RES-B5B4

C1 0.001 C2 6.621 C3 6.621 FAD 1.839

XEST	XI(K)	XIEST	XII(K)	Z
0.060	0.064	55.328	40.4	0.000
0.085	0.074	70.252	68.2	27.770
0.104	0.096	95.055	88.0	20.410
0.120	0.114	110.643	104.8	15.260
0.134	0.128	123.713	117.7	12.820
0.147	0.142	135.527	130.5	12.830
0.159	0.154	146.007	141.6	11.110
0.170	0.165	156.502	152.0	10.410
0.180	0.176	166.032	161.6	9.590
0.190	0.186	174.677	171.4	9.800
0.199	0.195	183.490	179.8	8.380
0.208	0.205	191.653	188.4	8.590
0.217	0.214	199.481	195.4	8.080
0.225	0.222	207.013	204.4	7.980
0.233	0.229	214.281	211.1	6.670
0.241	0.237	221.309	218.2	7.070
0.248	0.245	228.097	225.4	7.270

ST ERR 0.006524 ST DEV 0.057762 CORR COEFF 0.995055

DOCUMENT RES-B3F6

C1 0.004 7.239 7.289 9.731  
 C2 C3 RAD

XEST	XI(K)	XIEST	XII(K)	Z
0.063	0.065	57.834	59.7	0.000
0.089	0.091	81.796	83.7	24.210
0.109	0.111	100.176	101.8	18.170
0.126	0.128	115.654	118.0	16.140
0.141	0.142	129.316	131.0	13.080
0.154	0.156	141.656	145.1	14.090
0.166	0.170	152.621	156.3	11.160
0.178	0.182	163.501	167.3	11.040
0.189	0.192	173.552	177.0	9.640
0.199	0.202	182.871	185.9	8.970
0.208	0.213	191.603	195.6	9.650
0.218	0.221	200.334	203.7	8.070
0.227	0.231	208.517	212.7	8.990
0.235	0.239	216.391	219.7	7.050
0.243	0.248	223.988	227.9	8.160
0.251	0.255	231.335	234.9	7.050
0.259	0.264	238.430	242.5	7.520

ST EKR 0.003501 ST DEV 0.058076 CORR COEFF 0.993143

DOCUMENT RES-6386

C1 0.000 C2 6.403 C3 6.403 RAD 5.549

XEST	XI(K)	XIEST	XI(K)	Z
0.059	0.059	54.381	54.3	0.000
0.084	0.084	75.915	77.0	22.710
0.102	0.102	94.195	94.2	17.160
0.118	0.118	108.749	108.6	14.390
0.132	0.132	121.595	121.6	12.830
0.145	0.145	133.207	133.3	11.890
0.156	0.156	143.508	143.8	10.530
0.167	0.166	153.823	152.7	8.910
0.177	0.179	163.189	164.2	11.670
0.187	0.187	171.952	171.9	7.510
0.196	0.196	180.349	180.2	8.250
0.205	0.204	188.571	188.1	7.930
0.213	0.213	196.066	196.0	7.920
0.221	0.221	203.469	203.5	7.540
0.229	0.229	210.612	210.7	7.190
0.236	0.236	217.520	217.5	6.780
0.244	0.244	224.191	224.3	6.760

ST ERR 0.000457 ST DEV 0.053971 CORR COEFF 0.999964

DOCUMENT RES-F3F2

C1 -0.004 C2 7.127 C3 7.127 RAD 9.514

XEST	XI(K)	YIEST	XII(K)	Z
0.062	0.060	56.330	54.8	0.000
0.087	0.085	80.389	78.3	23.430
0.107	0.105	98.453	96.3	18.030
0.124	0.122	113.665	112.1	15.760
0.138	0.136	127.091	124.3	12.730
0.151	0.149	139.229	137.0	12.120
0.163	0.161	149.995	148.1	11.110
0.175	0.173	160.777	159.1	11.000
0.185	0.183	170.567	168.7	9.600
0.195	0.194	179.726	178.3	9.590
0.205	0.204	188.502	187.5	9.200
0.214	0.212	196.833	195.2	7.770
0.223	0.222	204.930	203.8	8.590
0.231	0.230	212.668	211.3	7.470
0.239	0.238	220.134	218.9	7.580
0.247	0.246	227.355	226.0	7.170
0.255	0.253	234.328	233.1	7.070

ST ERR 0.001958 ST DEV 0.056609 CORR COEFF 0.999456

DOCUMENT RES-F582

C1 -0.005 C2 6.710 C3 6.710 RAD 2.958

XEST	XI(K)	XIEST	XII(K)	Z
0-060	0-052	55-492	53-3	0-000
0-085	0-083	78-470	76-3	22-910
0-104	0-103	96-102	94-6	18-380
0-121	0-118	110-951	108-7	14-040
0-135	0-133	124-058	122-7	13-970
0-148	0-146	135-905	134-4	11-780
0-159	0-157	146-414	144-7	10-250
0-171	0-168	156-933	154-7	10-050
0-181	0-179	166-495	164-5	9-800
0-191	0-183	175-535	172-3	8-280
0-200	0-198	184-002	181-9	9-090
0-209	0-207	192-137	190-9	8-590
0-217	0-215	200-037	198-2	7-670
0-226	0-221	207-591	203-3	5-190
0-234	0-232	214-878	213-1	9-760
0-241	0-239	221-926	220-2	7-070
0-249	0-248	228-733	228-1	7-940

ST ERR 0.002283 ST DEV 0.054934 CORR COEFF 0.999139

DOCUMENT RES-F3F4

C1 0.001 C2 7.105 C3 7.105 RAD 9.486

YEST	XI(K)	XIEST	XII(K)	Z
0.062	0.067	56.839	61.0	0.000
0.087	0.091	60.384	63.3	21.720
0.107	0.110	93.453	101.5	18.190
0.124	0.127	113.665	116.7	15.160
0.138	0.141	127.091	129.6	12.930
0.151	0.154	139.229	142.0	12.430
0.163	0.167	149.995	153.5	11.510
0.175	0.179	160.777	164.3	10.810
0.185	0.189	170.567	173.6	9.290
0.195	0.199	179.726	182.8	9.190
0.205	0.209	188.502	191.4	8.580
0.214	0.218	196.888	200.3	8.390
0.223	0.227	204.930	208.7	8.390
0.231	0.235	212.668	215.8	7.170
0.239	0.243	220.134	223.6	7.770
0.247	0.251	227.355	230.3	7.170
0.255	0.258	234.328	237.4	6.670

ST ERR 0.003583 ST DEV 0.656217 CORR COEFF 0.997537

DOCUMENT RES-F304

C1

-0.000

C2

6.468

C3

6.468

RM

4.635

XEST  
 0-.059  
 0-.084  
 0-.102  
 0-.118  
 0-.132  
 0-.145  
 0-.156  
 0-.167  
 0-.177  
 0-.187  
 0-.196  
 0-.205  
 0-.213  
 0-.221  
 0-.229  
 0-.236  
 0-.244

XI(K)  
 0-.057  
 0-.081  
 0-.101  
 0-.117  
 0-.132  
 0-.144  
 0-.156  
 0-.167  
 0-.177  
 0-.187  
 0-.196  
 0-.205  
 0-.213  
 0-.221  
 0-.229  
 0-.237  
 0-.244

XIEST  
 54.381  
 76.913  
 94.195  
 109.749  
 121.595  
 133.207  
 143.506  
 153.823  
 163.189  
 171.952  
 180.340  
 188.371  
 196.066  
 203.469  
 210.612  
 217.520  
 224.191

X1I(K)  
 52.0  
 74.9  
 93.1  
 107.8  
 121.0  
 132.8  
 143.4  
 153.5  
 163.1  
 171.7  
 180.4  
 188.4  
 196.2  
 203.7  
 211.1  
 217.9  
 224.6

Z  
 0-.000  
 22-.930  
 18-.180  
 14-.650  
 13-.230  
 11-.810  
 10-.610  
 10-.100  
 9-.590  
 8-.590  
 8-.690  
 7-.970  
 7-.830  
 7-.530  
 7-.370  
 6-.770  
 6-.760

ST ERR  
 0.000647

ST DEV  
 0.054652

CORR COEFF  
 0.999645

DOCUMENT RES-F3F6

C1 -0.004 7.129 C2 7.129 C3 7.129 RAD 9.517

XEST	XI(K)	XIEST	XII(K)	Z
0-062	0-061	56-839	55-5	0-000
0-067	0-087	80-329	80-0	23-470
0-107	0-106	98-453	97-9	17-930
0-124	0-123	113-663	113-0	15-080
0-138	0-138	127-091	127-0	14-040
0-151	0-150	139-229	138-3	14-270
0-163	0-162	149-995	149-5	11-220
0-175	0-174	160-777	159-9	10-600
0-185	0-184	170-567	169-7	9-800
0-195	0-194	179-726	178-5	8-820
0-205	0-204	188-502	187-3	8-820
0-214	0-213	196-838	195-9	8-600
0-225	0-222	204-930	203-8	7-870
0-231	0-230	212-668	211-4	7-620
0-239	0-238	220-134	219-0	7-550
0-247	0-246	227-355	226-5	7-540
0-255	0-255	254-328	254-8	8-320

ST ERR 0-000934 ST DEV 0-056144 CORR COEFF 0-999842

DOCUMENT RES-F396

C1 0.002 C2 6.205 C3 6.205 RAD 3.224

XEST	XI(K)	XIEST	X1I(K)	Z
0.058	0.050	53.621	53.7	0.000
0.062	0.063	75.354	76.1	22.480
0.101	0.100	92.531	92.4	16.320
0.116	0.118	106.828	109.0	16.600
0.130	0.131	119.447	120.8	11.800
0.142	0.144	130.854	132.5	11.700
0.153	0.156	140.973	143.2	10.700
0.164	0.165	151.106	151.8	8.600
0.174	0.176	160.307	161.6	9.800
0.184	0.186	168.914	170.7	9.100
0.193	0.195	177.163	179.0	8.300
0.201	0.204	185.044	187.9	8.900
0.209	0.210	192.602	193.6	5.700
0.217	0.219	199.874	201.6	8.000
0.225	0.227	206.891	208.7	7.100
0.232	0.235	213.677	215.9	7.200
0.239	0.242	220.230	222.5	5.600

ST ERR 0.001842 ST DEV 0.053441 CORR. COEFF 0.999395

DOCUMENT RES-J3FZ

C1 -0.500 C2 6.775 C3 6.775 RAD 9.044

TEST	XI(K)	XIEST	XI(K)	Z
0.061	0.056	55.856	60.6	0.000
0.085	0.089	77.999	82.0	21.410
0.105	0.108	96.749	99.5	17.470
0.121	0.125	111.694	114.6	15.150
0.136	0.138	124.892	127.3	12.650
0.149	0.151	136.220	138.9	11.610
0.160	0.162	147.400	149.5	10.610
0.172	0.173	157.995	159.6	10.100
0.182	0.184	167.615	168.9	9.200
0.192	0.194	176.615	178.1	9.190
0.201	0.203	185.240	186.8	8.790
0.210	0.212	193.480	195.4	9.580
0.219	0.221	201.383	203.0	7.580
0.227	0.229	208.988	210.4	7.370
0.235	0.236	216.324	217.5	6.970
0.243	0.244	223.420	224.7	7.370
0.250	0.252	230.272	231.9	7.160

ST ERR 0.002420 ST DEV 0.154462 COEFF 0.999546



DOCUMENT RES-J3F4

C1	C2	C3	RAD	XI(K)	XI(K)	XI(K)	Z
-0.003	6.715	6.715	6.964	46.0	46.0	46.0	0.000
XEST	0.050	55.256		72.2	72.2	72.2	26.260
0.061	0.078	72.092		90.4	90.4	90.4	18.180
0.086	0.092	96.749		105.6	105.6	105.6	15.150
0.105	0.115	111.698		119.4	119.4	119.4	13.840
0.121	0.130	124.292		131.3	131.3	131.3	11.920
0.136	0.143	136.820		142.7	142.7	142.7	11.410
0.149	0.155	147.400		152.7	152.7	152.7	10.000
0.160	0.166	157.995		162.2	162.2	162.2	9.500
0.172	0.175	167.615		171.3	171.3	171.3	9.090
0.182	0.186	176.615		179.6	179.6	179.6	8.480
0.192	0.195	185.240		188.3	188.3	188.3	8.480
0.201	0.205	193.480		196.1	196.1	196.1	7.820
0.210	0.213	201.365		203.6	203.6	203.6	7.480
0.219	0.221	208.968		211.6	211.6	211.6	7.970
0.227	0.230	216.324		218.4	218.4	218.4	6.770
0.235	0.237	223.420		226.0	226.0	226.0	7.600
0.243	0.246	230.272					
0.250							

ST ERR 5.006298 ST DEV 0.036345 CORR COEFF 0.993655

DOCUMENT RES-J3B4

C1 -0.000 C2 6.235 C3 6.235 PAD 8.324

XEST	XI(K)	YIEST	X1I(K)	Z
0.058	0.054	53.421	53.1	0.050
0.022	0.032	75.554	75.8	22.620
0.101	0.100	92.531	92.2	16.430
0.116	0.116	106.323	106.8	14.620
0.130	0.130	119.447	119.5	12.500
0.142	0.142	130.254	130.7	11.390
0.153	0.154	140.973	141.5	-10.720
0.164	0.165	151.106	151.4	9.880
0.174	0.175	160.307	160.3	9.320
0.184	0.184	168.914	169.3	8.560
0.193	0.193	177.163	177.6	8.270
0.201	0.202	185.064	185.0	8.160
0.209	0.210	192.602	193.1	7.360
0.217	0.218	199.874	200.2	7.060
0.225	0.226	206.891	207.7	7.460
0.232	0.233	213.677	214.4	6.750
0.239	0.240	220.230	220.7	6.350

ST ERR 0.000475 ST DEV 0.053192 CORR COEFF 0.999955

DOCUMENT RES-J3F6

C1 -0.004 C2 6.246 C3 6.846 RAD 9.139

XEST	XI(K)	XIEST	XII(K)	Z
0.061	0.060	55.856	55.5	0.000
0.086	0.086	71.363	78.4	22.923
0.105	0.105	95.749	96.3	17.840
0.121	0.121	111.692	111.0	14.750
0.136	0.134	124.892	123.2	12.160
0.149	0.147	136.820	135.1	11.940
0.160	0.158	147.400	145.6	10.500
0.172	0.170	157.933	154.9	11.210
0.182	0.182	167.615	167.5	10.600
0.192	0.190	176.615	175.2	7.750
0.201	0.199	185.240	182.2	7.640
0.210	0.209	193.480	192.1	9.260
0.219	0.217	201.321	200.0	7.900
0.227	0.226	208.988	207.9	7.910
0.235	0.233	216.324	214.3	6.390
0.243	0.241	223.420	221.8	7.510
0.250	0.250	230.272	229.9	8.060

ST ERR 0.001459 ST DEV 0.055026 CORR COEFF 0.999652

DOCUMENT RES-J356

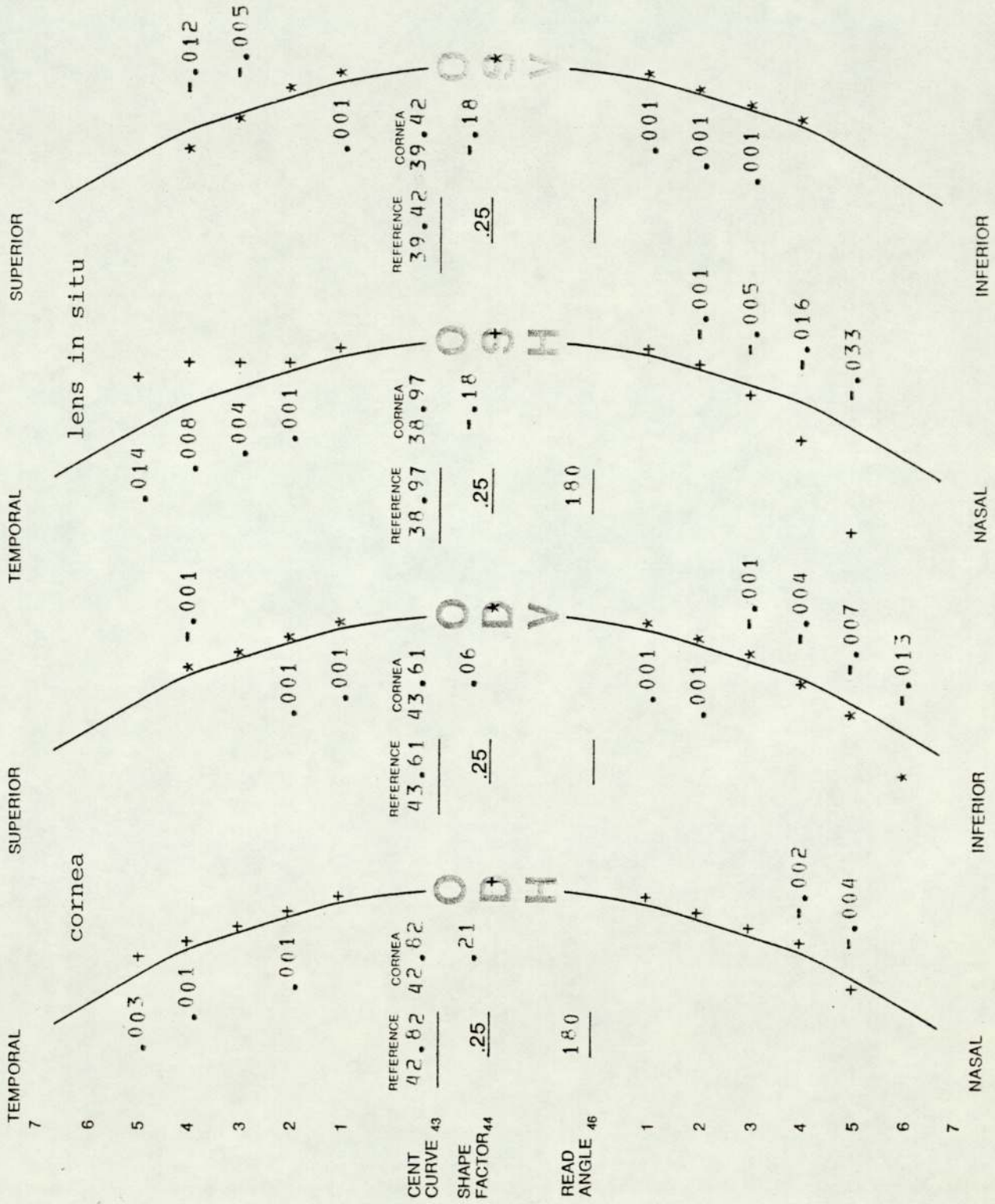
C1 C2 C3 PAD  
 0-001 5-933 5-933 7-920

XEST	XI(K)	XTEST	X1I(K)	Z
0-057	0-057	52-440	52-2	0-000
0-081	0-080	74-167	73-7	21-090
0-099	0-100	90-332	91-7	18-450
0-114	0-114	104-867	104-0	13-100
0-127	0-122	117-254	117-5	12-640
0-140	0-141	125-452	129-3	11-020
0-150	0-150	133-385	137-7	8-480
0-161	0-161	148-331	148-3	-10-520
0-171	0-171	157-364	157-5	9-120
0-180	0-181	165-513	166-0	9-290
0-189	0-188	173-910	172-9	6-070
0-197	0-197	181-646	181-4	8-590
0-206	0-206	189-065	189-4	5-500
0-213	0-214	196-204	196-6	7-190
0-221	0-221	203-092	203-1	6-470
0-228	0-228	209-753	209-5	6-360
0-235	0-236	216-126	216-8	7-330

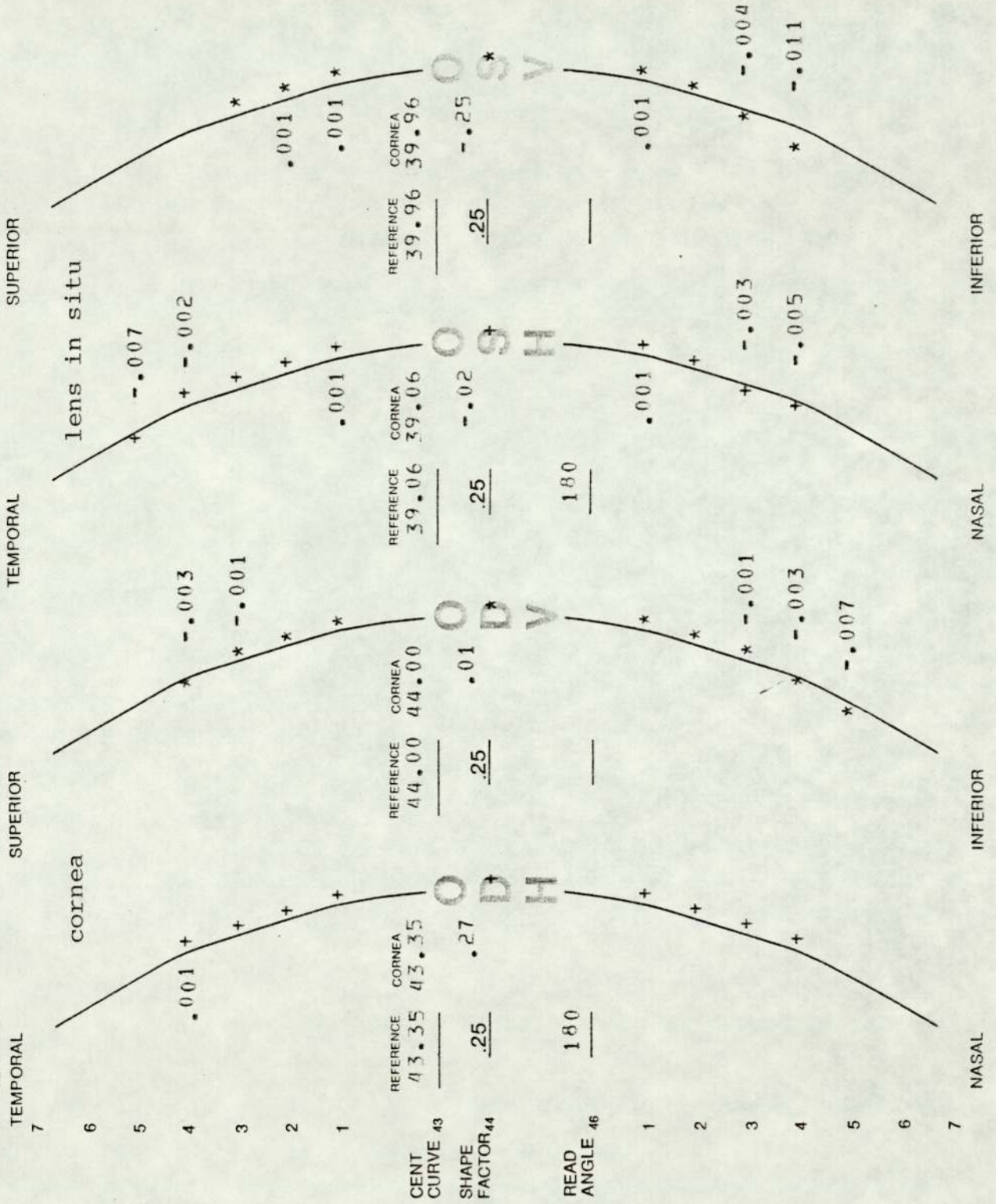
ST ERR 0-000629 ST DEV 0-052022 CORP COEFF 0-699927

APPENDIX III

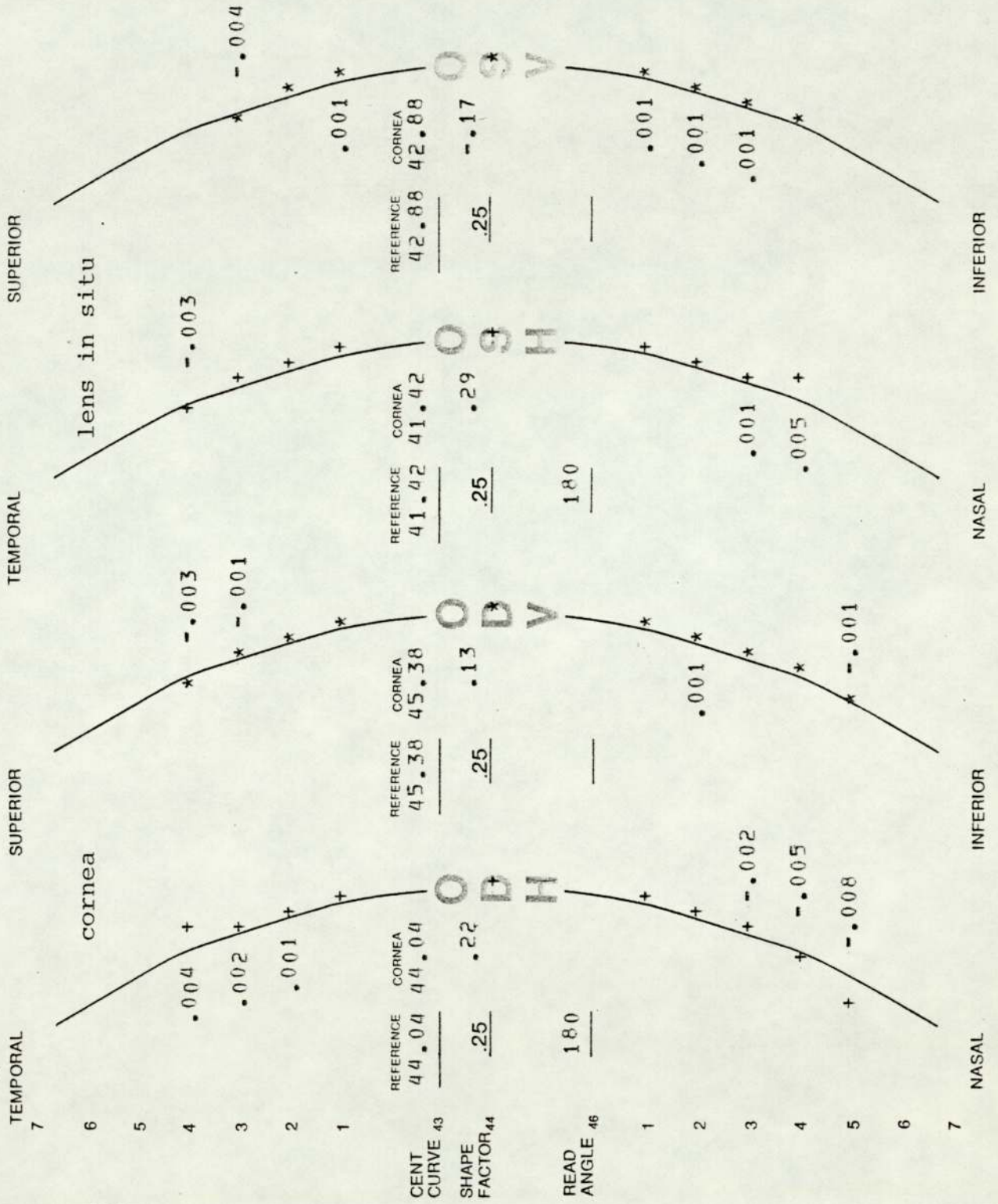
Subject 1



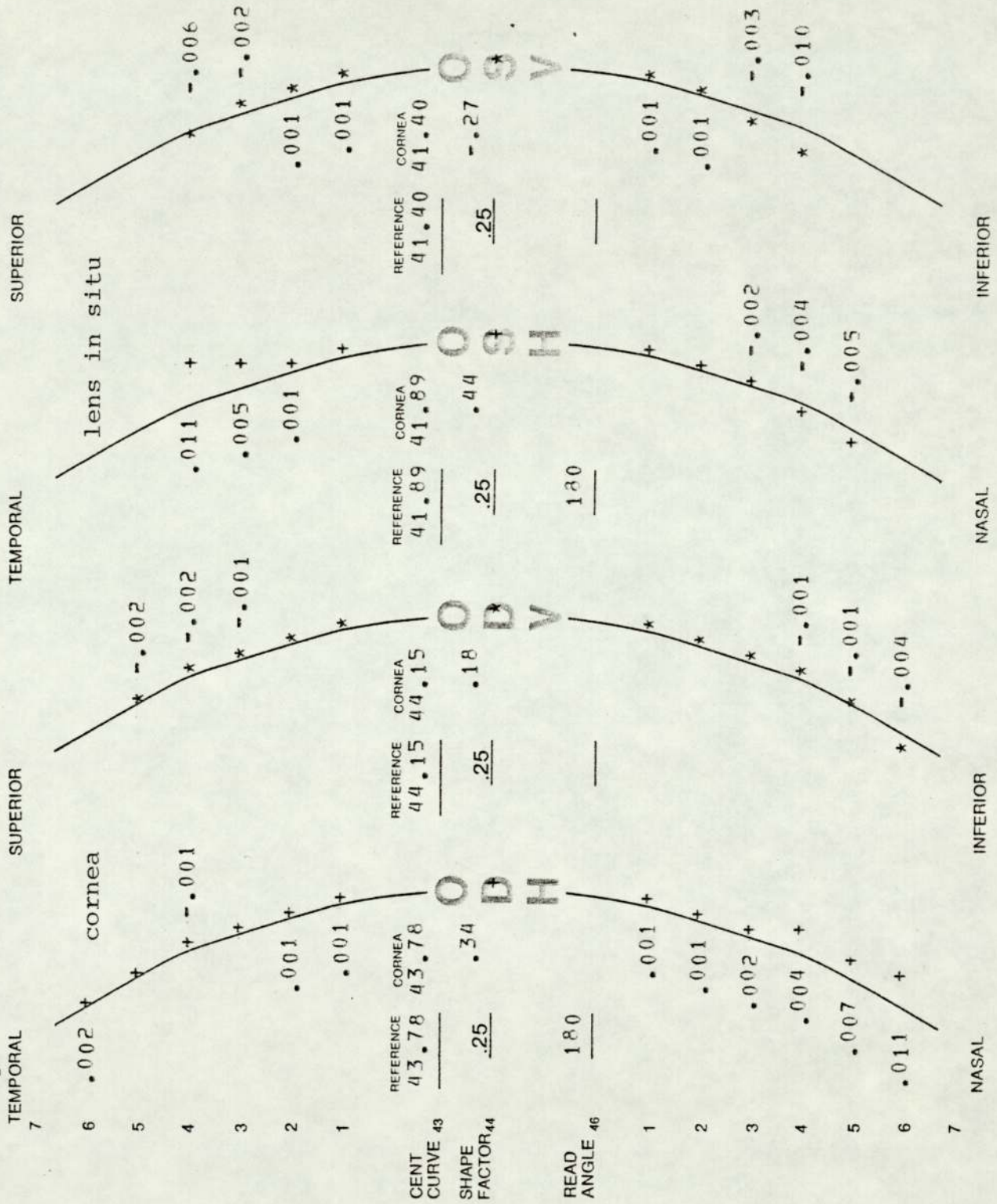
Subject 2



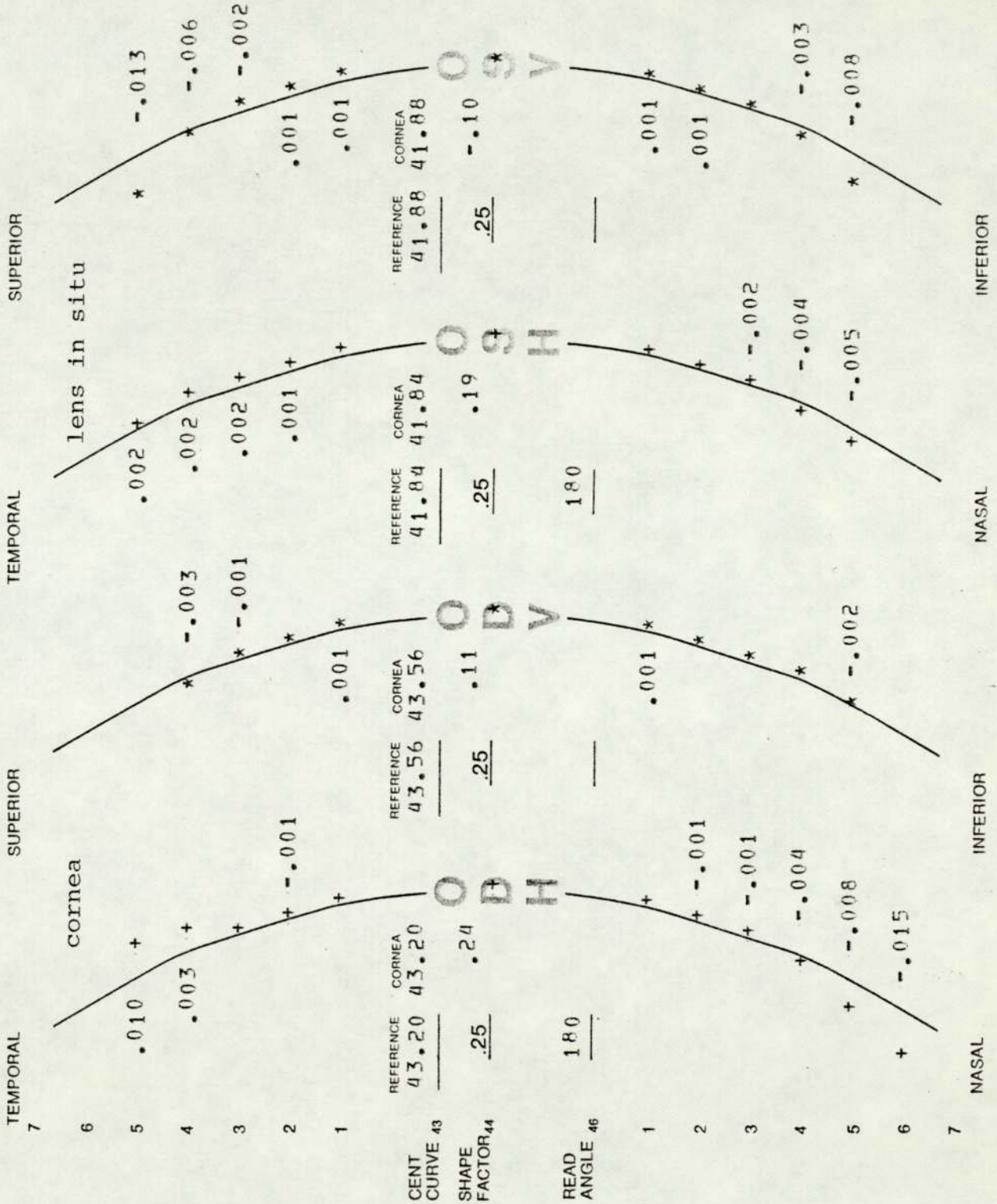
Subject 3



Subject 4



Subject 5



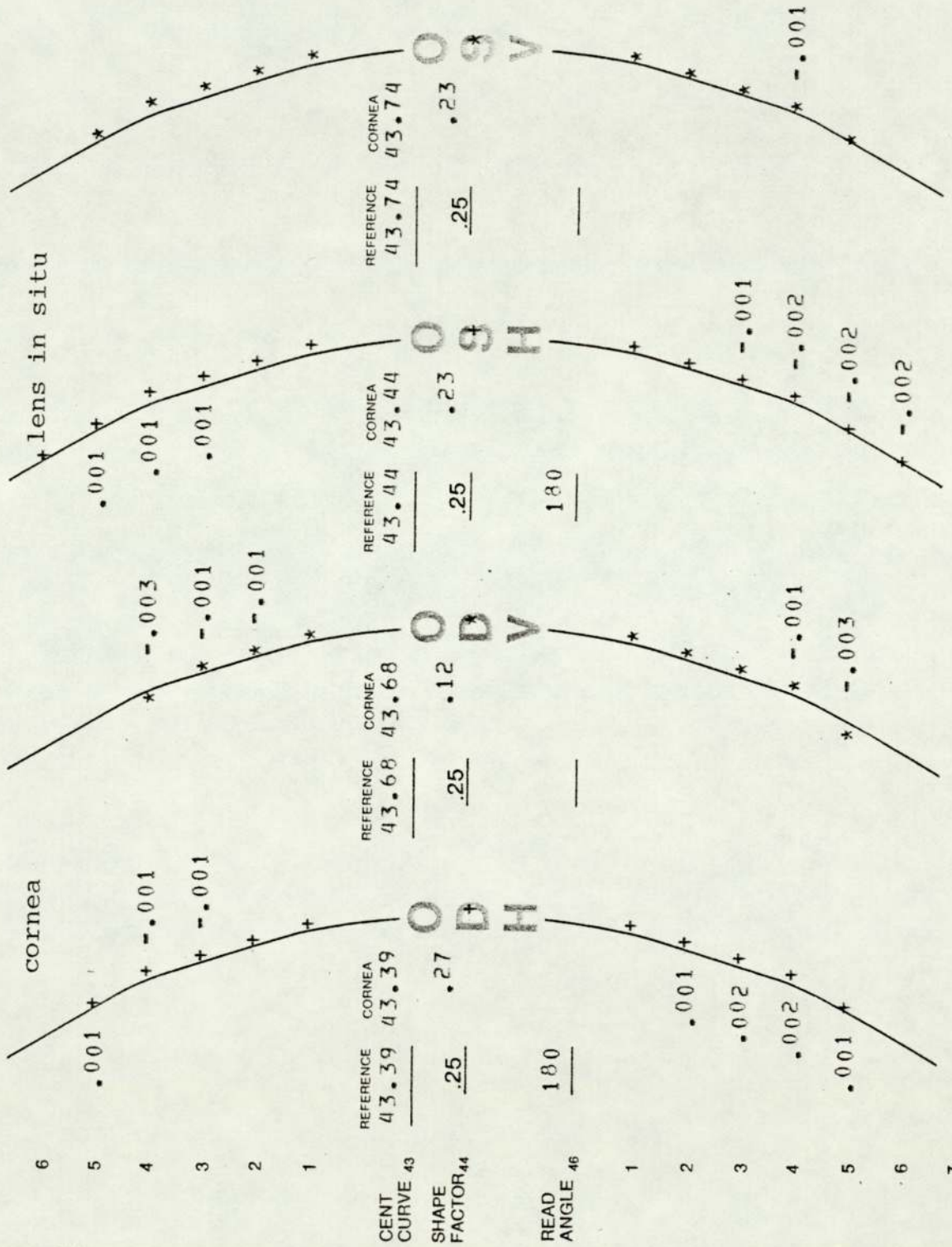
Subject 6  
TEMPORAL  
7

SUPERIOR

TEMPORAL

SUPERIOR

TEMPORAL  
7



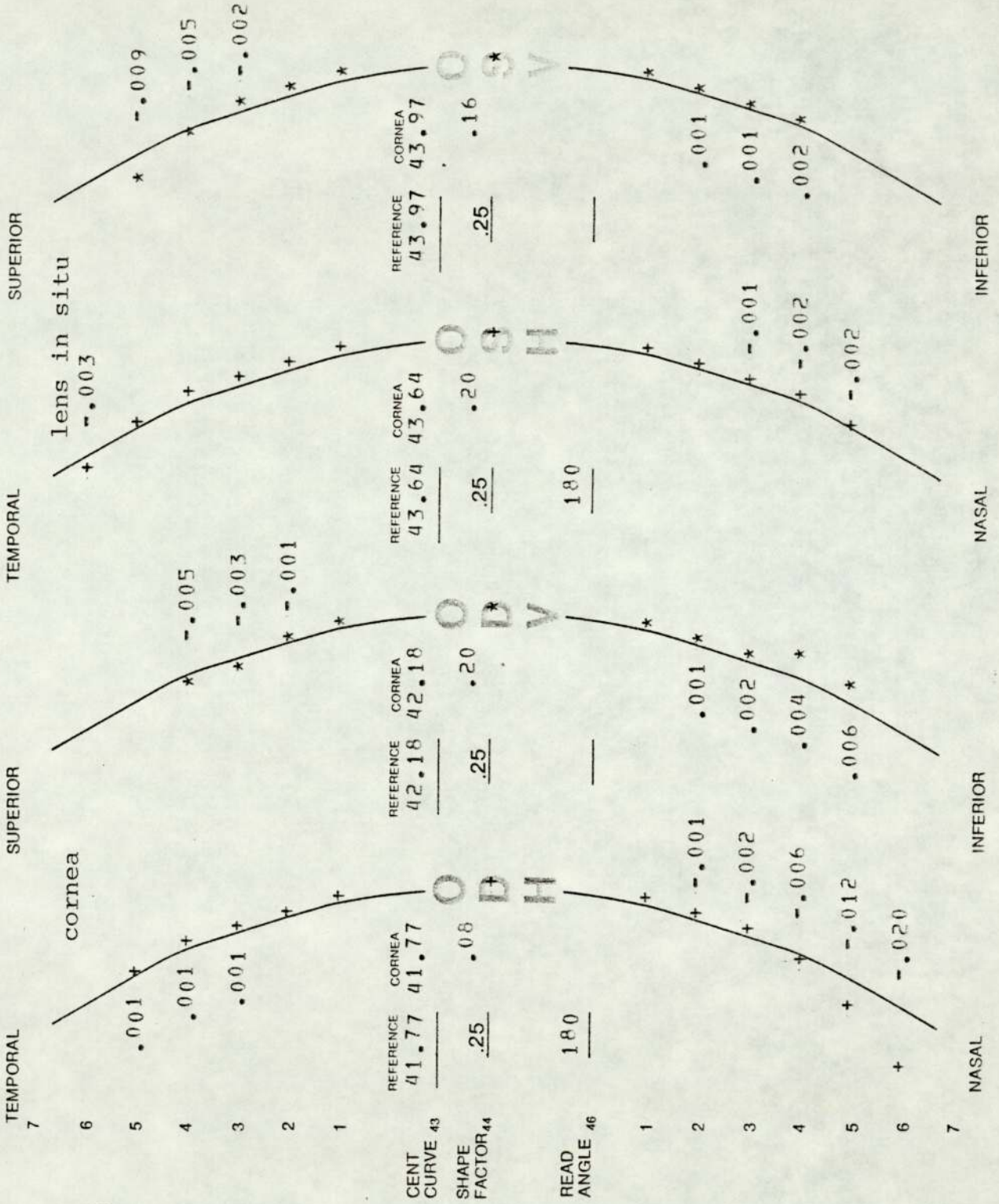
INFERIOR

NASAL

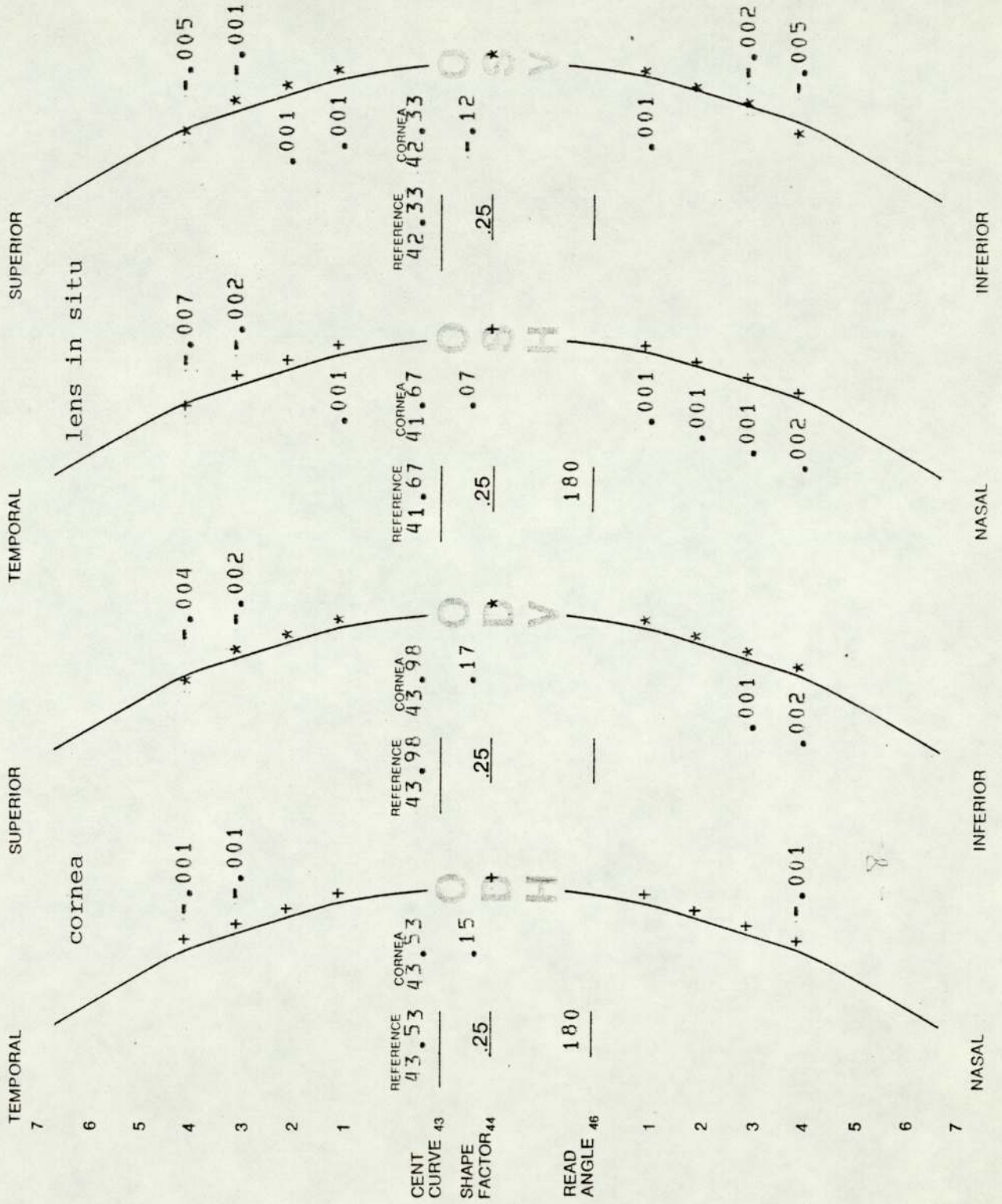
INFERIOR

NASAL  
7

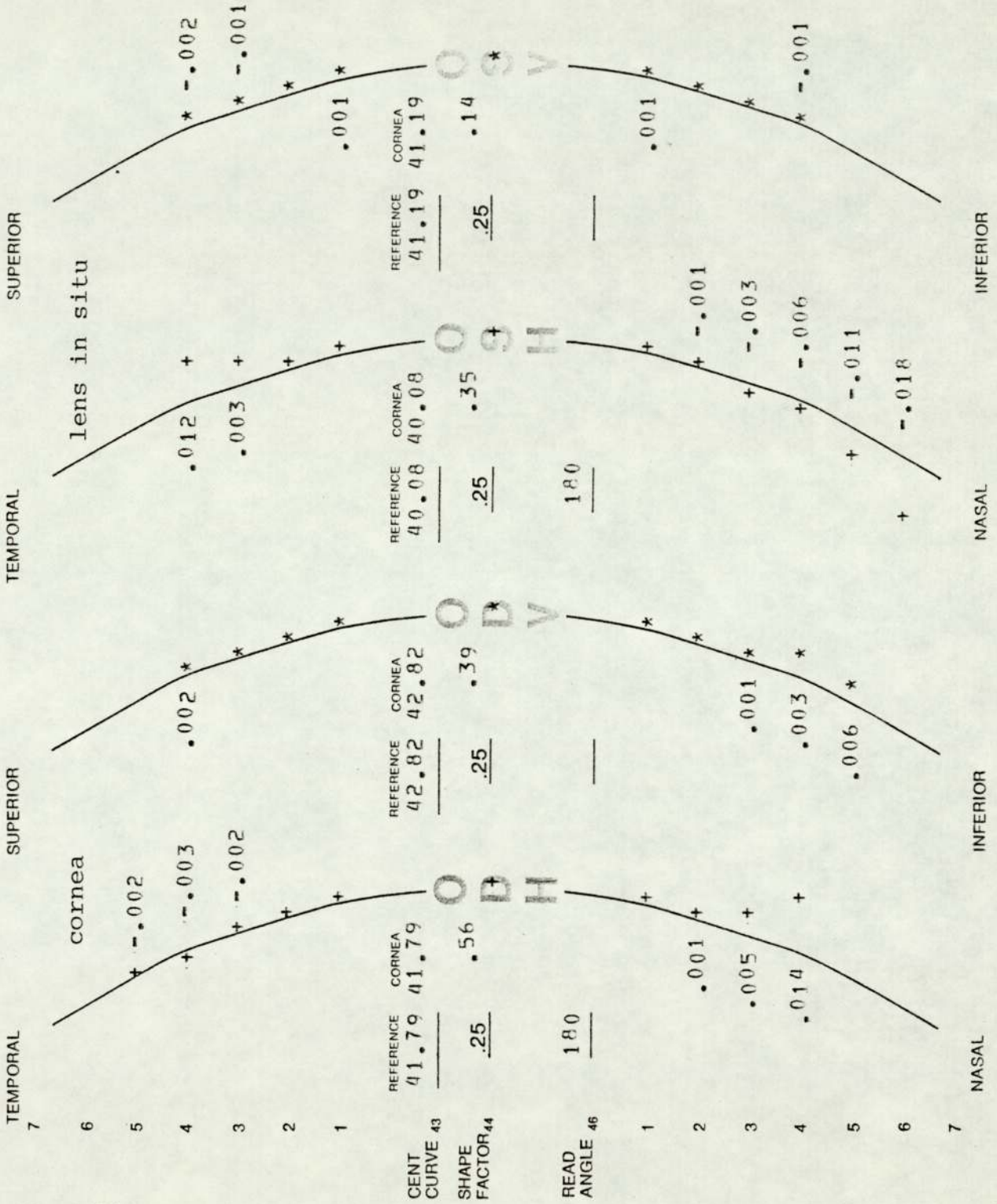
Subject 7



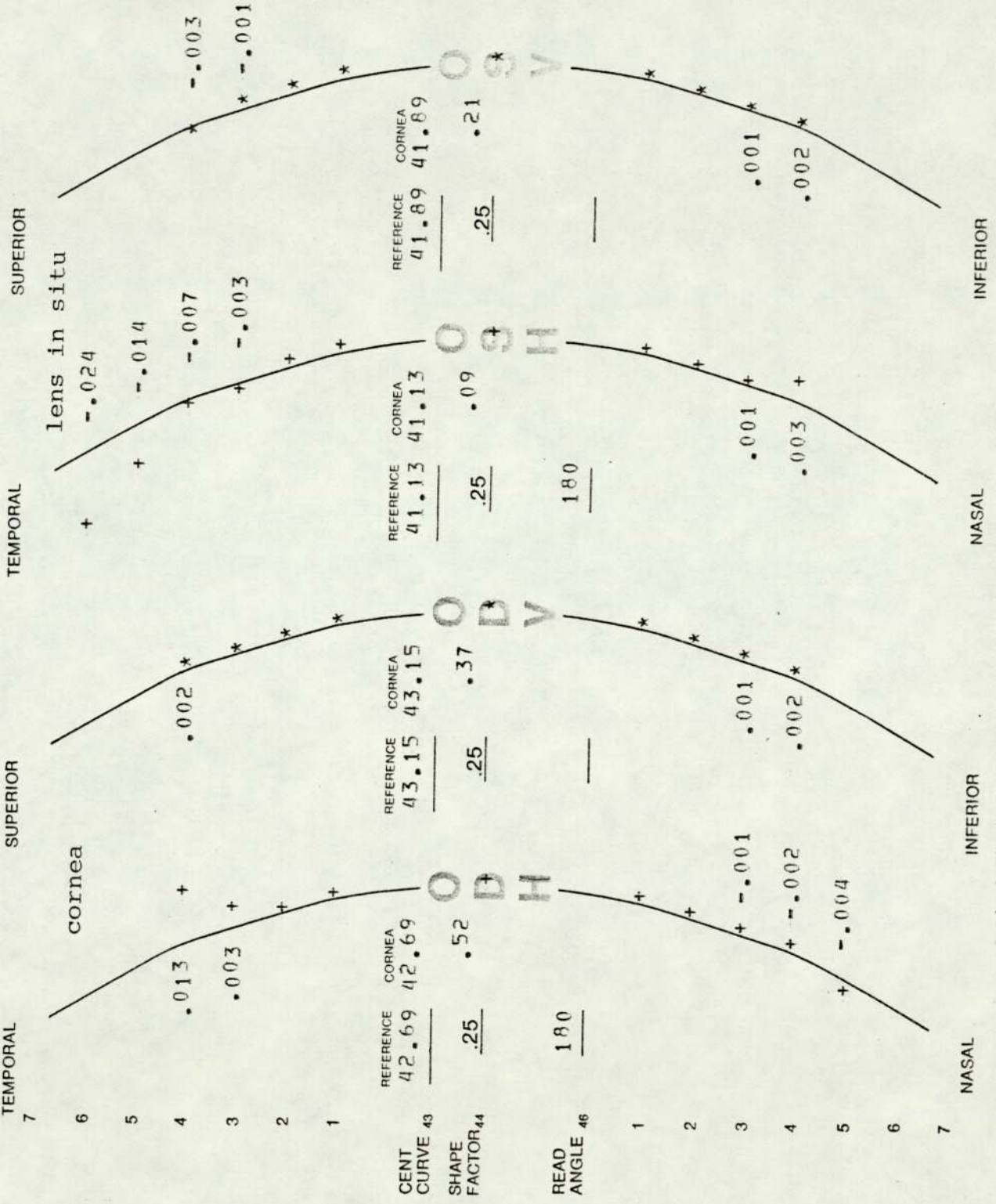
Subject 8



Subject 9



Subject 10



References

Adam, N. K. (1968)

The physics and chemistry of surfaces, Dover, 1968

Ames, A; Proctor, C. A. (1921)

J. Opt. Soc. Am. 5: 22-84

"Dioptrics of the Eye"

Anon (1954)

"Interference Microscope. Carl Zeiss Oberkochen"

Anon (1976)

Soflens International Fitting Guide

Bausch and Lomb Soflens division. Rochester USA

Bailey, N. J. (1961)

Opt. J. Rev. Optom. 98(3): 31-32

"Residual astigmatism contact lenses"

Banko, P.E. (1976)

Aus. J. Optom. 59(8): 286-289

"Production of contact lenses by spin casting"

Bennett, A. G. (1964)

Brit. J. Phys. Opt. 21: 234-238

"A new keratometer and its application to corneal topography"

Bennett, A. G. (1966)

Optics of contact lenses, 4th ed. Assoc. of dispensing opticians, Nottingham Place, London

Bennett, A. G. (1966)

The optician 151 (3913): 317-322

"The calibration of keratometers"

Becker, W. E. (1966)  
U.S. Patent 3, 22, 741

Biddles, B. J. (1969)  
Optica acta 16(2): 137-157  
"A non contacting interferometer for testing steeply  
curved surfaces"

Bier, N. (1957)  
Contact lens routine and practice, 2nd ed. London Butterworth

Bier, N (1956)  
Brit. J. Phys. Opt. 13: 79-92  
"A study of the cornea"

Bier, N. (1958)  
The optician 136(3512): 31-32  
"Two new contact lens instruments for measuring the corneal  
radius of contact lenses"

Bissel, J. L. (1974)  
Aust. J. Optom. 57(3): 79-80  
"An instrument for the measurement of hydrophilic lenses"

Blackstone, M. (1966)  
The optician 152 (3928): 38-39  
"The toposcope examined"

Bondarev, V. I. (1965)  
Measurement techniques 2: 137- 143  
"Measuring the radii of templet profiles by means of  
heads calibrated in radii"

Brailsford, M. I. D. (1972)

Oph. Optician 12(20): 1047-1048

"The importance of sag heights when fitting Bionte lenses"

Brezel, D. (1959)

J. Am. Optom. Assoc. 31(5): 379-380

"An instrument for measuring the base curve of contact lenses"

Brucker, D.; Malin, A.; Malin, H. (1972)

J. Am. Optom. Assoc. 43(3): 287-290

"Fitting soft corneascleral lenses"

Chamorro Tormo, C. J. (1974)

Gaceta Optica, Translation G. Nissel & Son

Carter, J. H. (1963)

Optom. Weekly. 54(27): 1271-1272

"Residual astigmatism of the human eye"

Chaston, J. (1973)

Optician 165(4271): 8-9, 12

"A method of measuring the radius of curvature of a soft contact lens."

Clements, L. D. (1978)

Soft contact lenses: Clinical and applied technology

Ed. Ruben, M. Willey & Sons, New York

Cooke, F. (1964)

Applied Optics, 3(1): 87-88

"The Bas spherometer"

Coombs, W. F.; Knoll, H. A. (1976)

Optical Engineering 15(4) July-August

Crombie, A. C.; Hoskins, M. A. (1967)  
History of Science 6: 90

Dellande, W. D. (1970)  
Am. J. Optom. & arch. am. acad.optom. 47(6): 459-463  
"A comparison of predicted and measured residual  
astigmatism in corneal contact lens wearers."

De Vany, A. S. (1966)  
Applied Optics 5(5): 867-868  
"A universal tester"

Dickens, R. (1966)  
The optician, 151(3911): 265-269  
"An investigation into the accuracy of the radius  
checking device"

Dickens, R.; Fletcher, R. (1964)  
Brit. J. phys. opt. 12: 107-115  
"A contact lens measurements: a comparison of several devices"

Dickinson, F. (1954)  
Optician 128: 316 23 July  
"A report on a new corneal lens"

Drysdale, C. V. (1900-1901)  
Transactions Optical Society 2: 1-12  
"On a simple direct method of determining the curvatures  
of small lenses"

Duke-Elder, S. (1970)  
System of ophthalmology "Ophthalmic optics and refraction"  
Kimpton, London

Dyson, J. (1970)

Interferometry as a measuring tool

The machinery publishing Co. Ltd., London

El-Nashar, N. F.; Larke, J.; Brookes, C. (1979)

Am. J. Optom. & physiol. Optics. 56(1): 10-15

Egorow, W. A. (1955)

Izmeritelnaja Technika 6: 48

"New interference device for the determination of the thickness of thin films"

Emsley, H. H. (1963)

The optician 146(3777): 161-168

"The keratometer - measurement of concave surfaces"

Enoch, J. M. (1956)

Am. J. Optom. & arch. am. acad. optom. 33: 77-85

"Descartes contact lens"

Fearn, W. W. (1970)

The contact lens 2: 20-22

"The use of the focimeter for measuring the central radii of corneal lenses"

Feinbloom, W. (1937)

Am. J. Optom. & arch. am. acad. optom. 14(2): 41-49

"A plastic contact lens"

Ferrero, N. (1952)

Am. J. Ophthal. 35: 507-521

Leonardi Da Vinci: of the eye

Fick, A. E. (1888)

Arch. F. Augenheilk 18: 279

"Ein Haftglas"

Forst, G. (1974)

Contacto, 18(6): 6-10

"A new method of measurement for controlling soft lens quality"

Freeman, M. H. (1965)

Am. J. Optom. & arch. am. acad. optom 42(11): 693-701

"The measurement of contact lens curvatures"

Garner, L. F. (1976)

Aust. J. Optom. 59(10): 349-354

"Design and tolerance for flexible contact lenses"

Gates, J. W. (1956)

J. Sci. instr. 33: 507

"Fringe spacing in interference microscopy"

Gilman, B. (1976)

Am. J. Optom and physiol. optics 53(3): 137-144

"Measurement of soft lens posterior curvature with moire fringes"

Gold, S. D.; Nikitin, V. A. (1964)

Measurement techniques 8: 679-681

"Superposition spherometer type IZS-8"

Goldberg, J. B. (1964)

Brit. J. phys. opt. 21(3): 169-173

"The correction of residual astigmatism with corneal contact lenses"

Goldberg, J. B. (1975)

Optometric weekly 66: 325-327

"Wet cell radius gauge"

Grosvenor, T. P. (1963)

Contact lens theory and practice. The professional press  
Inc. Chicago

Guild, J. (1918)

Transactions optical soc. 19: 103-111

"A spherometer of precision"

Guild, J. (1923)

Dictionary of applied physics 4: 786-797, Macmillan Co.  
Ltd., London

Gullstrand, A (1909)

Supplement to Helmholtz's physiological optics

Translated by Southall, J. opt. soc. am.: 437 (1924)

Hamano, H.; Kawabe, H. (1978)

Contacto 22(1): 4-8

"A method of measuring radii of a soft lens with an  
electronic device"

Hampson, R. M. (1973)

The optician 165 (4283): 4-16

"Considerations in the checking and predictability of  
hydrophilic lenses"

Harris, M. G. (1970)

J. am. optom. Assn. 41(3): 247-248

"Contact lens flexure and residual astigmatism on toric corneas"

Harris, M. G.; Appelquist, T. D. (1974)

am. J. optom & physiol. optics 51(4) 266-270

"The effect of contact lens diameter and power on flexure  
and residual astigmatism"

- Harris, M. G.; Hall, K.; Oye, R. (1973)  
Am. J. optom & arch. am. acad. optom. 50(7): 546-552  
"The measurement and stability of hydrophilic lens dimensions"
- Herschel, J. (1830)  
Encyclopedia Metropolitana, London 2: 389
- Holden, B. A. (1975)  
Aust. J. Optom. 58(12): 443-449  
"An accurate and reliable method of measuring soft contact lens curvatures"
- Holden, B. A. (1976)  
Aust. J. Optom 59: 117-129  
"Soft lens performance models; the clinical significance of the lens flexure effect"
- Holden, B. A. (1977)  
Aust. J. Optom. 60: 175-182  
"Checking soft lens parameters)
- Howland, B.; Howland, H. C. (1976)  
Science 193: 580-582  
"Subjective measurement of high-order aberrations of the eye"
- Howland, H. C.; Howland, B. (1977)  
J. Opt. Soc. am. 67: 1508-1518  
"A subjective method for the measurement of monochromatic aberrations of the eye"
- Ivanoff, A. (1947)  
J. opt. soc. am. 37: 730-731  
"On the influence of accommodation on spherical aberration in the human eye, an attempt to interpret night myopia"

Ivanoff, A. (1953)

Les aberrations de L'oeil (ed. de la Revue d'optique  
Theorique et instrumentale, Paris)

Ivanoff, A. (1956)

J. opt. soc. am. 46: 901-903

"About the spherical aberration of the eye"

Jenkins, T. C. A. (1963)

Br. J. Physiol. optics. 20: 59-91

"Aberrations of the eye and their effects on vision"

Johnson, B. K. (1960)

Optics and optical instrument. Dover Publications Inc. New York

Kalt, E. (1888)

Bull. Acad, Med. Paris 19: 400

Kaplan, M. M. (1966)

Optometric weekly, April 29-39

"Optical considerations of hydrogel contact lenses"

Kawabe, H.; Hamano, H. (1977)

Contacto, 21(3): 15-19

"Standardization of soft contact lenses (second report)"

Kerns, R. K. (1974)

Am.J. Optom. & physiol optics 51: 750-757

"Clinical evaluation of the merits of an aspheric front  
surface contact lens for patients manifesting residual  
astigmatism"

Kidger, M. J. (1978) Personal communication

Kinder, W. (1937)

Zeiss Nachrichten 2nd series 3: 91-99

"Ein Mikro-interferometer nach W. Linnik"

Koetting, R. A. (1973)

Opt. U. Rev. optom 110(20): 34-35

"Why not use the radiuscope to measure soft lenses?"

Koetting, R. A. (1975)

Am. I. optom & physiol. optics 52(7): 485-492

"Soft lens power and curvature: a comparison of "Label"  
and observed measurements"

Kolomiitsov, Yu. V.; Egudkin, A. S. (1962)

Measurement techniques, 10: 815-818

"Interferometer IZK-57 for measuring the diameter of balls"

Koomen, M.; Tousey, R.; Scolnik, R (1949)

J. opt. soc. am. 39: 370-376

"The spherical aberration of the eye"

Korb, D. R. (1960)

Optom Weekly 51(48): 2501-2505

"A preliminary report on toric contact lenses"

Kratz, J. D.; Walton, W. G. (1949)

Am. J. Optom & arch. am. acad. optom. 26(7): 295-306

"A modification of Javal's rule for the correction of  
astigmatism"

Krug, W.; Rienitz, J.; Schultz, G. (1960) Beitrage zur Interferenzmikroskopie, Akademie-Verlag, Berlin. Translated by Home Dickson, J. "Contributions to interference microscopy". Hilger and Watts Ltd., 1964

Kumar, R.; Singh, S. D.; Sabberwal, S. P. (1976)  
Ahi-Fondazione Giorgio Ronchi E Contributi istituto  
Nazionale Di ottica 31 (2): 234-244

Laycock, D. E. (1957)  
Am. J. optom & arch. am. acad. optom. 34(10): 538-539  
"A microlens measuring aid"

Le Grand, Y. V. E. S. (1952)  
Optique physiologique 1 2nd ed. de la "revue d'Optique"  
Paris

Lim, D.; Wichterle, O. (1956)  
Process for producing shaped articles from three-dimensional hydrophilic high polymers  
Czechoslovakia Patent ser. no. 580, 411

Linnik, W. (1933)  
Compt. Rend. Acad. Sci. URSS pp 21

Loran, D. F. C. (1974)  
Oph. optician 14(19): 980-985  
"Determination of hydrogel contact lens radii by projection"

Ludlam, W.; Kaye, M. (1966)  
Am. J. optom & arch. am. acad. optom. 43(8): 525-528  
"Optometry and new metrology"

Mandell, R. B. (1969)  
Contact lens practice: Basic and advanced 1st ed. Thomas, USA

Mandell, R. B. (1974)

Contact lens practice: Hard and flexible lenses  
2nd ed. Thomas, USA

Marano, J. A. (1962)

Optom. Weekly, 53(37): 1803-1804

"Front surface cylindrical contact lenses"

Martin, L. C. (1924)

"Optical measuring instruments", Blackie & son ltd., London

Millodot, M. (1969)

Arch. ophthal. 82: 461-465

"Variation of visual acuity with contact lenses"

Millodot, M. (1975)

Am. J. optom & physiol optics 52, 541-544

"Variation of visual acuity with soft contact lenses;  
A function of luminance"

Mizutani, Y.; Miwa, Y. (1977)

Contacto 21(1): 15-19

"Hydrophilic silicone rubber contact lens"

Muller, A. (1889)

Brillenglaser und Hornhautlinsen (Diss.), Kiel

Mykura, H. (1954)

Proc. phys. soc. 67B: 281-289

"Interference microscopy at high wedge angles"

Nakajima, A.; Shibata, H.; Magatami, H.; Hirano, A. (1974)

J. Jpn contact lens soc. 6(9): 123-131

"A method of soft contact lens measurement"

Ng, C. O. (1974)

"Synthetic hydrogels in contact lens applications"

PhD thesis, University of Aston in Birmingham

Nugent, M. W. (1949)

Trans. am. acad. ophthal. otol. 374-375

"The Tuohy corneal lens"

Obrig, T.; Salvatori, P. (1957)

"Contact lenses" 3rd ed., Phila., Chilton, Company.

Padula, C. F.; Spitzberg, L. A.; Kilborn, R. A. (1974)

Ref. Applied Optics 15(5): 1348 (1976)

Pfund, A. H. (1931)

J. Opt. Soc. am. 21: 182-186

"A plane-parallel plate refractometer"

Pi, H. T. (1925)

Trans. ophth. soc. of U.K. 45: 395

"The total peripheral aberration of the eye"

Polse, K. A. (1979)

Invest. ophthalmol. visual science April (1979)

"Tear flow under hydrogel contact lenses"

Port, M. (1976)

Oph. optician 16(25): 1079-1082

"New method of measuring hydrophilic lenses"

Rank, D. H. (1946)

J. opt. soc. am. 36(2): 108-110

"Measurement of the radius of curvature of concave spheres"

Rantsch, K. (1944)

Oberflächenprüfung mit Lichtinterferenz, Feinmech.

U. Prazis. 52, Part 7/12

Rantsch, K. (1945)

Optische Verfahren Zur oberflächenprüfung

Zeiss Nachr. 5, 189

Refojo (1978)

Soft contact lenses: clinical and applied Technology

Ed. Ruben, M. (J. Wiley & Sons, New York)

Sacharewski, A. N. (1952)

Interferometry, Moscow

Sagan, W. (1973)

J. am. optom. assoc. 44(10): 1053-1056

"Measurement of the hydrophilic contact lens"

Sandhu, H. S.; Friedmann, G. B. (1965)

Am. J. Phys. 33(10): 818-819

"Determination of radii of curvature of spherical surfaces using Newtons rings"

Sarma, M.; Seth, R.; Prasad, J. (1970)

J. Sci. industr. Res. (INDIA) 29(3): 149-151

"Measurement of radius of curvature of spherical optical surfaces"

Sarver, M. D. (1963)

Am. J. Optom. & arch. am. acad. 40(1): 20-28

"Calculation of the optical specifications of contact lenses"

Sarver, M. D. (1963)

Am. J. Optom & arch. am. acad. optom 40(12): 730-744

"The effect of contact lens tilt upon residual astigmatism"

Sarver, M. D. (1969)

Am. J. optom. & arch. am. acad. optom 46(8): 578-582

"A study of residual astigmatism"

Sarver, M.; Kerr, K. (1964)

Am. J. optom & arch. am. acad. optom 41(8): 481-489

"A radius of curvature measuring device for contact lenses"

Schober, H.; Hunker, H.; Zolleis, F. (1968)

Optica acta 15: 47-57

"Die aberration des menschlichen Auges und ihre messung"

Sohniges, C. P. (1974)

Contacto 18(5): 31-33

"A Sohniges control and measuring unit for hard and soft contact lenses"

Speyer, E. (1943)

Rev. Sci. instr. 14(11):336-338

"The interference spherometer"

Storey, S. (1969)

An assessment of the O.M.I. Toposcope", student project,  
The City University, London

Steel, W. H.; Noack, D. B. (1977)

Applied optics 16(4): 778-779

"Measuring the radius of curvature of soft corneal lenses"

Stine, G. H. (1930)

Am. J. Ophth. 13: 101-111

"Variation in refraction of the visual and extra visual pupillary zones"

Strachan, J. P. F. (1973)

Aus. J. Optom. 56: 25-33

"Some principles of the optics of hydrophilic lenses and geometrical optics applied to flexible lenses"

Strachan, J. P. F. (1975)

Contacto, 19(4): 24-32

"Geometrical optics applied to hydrophilic lenses and fitting hydrophilic lenses"

Tannehil, J. C.; Sampson, W. G. (1966)

Am. J. Ophthal.-mol 62(1): 132-139

"Extended use of the radiuscope in contact lens inspection"

Tocher, R. B. (1962)

Am. J. Optom & arch. am. acad. optom. 39(1): 3-16

"Astigmatism due to the tilt of a contact lenses"

Tolansky, S. (1948)

Multiple beam interferometry (Oxford: Clarendon Press)

Tolmon, F. R.; Wood, J. G. (1956)

J. Sci. Instr. 33: 236-238

"Fringe spacing in interference microscopes"

Townsley, M. (1970)

Contacto 14: 38-43

"New knowledge of the corneal contour"

Twyman, F. (1952)

"Prism and lens making". Hilger & Watt Ltd., London

Von Bahr, G. (1945)

Acta Opth. 23: 1-47

"Investigations into spherical and chromatic aberrations of the eye, and their influence on its refraction"

Wechsler, S. (1978)

J. am. optom assoc. 49: 251-256

"Visual acuity in hard and soft contact lens wearers: a comparison"

Westheimer, G. (1955)

Optica acta 2: 151-152

"Spherical aberration of the eye"

Westheimer, G. (1961)

Am. J. Optom & arch. am. acad. optom. 38(8): 445-448

"Aberrations of contact lenses"

Westheimer, G. (1961)

Transactions, International ophthalmic optical congress,  
London

"Design of bitoric contact lenses"

Wichterle, O. (1966)

"Mechanical and optical aspects in soft lens fitting"

Read at 20th int. cong. Ophthal, Munich-Feldajing

Wichterle, O. (1967)

"Corneal and scleral contact lenses", Ed. Girand, L. J.,  
Mosby, Saint Louis, p238-246

Wichterle, O. (1968) U.S. Patent no. 3,408, 429

Wilson, R. N. (1956)

J. Scient. instrum. 33: 12, 487-488

"Precision measurment of small radii of curvature"

Woo, G. C. S.; Sivak, J. G. (1976)

Am. J. Optom & physiol optics 53: 459-463

"The effect of hard and soft contact lenses (Soflens) on  
the spherical aberration of the human eye"

Young, T. (1801)

Phil. Trans. 91: 69

"On the mechanism of the eye"